

REPORT

**HYDRODYNAMIC MODEL COMPARISON
ADCIRC VS. RMA2
FDOT HURRICANE STORM SURGE MODELING**

SUBMITTED TO:

**FLORIDA DEPARTMENT OF TRANSPORTATION
DRAINAGE DESIGN OFFICE
TALLAHASSEE, FLORIDA**

SUBMITTED BY:

**OCEAN ENGINEERING ASSOCIATES, INC.
2531 NW 41st STREET, BUILDING D
GAINESVILLE, FLORIDA 32606**

MAY 2004

TABLE OF CONTENTS

LIST OF FIGURESi
LIST OF TABLESiii
EXECUTIVE SUMMARYiv
1.0 INTRODUCTION.....1
2.0 BACKGROUND3
 2.1 Numerical Models3
 2.2 Model Domain7
 2.3 Calibration Data.....8
 2.4 Hurricane storm surge hydrographs14
 2.5 Hydrology17
3.0 HYDRODYNAMIC SIMULATIONS28
 3.1 Model construction28
 3.2 Calibration.....37
 3.3 Model Simulations45
 3.3.1 RMA2 Simulations.....47
 3.3.2 ADCIRC Simulations59
4.0 MODEL COMPARISON.....67
 4.1 Qualitative Comparison67
 4.2 Quantitative Comparison.....69
5.0 SUMMARY AND RECOMMENDATIONS.....73
REFERENCES75
ACKNOWLEDGMENTS75

LIST OF FIGURES

Figure 2.1 Tide Gage Locations 10

Figure 2.2 Cross Section Locations for Flow Measurement 11

Figure 2.3 Measured Tidal Elevations 12

Figure 2.4 Measured Flow Rates..... 13

Figure 2.5 Palm Beach County Profiles near Lake Worth Inlet..... 16

Figure 2.6 Total Combined Storm Surge Hydrographs for the Lake Worth Inlet Model..... 17

Figure 2.7 Location Map for SFWMD Structure S-40..... 20

Figure 2.8 Location Map for SFWMD Structure S-41 21

Figure 2.9 Location Map for SFWMD Structure S-155 22

Figure 2.10 Location Map for SFWMD Structure S-44..... 23

Figure 2.11 Location Map for SFWMD Structure S-46 and USGS Gage LOX 8..... 24

Figure 2.12 Flow Rates and Bulletin 17B Estimate at Structure S-40..... 25

Figure 2.13 Flow Rates and Bulletin 17B Estimate at Structure S-41..... 25

Figure 2.14 Flow Rates and Bulletin 17B Estimate at Structure S-155..... 26

Figure 2.15 Flow Rates and Bulletin 17B Estimate at Structure S-44..... 26

Figure 2.16 Flow Rates and Bulletin 17B Estimate at Structure S-46..... 27

Figure 2.17 Flow Rates and Bulletin 17B Estimate at USGS Gage LOX 8..... 27

Figure 3.1 Lake Worth Inlet Model RMA2 Mesh (a) Elements and (b) Elevations 30

Figure 3.2 Lake Worth Inlet Model ADCIRC Mesh (a) Elements and (b) Elevations 31

Figure 3.3 RMA2 Model Mesh at Lake Worth Inlet..... 32

Figure 3.4 ADCIRC Model Mesh at Lake Worth Inlet 32

Figure 3.5 Flow Boundary Condition at the C-15 Canal..... 34

Figure 3.6 Flow Boundary Condition at the C-16 (Boynton) Canal 35

Figure 3.7 Flow Boundary Condition at the C-51 (West Palm Beach) Canal..... 35

Figure 3.8 Flow Boundary Condition at the C-17 Canal / Earman River 36

Figure 3.9 Flow Boundary Condition at the C-18 Canal..... 36

Figure 3.10 Flow Boundary Condition at the Loxahatchee River 37

Figure 3.11 Measured and Predicted Water Surface Elevations at Frenchman’s Marina..... 40

Figure 3.12 Measured and Predicted Water Surface Elevations at Bryant Park..... 41

Figure 3.13 Flow Rate Calibration at Lake Worth Inlet 43

Figure 3.14 Flow Rate Calibration at Peanut Island West..... 43

Figure 3.15 Flow Rate Calibration at Peanut Island East 44

Figure 3.16 Flow Rate Calibration at ICWW-South 44

Figure 3.17 Locations of the Bridges Employed for the Presentation of the Simulation Results..... 46

Figure 3.18 Contours of Velocity Magnitude and Velocity Vectors at the Time of Maximum Velocity near the Big Blue Heron Bridge for the 50-year Return Period Storm Surge Simulation (RMA2)..... 49

Figure 3.19 Contours of Velocity Magnitude and Velocity Vectors at the Time of Maximum Velocity near the Big Blue Heron Bridge for the 100-year Return Period Storm Surge Simulation (RMA2) 50

Figure 3.20 Contours of Velocity Magnitude and Velocity Vectors at the Time of Maximum Velocity near the Big Blue Heron Bridge for the 500-year Return Period Storm Surge Simulation (RMA2)..... 51

Figure 3.21 Contours of Velocity Magnitude and Velocity Vectors at the Time of Maximum Velocity near the Royal Palm Bridge for the 50-year Return Period Storm Surge Simulation (RMA2)..... 52

Figure 3.22 Contours of Velocity Magnitude and Velocity Vectors at the Time of Maximum Velocity near the Royal Palm Bridge for the 100-year Return Period Storm Surge Simulation (RMA2)..... 53

Figure 3.23 Contours of Velocity Magnitude and Velocity Vectors at the Time of Maximum Velocity near the Royal Palm Bridge for the 500-year Return Period Storm Surge Simulation (RMA2) 54

Figure 3.24 Velocity Magnitude Time Series at the Big Blue Heron Bridge for All Simulations 55

Figure 3.25 Water Surface Elevation Time Series at the Big Blue Heron Bridge for All Simulations 56

Figure 3.26 Velocity Magnitude Time Series at the Royal Palm Bridge for All Simulations 57

Figure 3.27 Water Surface Elevation Time Series at the Royal Palm Bridge for All Simulations 58

Figure 3.28 Contours of Velocity Magnitude and Velocity Vectors at the Time of Maximum Velocity near the Big Blue Heron Bridge for the 50-year Return Period Storm Surge Simulation (ADCIRC) 61

Figure 3.29 Contours of Velocity Magnitude and Velocity Vectors at the Time of Maximum Velocity near the Big Blue Heron Bridge for the 100-year Return Period Storm Surge Simulation (ADCIRC) 62

Figure 3.30 Contours of Velocity Magnitude and Velocity Vectors at the Time of Maximum Velocity near the Big Blue Heron Bridge for the 500-year Return Period Storm Surge Simulation (ADCIRC) 63

Figure 3.31 Contours of Velocity Magnitude and Velocity Vectors at the Time of Maximum Velocity near the Royal Palm Bridge for the 50-year Return Period Storm Surge Simulation (ADCIRC) 64

Figure 3.32 Contours of Velocity Magnitude and Velocity Vectors at the Time of Maximum Velocity near the Royal Palm Bridge for the 100-year Return Period Storm Surge Simulation (ADCIRC) 65

Figure 3.33 Contours of Velocity Magnitude and Velocity Vectors at the Time of Maximum Velocity near the Royal Palm Bridge for the 500-year Return Period Storm Surge Simulation (ADCIRC) 66

Figure 4.1 ADCIRC Model Mesh in the Vicinity of the Big Blue Heron Bridge 71

Figure 4.2 RMA2 Model Mesh in the Vicinity of the Big Blue Heron Bridge 71

LIST OF TABLES

Table ES.1 Error Summary for Water Level Calibration..... v
Table ES.2 Error Summary for Flow Rate Calibration..... v
Table ES.3 Summary of Simulation Results..... v
Table 2.1 Tide Gage Information 9
Table 2.2 Total Storm Surge Elevations for the Lake Worth Inlet Model..... 15
Table 2.3 Flow Gage Summary 19
Table 3.1 Friction Assignment within the RMA2 Lake Worth Inlet Model Mesh..... 39
Table 3.2 Error Summary for Water Level Calibration..... 42
Table 3.3 Error Summary for Flow Rate Calibration..... 42
Table 3.4 Summary of Simulation Results..... 48

EXECUTIVE SUMMARY

The objective of this work was to evaluate the capabilities of the ADCIRC and RMA2 models to simulate hurricane storm surge propagation through inland waterways for the purpose of determining design flow properties in support of FDOT's bridge hydraulics interests. This report presents the work associated with constructing a model of Lake Worth Inlet, its neighboring inlets, and connecting waterways, debugging and calibrating the model, and employing the model to simulate the storm surge propagation associated with the 50-, 100-, and 500-year return period hurricane storm surge open coast boundary conditions. Results from these simulations were compared at the Royal Palm Bridge and the Big Blue Heron Bridge in Palm Beach County, FL. This work built upon work previously performed for FDOT District 4 in support of its scour evaluation program. The models' performance was judged both qualitatively on ease of application and time to construct and run and quantitatively on capability to reproduce measured water surface elevations and flow rates near Lake Worth Inlet.

Both models took roughly the same amount of time to construct, calibrate, and run. Both models achieved good calibration when compared with measured flow and water surface elevations. Tables ES.1 and ES.2 present the results of the calibration. Although the ADCIRC model performed slightly better in the overall calibration than did the RMA2 model, the differences were minor. The models did exhibit slight differences in flow behavior during the storm surge simulations at the two bridges examined. Table ES.3 presents a summary of the storm surge simulations. The differences (10% to 15%) in maximum velocity and may be attributed to different choices made by the model developer concerning model resolution and topography smoothing during the model development and debugging processes. Additionally, differences occurred in the flow behavior offshore of the inlet. This resulted from the offshore boundary located too close to the inlet for the ADCIRC model. This underscores the importance of placing the boundary conditions far from the area of interest. In summary, the models appear roughly equivalent in both their accuracy and their ease of application for the near shore application described above.

Table ES.1 Error Summary for Water Level Calibration

Model	Error Type	Frenchman's Marina	Bryant Park
ADCIRC	Mean Error (cfs)	0.24	0.13
	RMS Error (cfs)	0.29	0.34
	Percent Error (%)	7.7%	9.3%
RMA2	Mean Error (cfs)	0.21	0.15
	RMS Error (cfs)	0.47	0.39
	Percent Error (%)	12.5%	10.8%

Table ES.2 Error Summary for Flow Rate Calibration

Model	Error Type	Lake Worth Inlet	ICWW-S	Peanut Island East	Peanut Island West
ADCIRC	Mean Error (cfs)	-647	-437	-811	-331
	RMS Error (cfs)	3881	3809	1768	1278
	Percent Error (%)	3.4%	5.5%	6.1%	6.6%
RMA2	Mean Error (cfs)	-137	5180	-1359	1433
	RMS Error (cfs)	4154	6332	1731	1936
	Percent Error (%)	3.6%	9.1%	6.0%	10.1%

Table ES.3 Summary of Simulation Results

Bridge	Model	Maximum Velocity (fps)			Maximum Water Surface Elevation (ft-NAVD88)		
		50-year	100-year	500-year	50-year	100-year	500-year
Royal Palm Bridge	ADCIRC	3.7	3.9	4.8	8.4	9.2	12.5
	RMA2	3.4	4.2	4.8	8.2	9.9	12.5
	Difference (RMA2-ADCIRC)	-0.3	0.3	<0.1	-0.2	0.7	0.0
Big Blue Heron	ADCIRC	3.6	3.8	4.4	8.3	9.1	12.3
	RMA2	3.4	4.4	5.0	8.1	9.8	12.5
	Difference (RMA2-ADCIRC)	-0.2	0.6	0.6	-0.2	0.7	0.2

Given the minor differences in the results from the two models, both models appear acceptable for this type of application. As such, OEA recommends the application of either model for the simulation of hurricane storm surge propagation into coastal waters for FDOT applications. Selection of a model should therefore fall to which model contains the features most appropriate to the model domain and available boundary conditions. For example, the ADCIRC model is more appropriate for simulation of specific hurricanes through meteorological

forcing. Conversely, if a bridge site contains numerous control structures such as culverts or flap gates, then the RMA2 model would be more appropriate.

1.0 INTRODUCTION

Two-dimensional hydrodynamic modeling is an important tool for design water levels, flows, and scour depths at bridge crossings. This tool is particularly useful when examining coastal bridges since the design flows are oftentimes produced by hurricane storm surge propagation. Currently, the Florida Department of Transportation (FDOT) does not require a specific hydraulic model for modeling such conditions. One of the more popular models employed by many consultants is the U.S. Army Corps of Engineers (USACE) RMA2 hydrodynamic model. RMA2, originally designed as a steady state model for riverine applications and later modified to simulate time-dependent flows, is a finite element model which solves the two-dimensional, depth averaged Navier-Stokes equations. More recently, the USACE developed an alternate hydraulic model ADCIRC (ADvanced CIRCulation model) designed specifically for applications in tidally dominated environments. This model was designed to address circulation problems associated with dredging activities. One of the guiding principles regarding model development included ensuring that the model lends itself to coastal and ocean applications (i.e., the capability to cover very large domains such as the North Atlantic and/or the Gulf of Mexico). This capability ensures proper specification of boundary conditions (i.e., far removed from the area of interest). Recent ADCIRC applications include hindcasting hurricane storm surges. In an effort to determine the more appropriate model for examining the design hydraulic conditions at its coastal bridges, the FDOT contracted Ocean Engineering Associates, Inc. (OEA) to compare and contrast these two models. This report details the work comparing the two models by simulating both the storm surge propagation and tidal circulation at specified locations within both models. It includes a quantitative comparison of the two models' solutions as well as a qualitative comparison of the modeling process (mesh construction, model stability, etc.). Finally, this report provides a recommendation as to which model the FDOT should advocate for this type of modeling.

Following this introduction, the report presents background information needed for the comparison including a review of each models' capabilities, the model domain, measured calibration data, and the storm surge hydrograph boundary conditions. Chapter 3.0 details the results of both the tidal circulation and storm surge propagation simulations for both models.

Chapter 4.0 gives both a qualitative and quantitative comparison of the results. Finally, Chapter 5.0 presents a summary of the work and recommendations. Notably, OEA has recently completed a project that simulated hurricane storm surge propagation for FDOT District 4 via the RMA2 model. The work outlined in this report builds upon this existing work for this project. As such, the work sponsored for this project largely covered the costs associated with setup and simulation with the ADCIRC model over the same domain as one of the FDOT District 4 models.

2.0 BACKGROUND

Calculation of a bridge's hydraulic characteristics during a hurricane storm surge via both ADCIRC and RMA2 requires detailed knowledge of the study area, an adequate set of calibration data for the model, and appropriate selection of boundary conditions. This chapter details the factors necessary for performing the modeling simulations and the comparison of the model results.

2.1 Numerical Models

Before one can make an accurate comparison of the models, it is appropriate to present an overview of each model as well as a review of each models' capabilities. Notably, the information presented in this section comes almost verbatim from the websites for the models. For a more complete description of the models, the reader is referred to the following sites:

RMA2 — <http://chl.wes.army.mil/software/tabs/rma2.htm>

ADCIRC — http://www.marine.unc.edu/C_CATS/adcirc/adcirc.htm

Application of RMA2 required three individual programs to resolve the flows through the Intracoastal Waterway (ICWW). Each of the programs performs a unique function. The Surfacewater Modeling System (SMS) aided in model creation and pre and post-processing of the model results. The program, originally developed by the USACE Coastal and Hydraulics Laboratory and further developed and currently maintained by the Environmental Modeling Research Laboratory (EMRL) at Brigham Young University, provides complete support for RMA2 (two-dimensional hydrodynamic and contaminant transport), SED2D (two-dimensional sediment transport and deposition), HIVEL2D (two-dimensional hydrodynamic supercritical and subcritical flow), the U.S. Federal Highway Administration's FESWMS (two-dimensional hydrodynamic and contaminant transport) finite element models, as well as the USACE ADCIRC model. This support includes automatically constructing finite element meshes for the modeled regions. SMS provides interactive graphics and easy-to-use dialog boxes for entering all modeling parameters. The software is well-suited for the construction of large, complex two-dimensional meshes of arbitrary shape. The software enables quick construction of large meshes

from sets of scattered point data by employing the Delauney triangulation technique. It also provides a means of importing existing digital elevation models to provide background data to generate bed elevations for the mesh. An adaptive tessellation meshing scheme allows the mesh to change its density based upon how rapidly the background data elevations change. Following the simulation, the software can output or display the results graphically through a variety of plots, including vector plots, contour plots, color-shaded contour plots, and time-history plots. SMS can easily generate contour plots and color-shaded contour plots of water surface elevation, velocity, and discharge for any of the computed time-steps. The user can request time-history plots at any location to illustrate fluctuations in water surface elevation, velocity, and discharge. For transient solutions, vector and contour animation allows the user to observe how water surface elevation, velocity, and discharge vary with time.

The second program employed in this analysis is GFGEN (Geometry File GENeration). This program provides a pre-processor for RMA2. It creates a binary finite element mesh geometry file from the ASCII finite element mesh geometry file generated by SMS. GFGEN also performs routine mesh diagnostics and element reordering.

The final program employed is the USACE supported RMA2 hydrodynamic solver. RMA2 is a one- and two-dimensional, dynamic, depth-averaged, finite-element, hydrodynamic model. It computes water surface elevations and depth-averaged horizontal velocity for subcritical, free-surface flow in two-dimensional flow fields. Norton, King and Orlob of Water Resources Engineers originally developed RMA2 for the Corps of Engineers Walla Walla District, in 1973. King and Roig at the University of California, Davis carried out further development of the model. King and Norton, of Resource Management Associates (RMA) and the Waterways Experiment Station (WES) Hydraulics Laboratory made subsequent enhancements which culminated in the current version of the code.

The code's governing equations treat conservation of mass, conservation of momentum in the x and y -direction, and turbulence closure. RMA2 computes a finite element solution of the Reynolds form of the Navier-Stokes equations for turbulent flows. The code treats bottom friction via the Manning's or Chezy equation. Eddy viscosity coefficients define the flow

turbulence characteristics. The program contains the capability of analyzing both steady and unsteady state (dynamic) problems. RMA2 is a general purpose model designed for far-field problems with negligible vertical accelerations and depth-uniform velocity directions at any instant of time. It expects a vertically homogeneous fluid with a free surface. Model capabilities include: identifying errors in the mesh; accepting either English or standard SI units; simulating wetting and drying events; accounting for Coriolis effects; applying wind stress involving frontal (storm) passages; modeling up to five different types of flow control structures; and applying a wide variety of boundary conditions. Users of the model may specify turbulent exchange coefficients, Manning's n-values, water temperature, or select equations for automatic dynamic assignment of Manning's n-value by depth or Peclet number for automatic dynamic assignment of turbulent exchange coefficients.

RMA2 is a rigorously tested and well maintained hydrodynamic model with wide applicability. Applications of the model include calculating water levels and flow distribution around islands; flow at bridges having one or more relief openings; in contracting and expanding reaches; into and out of off-channel hydropower plants; at river junctions; and into and out of pumping plant channels; circulation and transport in waterbodies with wetlands; and general water levels and flow patterns in rivers; reservoirs; and estuaries.

Calculation of hurricane storm surge via ADCIRC required the application of individual programs. As with the RMA2 model, the program SMS provides the user interface. ADCIRC (Advanced Circulation Model for Coastal Ocean Hydrodynamics) is a numerical model developed specifically for generating long time periods of hydrodynamic circulation along shelves, coasts, and within estuaries. The intent of the model is to produce long numerical simulations for very large computational domains in a unified and systematic manner. The collaboration of many researchers have led to the development of the ADCIRC model including investigators at the University of Notre Dame (J.J. Westerink), the University of North Carolina at Chapel Hill (R.A. Luettich), the University of Texas at Austin (M.F. Wheeler and C. Dawson), the University of Oklahoma (R. Kolar), the State of Texas (Jurji), and the Waterways Experiment Station (N. Scheffner).

Both the U.S. Army and Navy have extensively applied ADCIRC for a wide range of tidal and hurricane storm surge predictions in regions including the western North Atlantic, Gulf of Mexico and Caribbean Sea, the Eastern Pacific Ocean, the North Sea, the Mediterranean Sea, the Persian Gulf, and the South China Sea. The model employs computational models of flow and transport in continental margin waters to predict free surface elevation and currents for a wide range of applications including evaluating coastal inundation, defining navigable depths and currents in near shore regions, to assessing pollutant and/or sediment movement on the continental shelf.

ADCIRC is a highly developed computer program for solving the equations of motion for a moving fluid on a rotating earth. The equation formulation includes applying the traditional hydrostatic pressure and Boussinesq approximations and discretizing the equations in space via the finite element (FE) method and in time via the finite difference (FD) method. The ADCIRC program includes both a two-dimensional depth integrated (2DDI) mode and a three-dimensional (3D) mode. For both, the models solve for elevation via the depth-integrated continuity equation in Generalized Wave-Continuity Equation (GWCE) form. The model solves for velocity via either the 2DDI or 3D momentum equations. These equations retain all the nonlinear terms. ADCIRC includes solution capabilities in either a Cartesian or a spherical coordinate system.

The GWCE is solved via either a consistent or a lumped mass matrix and an implicit or explicit time stepping scheme. If a lumped, fully explicit formulation is specified, no matrix solver is necessary. In all other cases, the GWCE is solved using the Jacobi preconditioned iterative solver from the ITPACKV 2D package. The 2DDI momentum equations are lumped and therefore require no matrix solver.

Possible boundary conditions for the model include specified elevation (harmonic tidal constituents or time series); specified normal flow (harmonic tidal constituents or time series); zero normal flow; slip or no slip conditions for velocity; external barrier overflow out of the domain; internal barrier overflow between sections of the domain; surface stress (wind and/or wave radiation stress); atmospheric pressure; or outward radiation of waves (Sommerfield condition). ADCIRC can be forced with: elevation boundary conditions; normal flow boundary

conditions; surface stress boundary conditions; tidal potential; or an earth load/self attraction tide.

2.2 Model Domain

As stated previously, this study builds on work previously performed for FDOT District 4. Specifically, OEA recently completed work that involved hurricane storm surge modeling for all the tidally influenced waterways within FDOT District 4. This work was performed in support of the District's effort to comply with the FHWA Scour Evaluation requirements. Employing a novel approach, the District chose to perform all the hurricane storm surge hydrodynamic modeling of its tidally influenced bridges en masse rather than on a bridge by bridge basis. The District contracted Kimley-Horn and Associates with subcontractor OEA to perform this work. The work involved the creation of nine individual hydrodynamic models (corresponding to the nine inlets that lie within the District). Each model is centered on one of the inlets and also includes the inlets to the north and south. This ensures that the communication between the subject inlet and each of its neighboring inlets is properly accounted for. Each model also includes the topography surrounding the waterbodies so that the storage associated with the expected flooded areas is included. The models were forced by both flow and elevation boundary conditions. The ocean boundaries (located approximately 2 miles offshore) were forced with an elevation time series that represents a hurricane storm surge hydrograph. These hydrographs were developed by the Florida Department of Environmental Protection (DEP) for each of Florida's coastal counties with sandy beaches. The hydrographs correspond to the 100-year storm surge events. The DEP also provides maximum elevations for the 50- and 500-year events. To obtain the boundary conditions associated with these events, the 100-year hydrographs were scaled such that the maximum elevations equaled the reported value. The flow boundary conditions for the hurricane simulations corresponded to the 5-year return period flow for each of the creeks and rivers that discharge into the Intracoastal Waterway. More information on the boundary conditions employed in this study is contained in Section 2.4. The work performed for District 4 also included a substantial field data collection effort in support of model setup and model calibration. Section 2.3 presents more information on the data collection effort vis-à-vis the calibration data collection.

Of the nine hydrodynamic models, the model deemed most appropriate for this comparison was the Lake Worth Inlet model. This model includes several of the features typical of Florida's coastal waterways including coastal barrier islands, low lying topography that abuts the waterways, and intercommunication of neighboring inlets. In fact, this model actually contains four inlets rather than three — Boca Raton Inlet, Boynton Inlet, Lake Worth Inlet, and Jupiter Inlet. Boca Raton Inlet was added into the model because initial modeling of the system indicated that significant communication occurred between this inlet and Lake Worth Inlet. This communication results from the relatively small cross sectional area, and hence small flow rates, associated with Boynton Inlet which lies immediately to the south of Lake Worth Inlet. Additionally, this model contained the largest number of nodes and elements, by a large margin, of any of the models constructed for this project. All these factors contributed to the selection of this model for this comparison.

2.3 Calibration Data

The field investigation in support of the Lake Worth Inlet model included water surface elevation measurements at three tide gages and flow discharge measurements at four cross sections over a tidal cycle. Figure 2.1 and 2.2 show the locations of the tide gages and the cross sections for discharge measurement. Table 2.1 summarizes the tide gage information for the field investigation. Figure 2.3 presents the water surface elevation data obtained from all gages for March to April 2001. From the table, the overlap in the tide gage measurements for the inshore gages spanned from February 28, 2001 to March 30, 2001 and from April 6, 2001 to April 26, 2001. Unfortunately, this coverage did not include the date (April 5, 2002) of flow measurement for Lake Worth Inlet at the cross sections indicated in Figure 2.2. Figure 2.3 includes the water surface elevation recorded at the Frenchman's Marina and Bryant Park gages, which provide information for calibration, and at the (open coast) Lake Worth Pier gage, which provides the Atlantic Ocean elevation boundary conditions for the calibration and spring tides simulations.

Table 2.1 Tide Gage Information

Name	Gauge Type	Latitude	Longitude	Associated Benchmark	Dates of Operation (2001)
Frenchman's Marina	Pressure Transducer	26° 52.800' N	80° 04.400' W	GPS Survey	Feb. 28- Apr. 26
Lake Worth Pier	Pressure Transducer	26° 36.7' N	80° 2.0' W	PID # AD0671	Mar. 1 – Apr. 26 May 31 – Oct. 4
Bryant Park	Pressure Transducer	26° 36.810' N	80° 02.820' W	GPS Survey	Feb. 28- Mar. 30 Apr. 6 - 26

Figure 2.4 presents the measured discharge data. The sign convention for the flow measurements obeys the following rule. If one draws lines connecting the edges of the cross sections to form a polygon, then the flow into the polygon is positive and flow out is negative. From 2.4, the flow measurement began on a flood tide, captured a complete ebb tide, and completed during a flood tide. Measured flow rates reached as high as 58,200 cfs on ebb tide and 56,100 cfs on flood tide. From the measurements, the tidal prism appears to flow evenly both north and south through the ICWW.

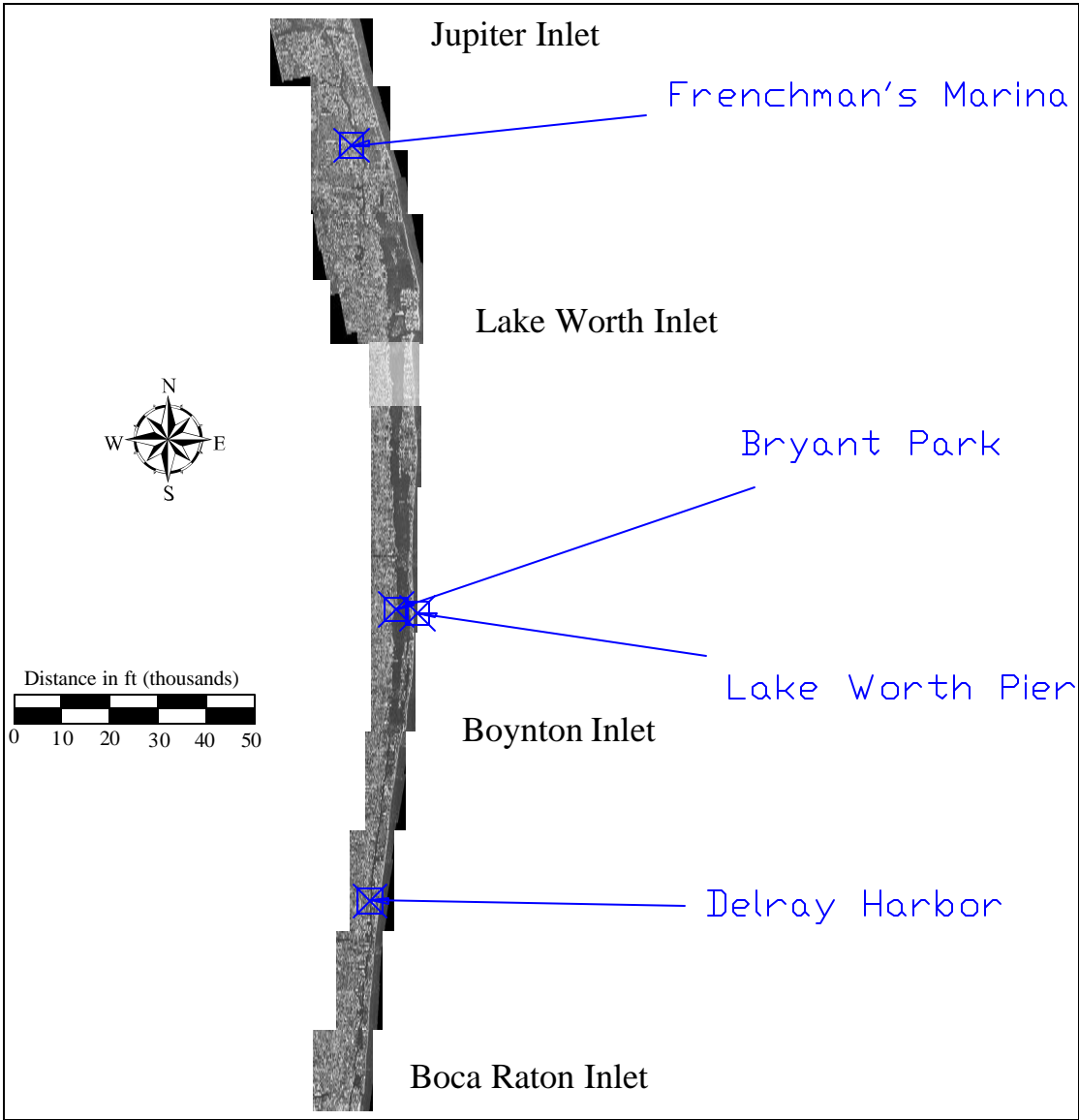


Figure 2.1 Tide Gage Locations

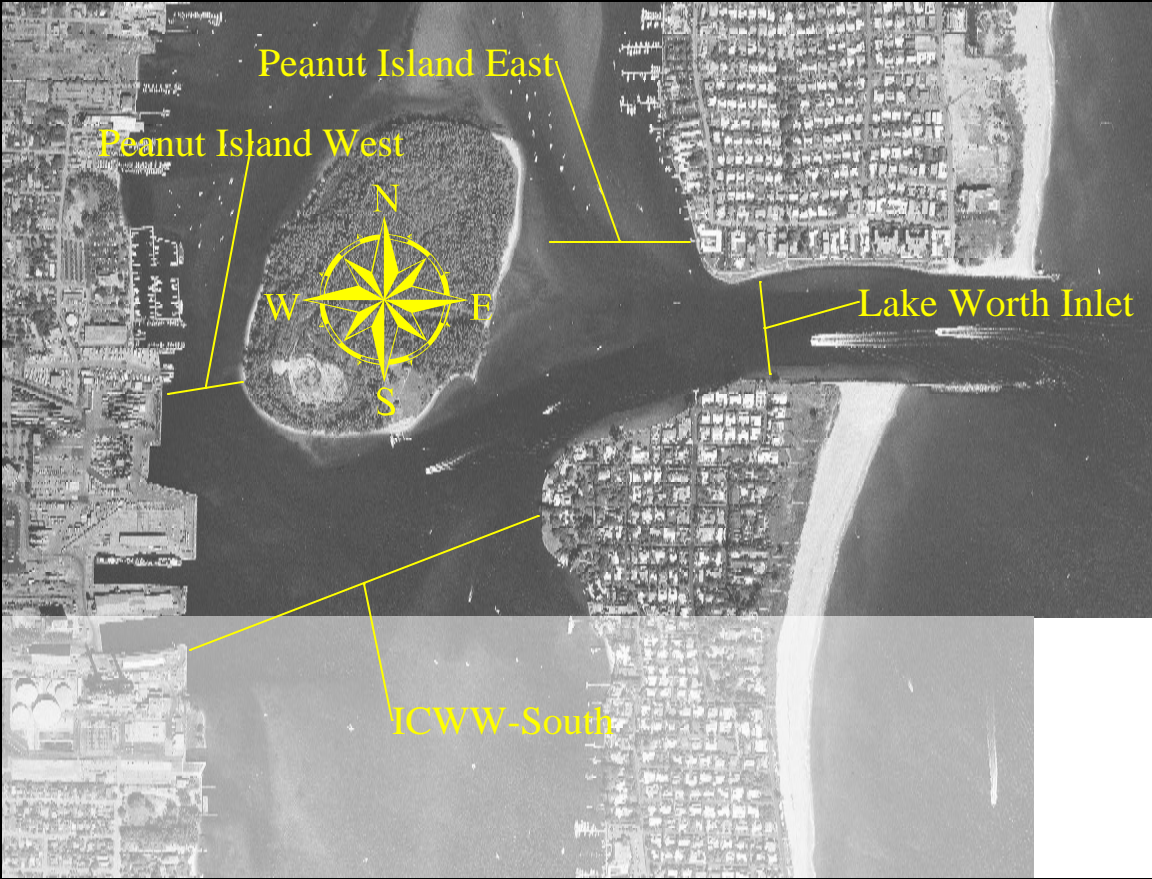


Figure 2.2 Cross Section Locations for Flow Measurement

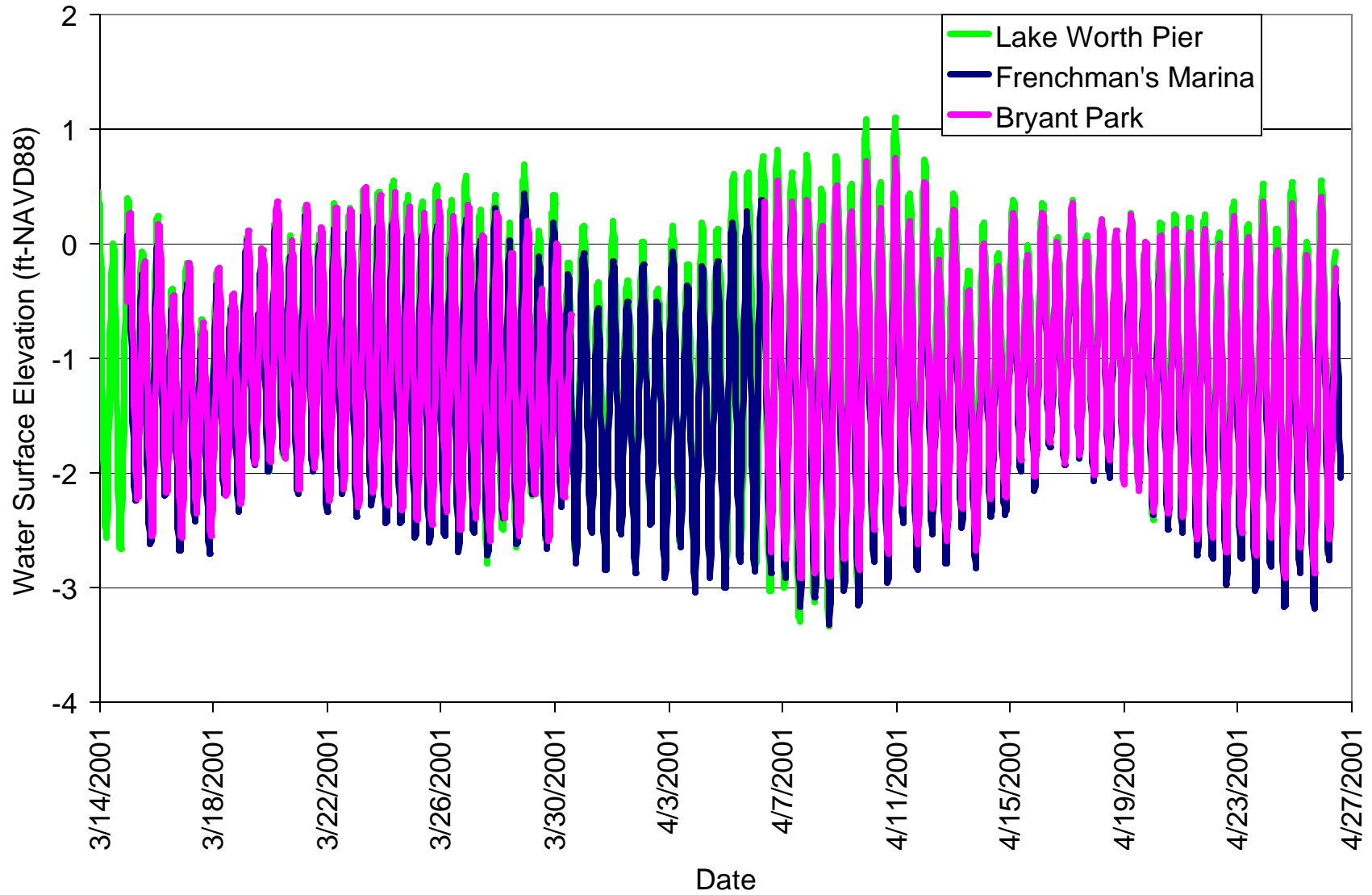


Figure 2.3 Measured Tidal Elevations

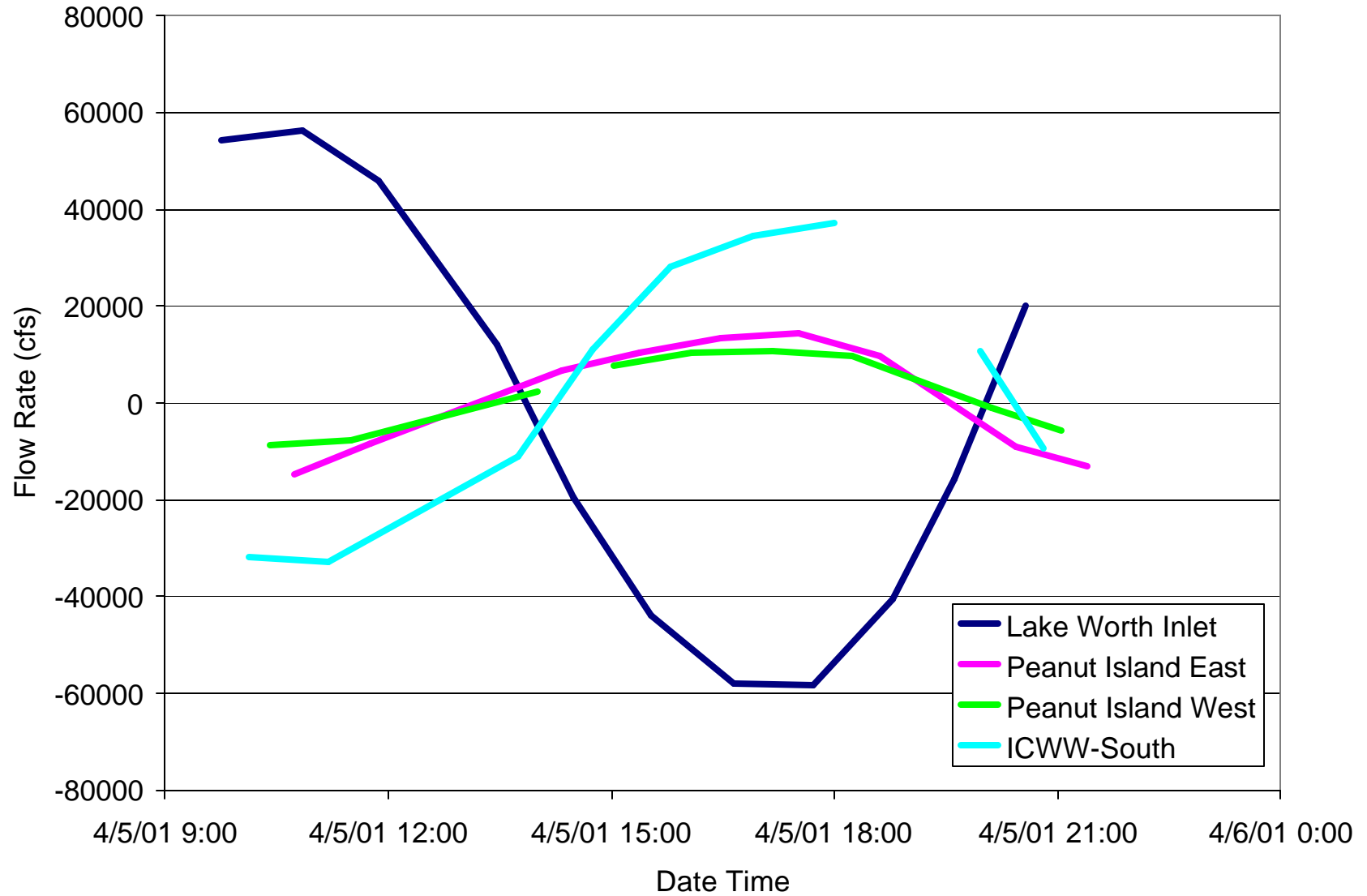


Figure 2.4 Measured Flow Rates

2.4 Hurricane storm surge hydrographs

Modeling the storm surge propagation through the ICWW requires knowledge of the offshore water surface elevation hydrograph associated with the passage of the design hurricane events. Several agencies have developed estimates of storm surge hydrographs and peak elevations both statewide and nationally. These agencies include NOAA, the Florida Department of Environmental Protection (FDEP), the Federal Emergency Management Agency (FEMA), and the Federal Highway Administration (FHWA, Pooled Fund Study). For this study, consensus opinion among the study participants held that the FDEP provided the most appropriate estimates for both storm surge peak elevations and storm surge hydrographs. In support of its Florida Coastal Construction Control Line (CCCL) program, the FDEP funded a study to determine the combined total tides including storm surges, astronomical tide and dynamic wave set-up for most of Florida's coastal counties. The objective of the study was to develop, through numerical modeling, valid estimates of the combined total storm tides for return periods of 5, 10, 20, 50, 100, 200 and 500 years. Output of the numerical modeling included the storm surge hydrograph that produced the 100-year elevation as well as the peak elevation for each of the return periods. The study reported results for three to four locations (profiles) for counties covered by the study.

The Lake Worth Inlet model spans the length of Palm Beach County. This range covers 4 FDEP profiles listed in reference Dean, et al. (1992). The offshore boundary condition for the Lake Worth model will include only one time series per storm surge event applied uniformly across the entire offshore boundary. As a conservative estimate, the hydrograph from the FDEP study profile on either side of the subject inlet that produced the highest elevation served as the boundary condition for the 100-year return period event. For the Lake Worth Inlet model, this hydrograph fell along Palm Beach County Profile Two (Figure 2.5). Developing the 50- and 500-year hydrographs required subtracting the astronomical tide from the 100-year hydrograph to obtain the storm surge signal. Next, the signal was scaled such that, when added back to the astronomical tide, the peak equaled the 50- and 500-year FDEP peak estimates. Again, for this study, the elevation of the peak for the 50- and 500-year events equaled the largest elevation from the profiles found on either side of the inlet (Palm Beach County Profile Two). Table 2.2

lists the peak elevations for the 50-, 100-, and 500-year events. Figure 2.6 illustrates the surge hydrographs for the 50-, 100-, and 500-year events.

Table 2.2 Total Storm Surge Elevations for the Lake Worth Inlet Model

Return Period (years)	Combined Total Storm Tide Level Above NAVD88 (ft)
500	13.5
100	10.0
50	8.2

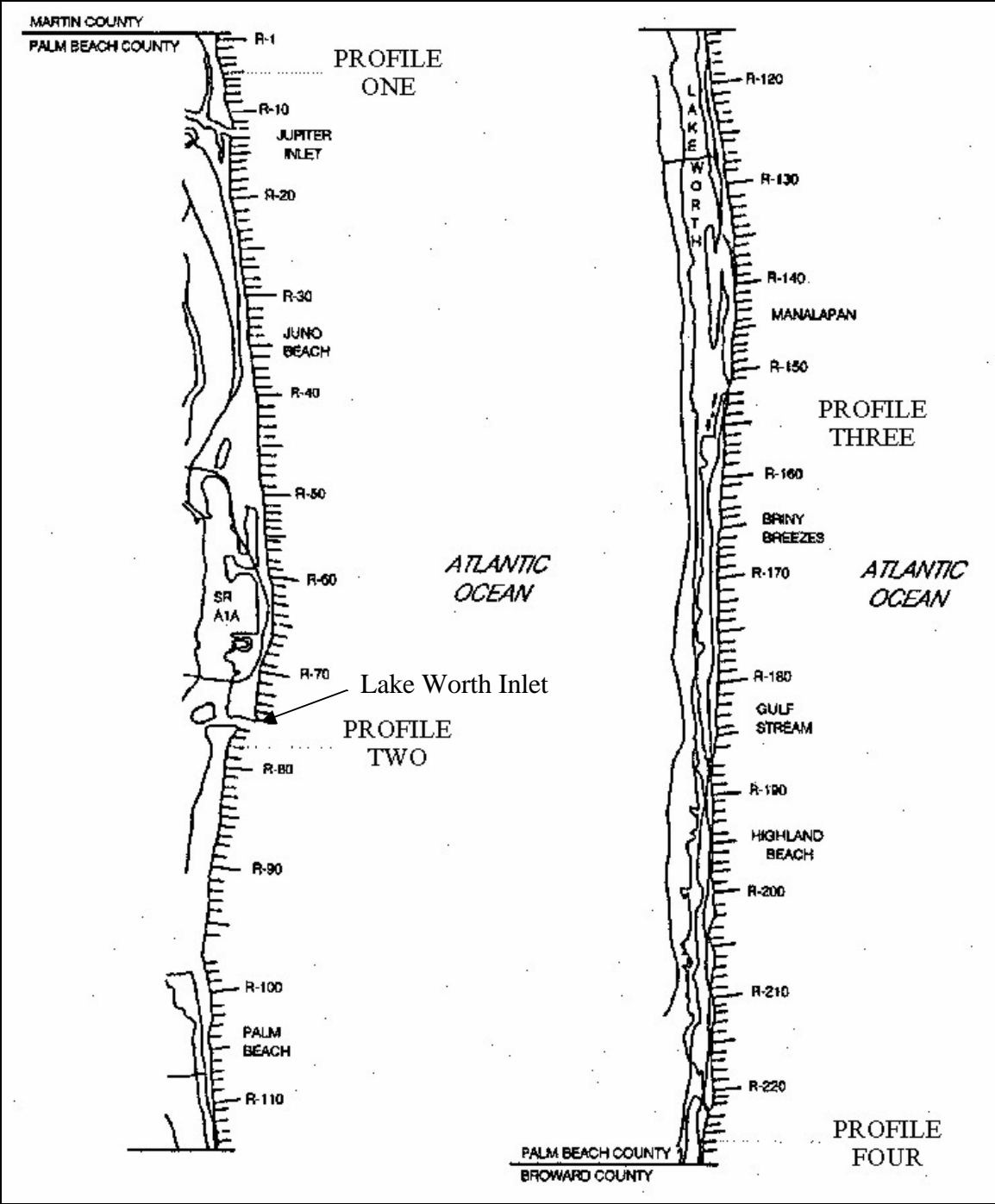


Figure 2.5 Palm Beach County Profiles near Lake Worth Inlet

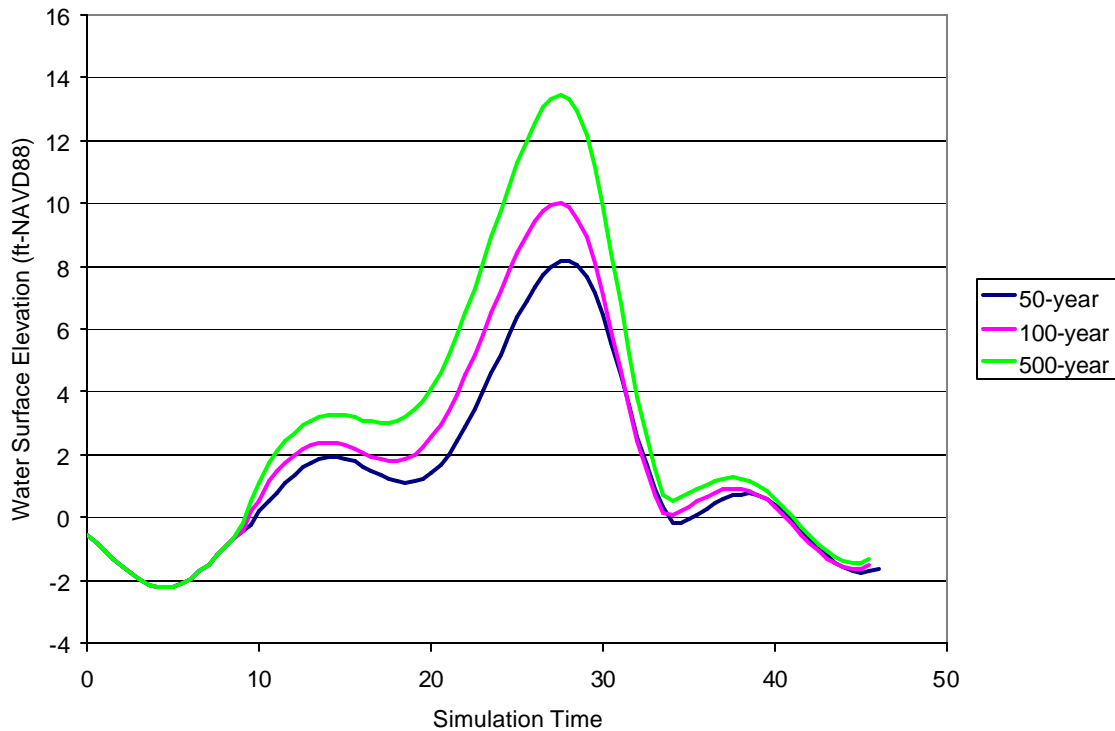


Figure 2.6 Total Combined Storm Surge Hydrographs for the Lake Worth Inlet Model

2.5 Hydrology

Construction of the hydrodynamic models requires knowledge of the upland hydrology for specifying the upland flow boundary conditions for the canals and rivers that terminate in the ICWW. Few methodologies exist for determining rainfall runoff that occurs during hurricane landfall events. The reference U. S. Army Corps of Engineers (1986) lists one such methodology. This procedure requires a priori knowledge of hurricane parameters, such as hurricane speed and storm landfall location. Unfortunately, this investigation does not distinguish the hurricane parameters as a function of return period. This fact makes calculation of the flows associated with the 50-, 100-, and 500-year return periods a daunting task. Additionally, many flow boundaries (canals and rivers) for this model comprise waterways managed by flow control structures. If the South Florida Water Management District (SFWMD) expects hurricane landfall within this domain, standard control structure management policies call for pumping down the water levels to mitigate for possible flooding following the storm. As such, accurate calculation of the storm runoff hydrographs must include detailed modeling that incorporates the SFWMD procedures at the flow control structures. Finally, sensitivity analyses

have demonstrated that specification of upland flow boundary conditions to values representative of rainfall runoff associated with hurricane landfall produce only negligible effects on flow and water surface elevation values at cross sections on the ICWW. Given this fact, the effort of modeling the hydrology associated with these flows far outweighs the almost negligible gain in accuracy. For the scope of this study, this resolution is not warranted.

For the purposes of this study, the model developers selected a 5-year return period flow for the upland boundary conditions applicable for all storm surge cases. Application of these flows at a constant rate during the entire simulation builds a measure of conservatism into this estimate. Flow boundary conditions for the calibration and spring tide simulations equaled a constant, nominal value.

Determination of the of the 5-year return period flow rates requires knowledge of the annual peak flow rates through the subject waterways over a sufficiently long time to develop meaningful statistics. Fortunately, the South Florida Water Management District (SFWMD) and U.S. Geologic Survey (USGS) maintain gages and record flow rates at the majority of the main waterways within the Lake Worth Inlet model. Figure 2.7 through 2.11 show the gage stations for determining flow rate information. For the Lake Worth Inlet models, six gages provide information to determine the 5-year flow rates for the interior boundary conditions. Table 2.3 summarizes this information.

Data reduction began with compilation of the peak annual flow rate over the years of available data. Next, the USGS freeware program PEAKFQ ranked the annual peaks and assigned the data Weibull plotting positions. The program then fits the data to a log-Pearson Type III distribution function according to the procedure recommended in Interagency Advisory Committee on Water Data (1982). Figure 2.12 through 2.17 show the peak annual flow rates as well as the Bulletin 17B estimate for each of the gages.

Table 2.3 Flow Gage Summary

Gage Identifier (Structure)	Agency	Waterway	Latitude	Longitude	Years of Available Data	5-year Return Period Flow (cfs)
S-40	SFWMD	C-15 Canal	26.419° N	80.074° W	1984-2002	2,280
S-41	SFWMD	C-16 Canal (Boynton Canal)	26.539° N	80.053° W	1941-1943 1983-2002	2,768
S-155	USGS	C-51 Canal (West Palm Beach Canal)	26.645° N	80.055° W	1939-2002	4,173
S-44	SFWMD	C-17 Canal / Earman River	26.817° N	80.082° W	1977-2002	1,116
S-46	SFWMD	C-18 Canal	26.934° N	80.142° W	1959-1965 1979-2002	1,898
LOX 8	USGS	Loxahatchee River	26.954° N	80.165° W	1972-1999	789

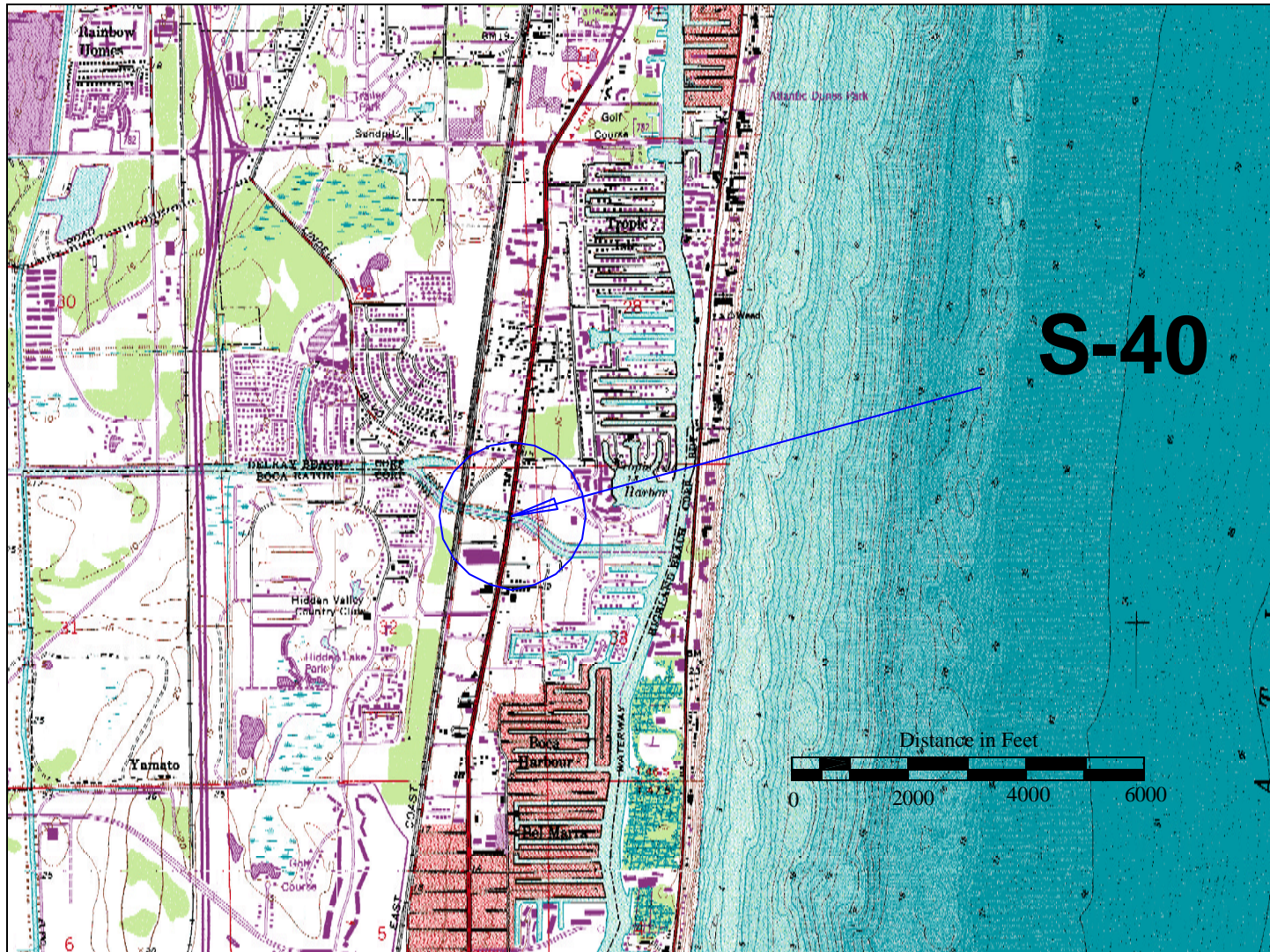


Figure 2.7 Location Map for SFWMD Structure S-40

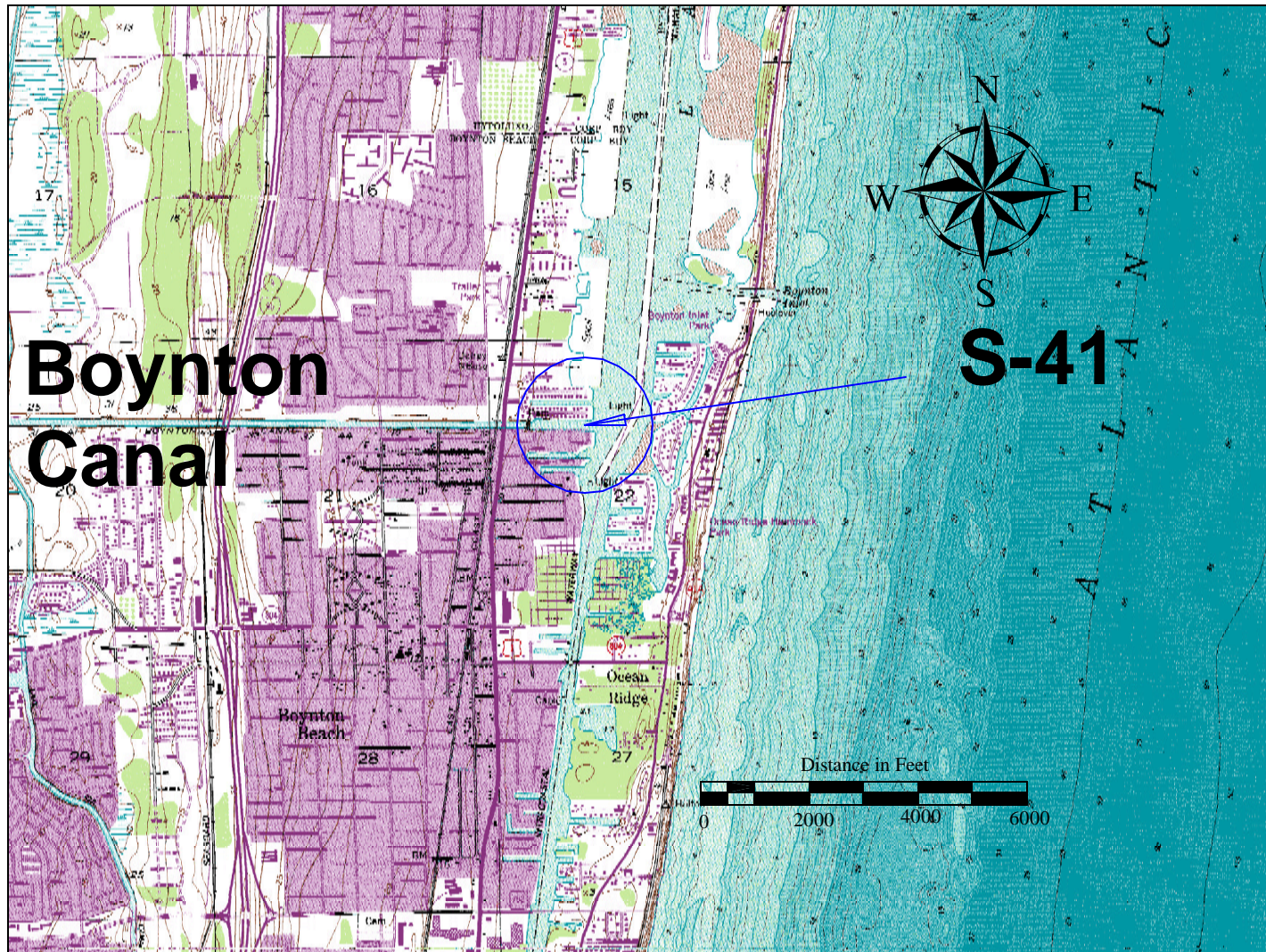


Figure 2.8 Location Map for SFWMD Structure S-41

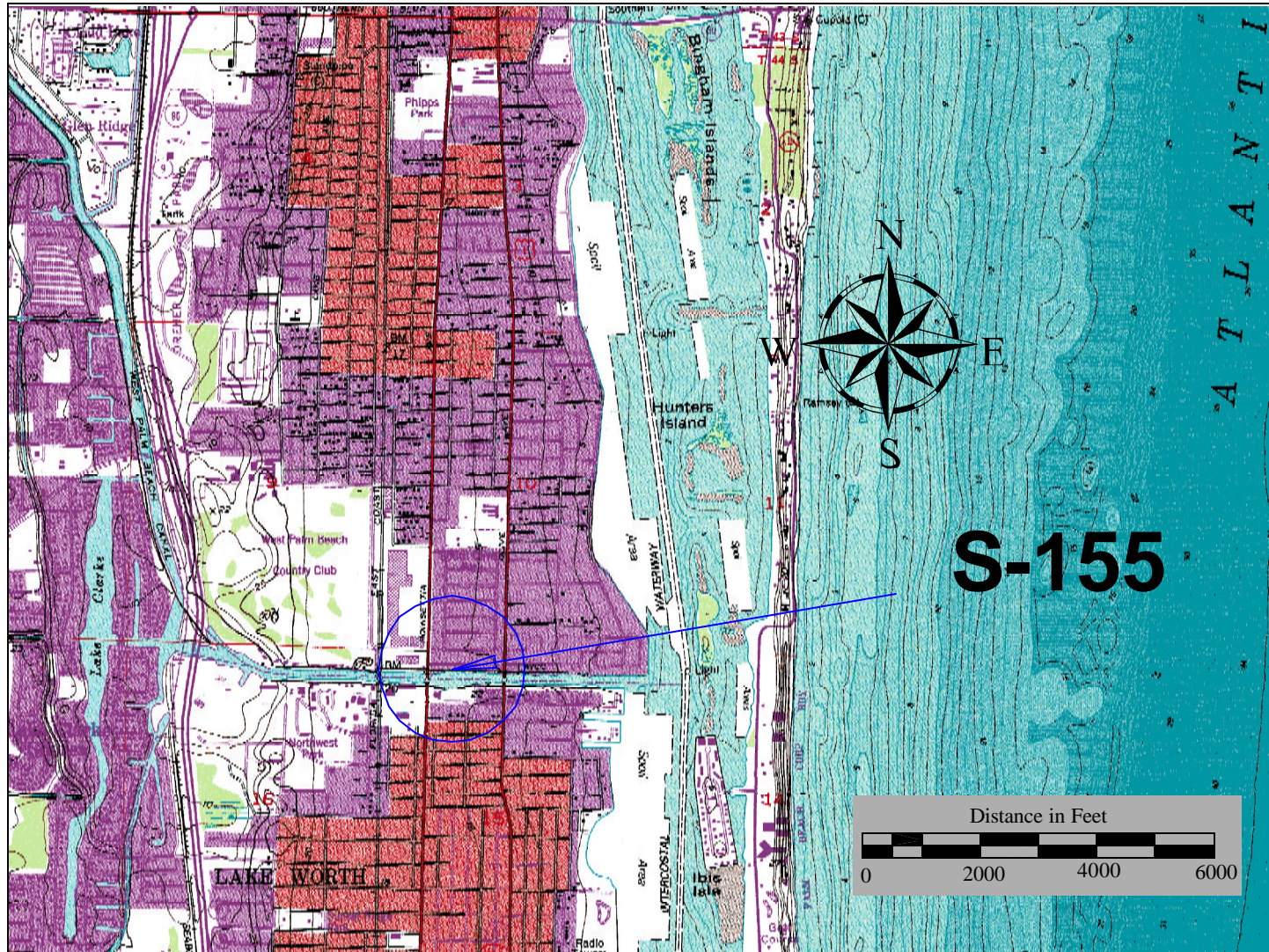


Figure 2.9 Location Map for SFWMD Structure S-155

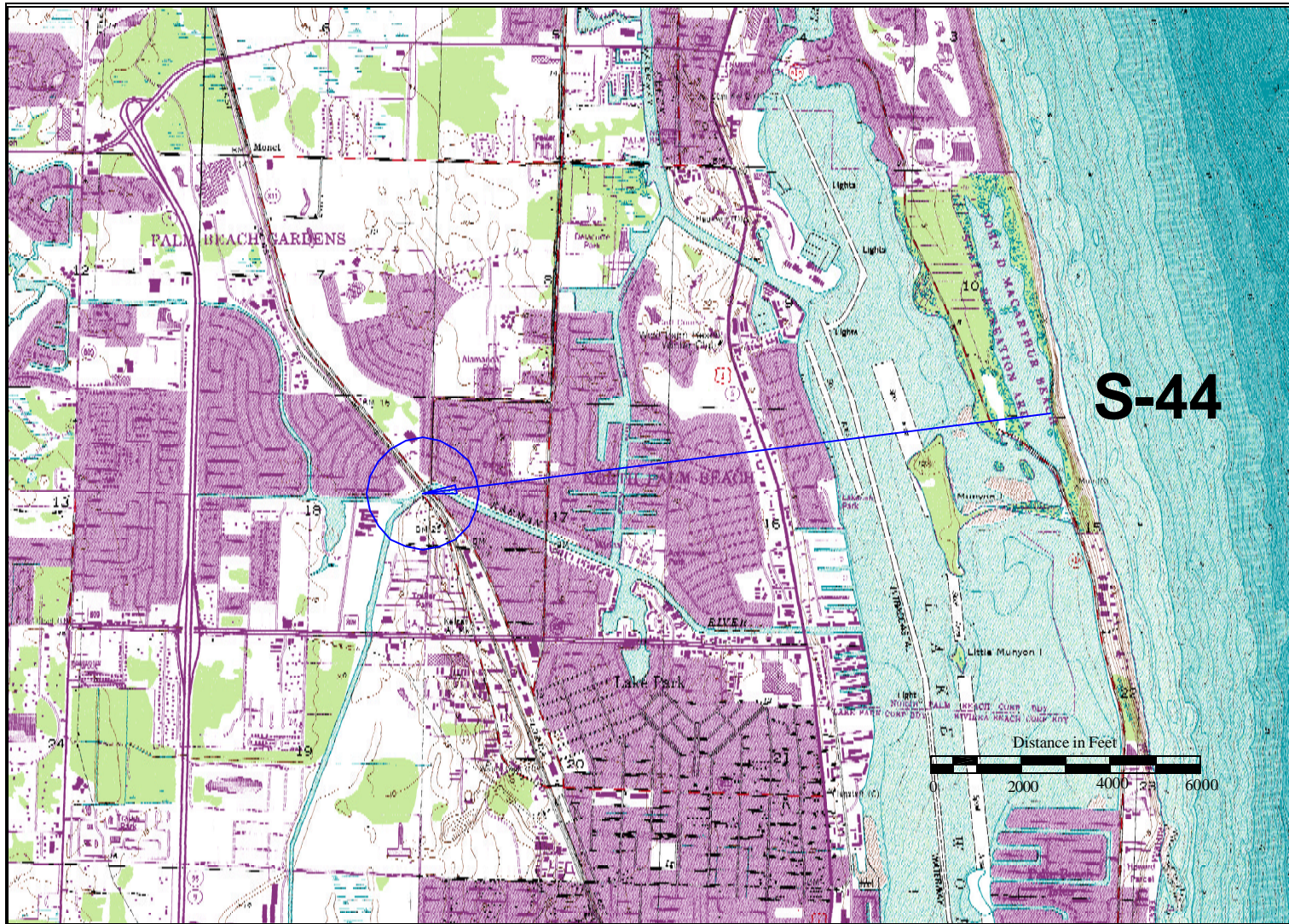


Figure 2.10 Location Map for SFWMD Structure S-44

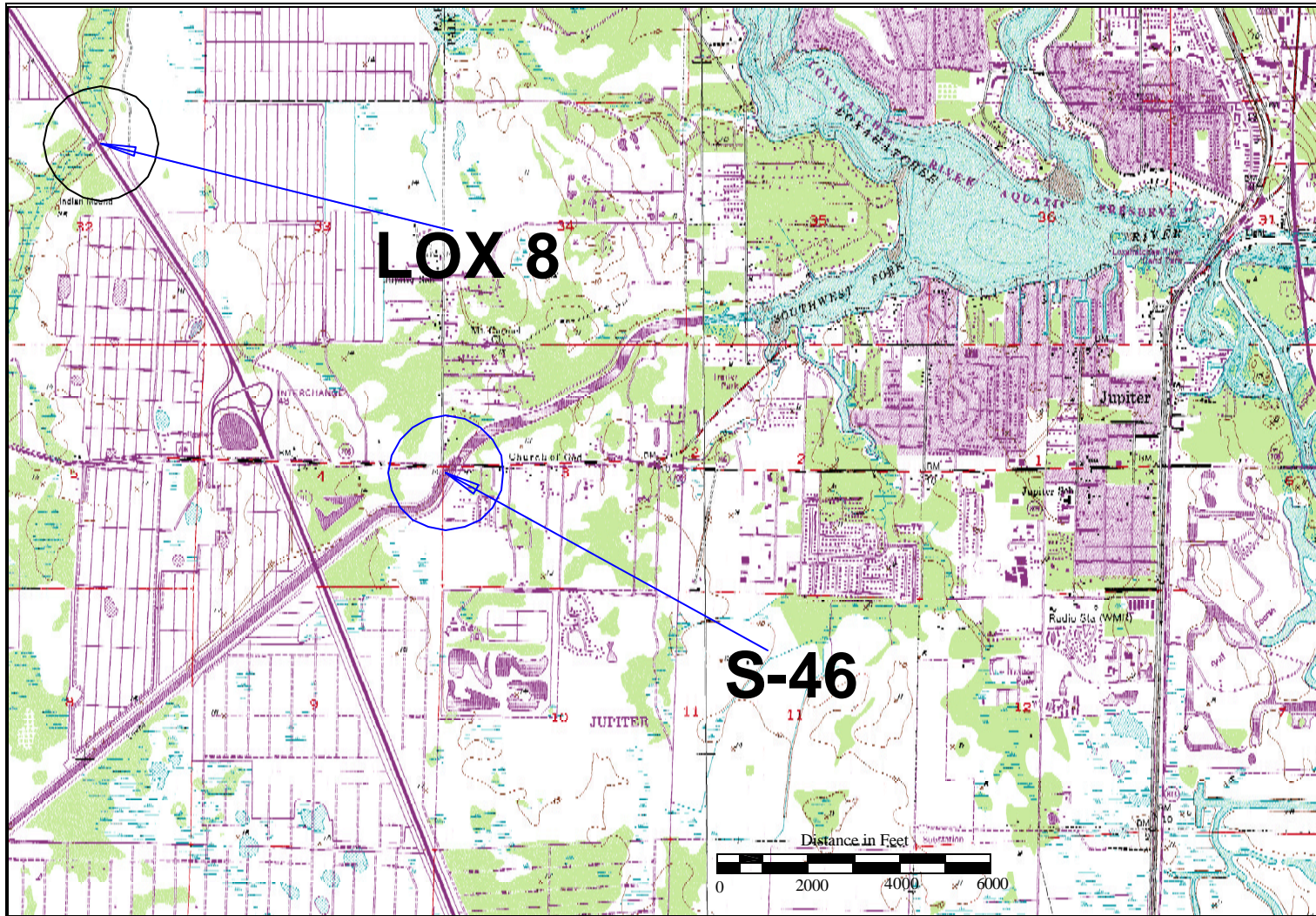


Figure 2.11 Location Map for SFWMD Structure S-46 and USGS Gage LOX 8

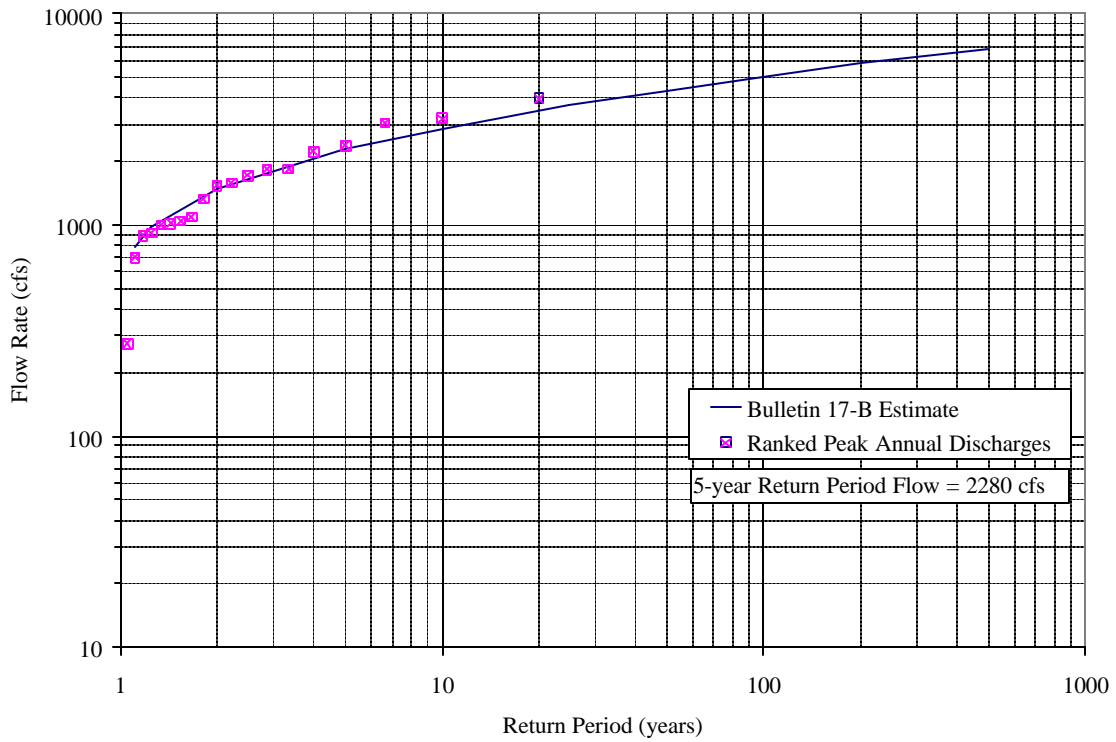


Figure 2.12 Flow Rates and Bulletin 17B Estimate at Structure S-40

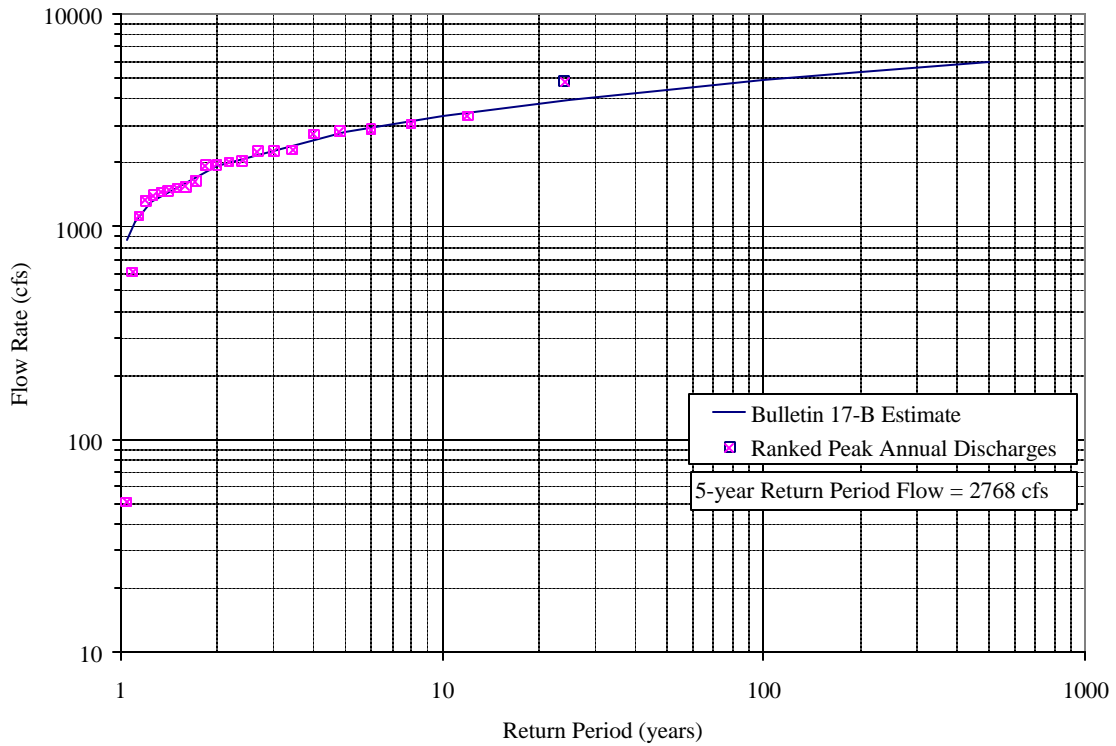


Figure 2.13 Flow Rates and Bulletin 17B Estimate at Structure S-41

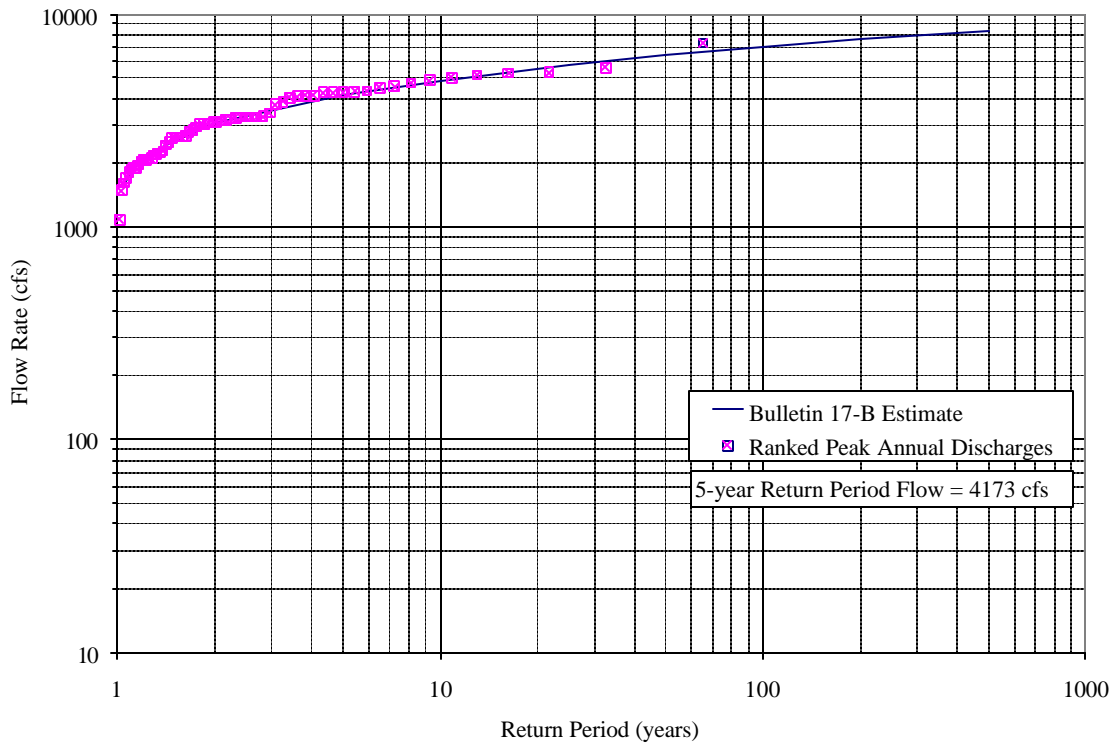


Figure 2.14 Flow Rates and Bulletin 17B Estimate at Structure S-155

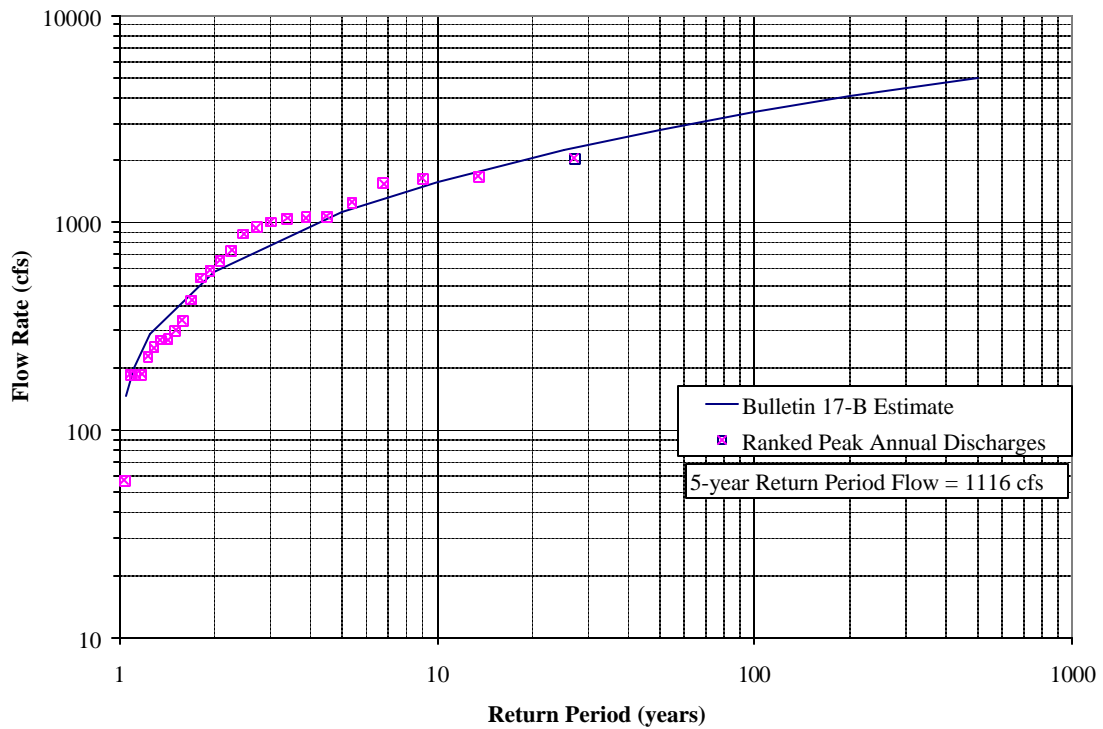


Figure 2.15 Flow Rates and Bulletin 17B Estimate at Structure S-44

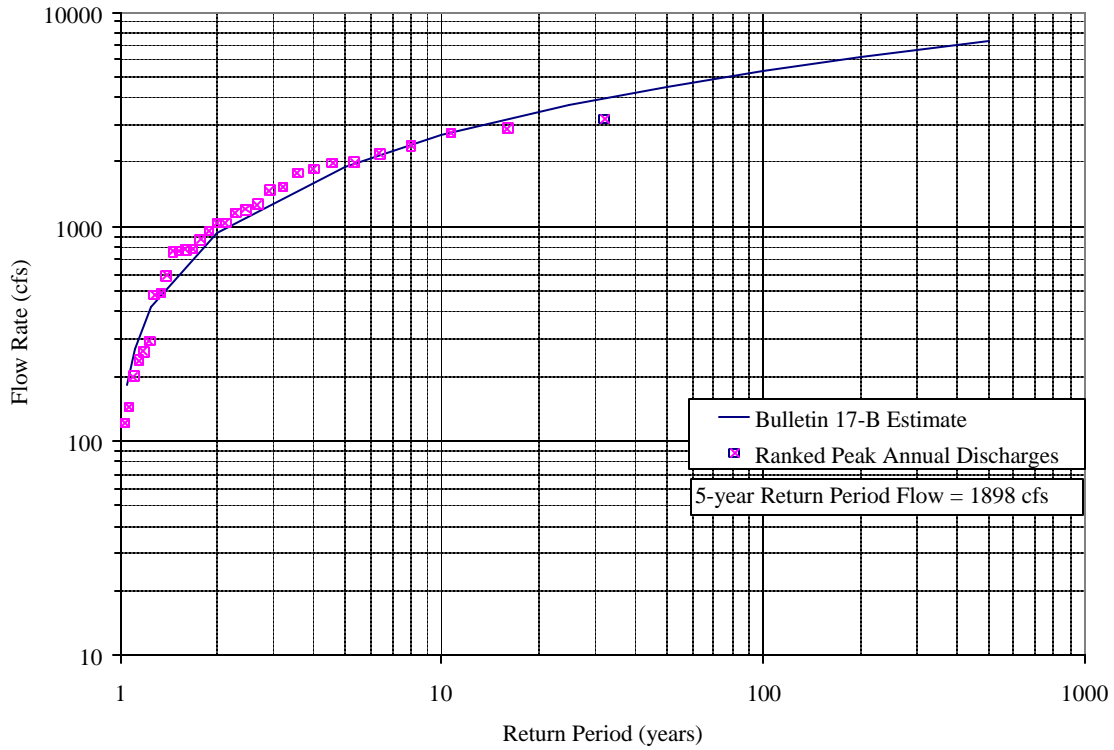


Figure 2.16 Flow Rates and Bulletin 17B Estimate at Structure S-46

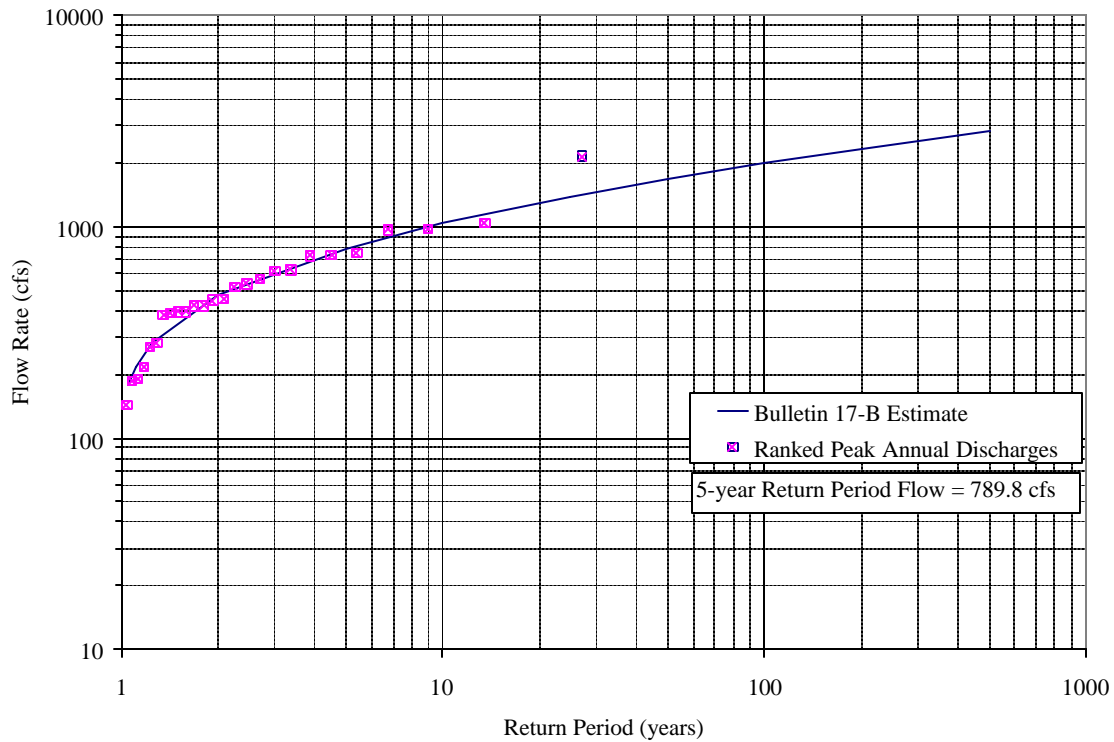


Figure 2.17 Flow Rates and Bulletin 17B Estimate at USGS Gage LOX 8

3.0 HYDRODYNAMIC SIMULATIONS

According to FHWA and FDOT guidelines, scour computation requires knowledge of specific hydraulic parameters. Determining these parameters requires a detailed hydraulic analysis of the study area. The complexity of flow conditions through multiple inlet systems typically found along Florida's coasts dictates employing two-dimensional modeling to discern design flows. These conditions typically result from two major factors. The first is the propagation of a hurricane surge into the study area. At the bridge locations along interior waterways, the magnitude of flow generated by an extreme hurricane surge certainly overshadows the flows created by an extreme rainfall event with an equal probability of occurrence. This results from the proximity of these waterways to the ocean. The second, and equally important, factor affecting the complexity of the flow regime is the study areas' physical geography. The proximity of multiple inlets and their interconnectivity influence the flow characteristics at the bridge locations. Additionally, the banks on either side of the interior waterways typically comprise low lying areas that would flood during a storm surge event. The wetting and drying of both the mainland and barrier islands significantly complicate the flows both within the interior waterways and at the bridge locations. These conditions make a single reach, steady-state hydraulic analysis inappropriate. Rather, these conditions dictate time-dependent, two-dimensional hydrodynamic modeling of the multi-inlet system to predict the complex nature of hurricane-generated flows at the bridges. For this study, both the RMA2 and ADCIRC software packages, supported by the U.S. Army Corps of Engineers (USACE), provide the two-dimensional modeling components. This chapter outlines the hydrodynamic modeling effort that determines the design flows for spring tides and the 50-, 100-, and 500-year storm events.

3.1 Model construction

The Lake Worth Inlet meshes (Figures 3.1 and 3.2) describe the specific topographic and bathymetric characteristics of Lake Worth Inlet, Jupiter Inlet, Boynton Inlet, and Boca Raton Inlet as well as the ICWW/Lake Worth, which connects these inlets. Figures 3.3 and 3.4 show the model meshes at Lake Worth Inlet. The mesh boundaries begin offshore approximately one to two miles from the shoreline and extend from north of Jupiter Inlet to south of Boca Raton

Inlet. The mesh extends westward through the four inlets into the interior waters. It follows the ICWW from Hobe Sound south to Boca Raton Inlet. The mesh also includes portions of the rivers and canals that terminate in the ICWW including the C-15 Canal, the C-16 Canal (Boynton Canal), the C-51 Canal (West Palm Beach Canal), the C-17 Canal, the Earman River, the C-18 Canal, and the Loxahatchee River. The westward extent of the model extends 2 to 3 mi landward of the Atlantic Ocean to approximately the Florida East Coast Railroad. Vertically, the mesh extends approximately to the +15-ft-NAVD contour. The RMA2 solution domain contains 32,252 triangular and quadrilateral elements with nodes at the corners and midpoints of the segments (95,715 nodes). In all, the elements cover 140 mi². The largest element covers 266 acres and the smallest covers 69 ft². This translates to a largest area to smallest area ratio of approximately 168,000:1. The ADCIRC solution domain contains 70,123 triangular elements with nodes at the corners of the segments (35,591 nodes). In all, the elements cover 130 mi². The largest element covers 12 acres and the smallest covers 352 ft². This translates to a largest area to smallest area ratio of approximately 1,500:1.

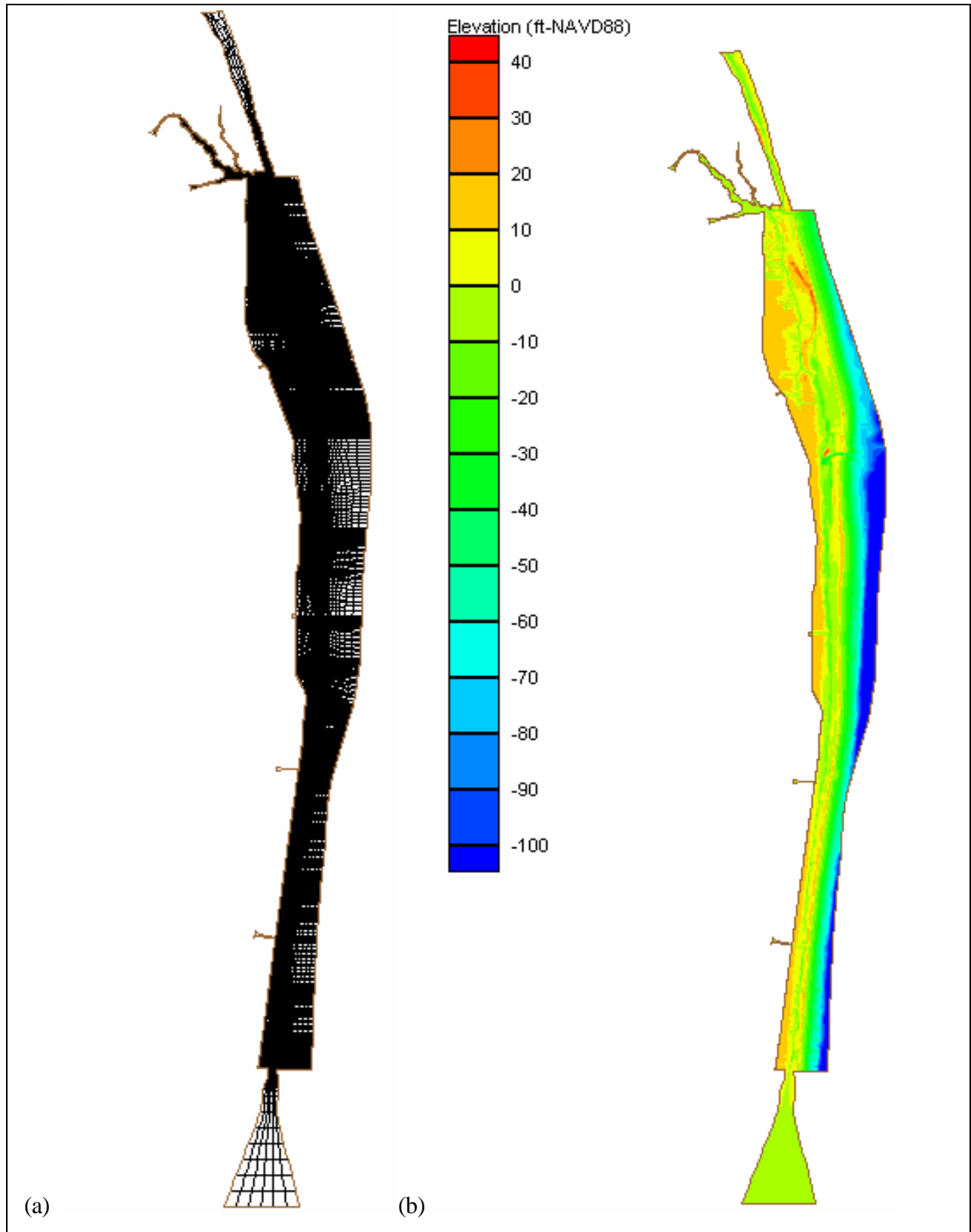


Figure 3.1 Lake Worth Inlet Model RMA2 Mesh (a) Elements and (b) Elevations

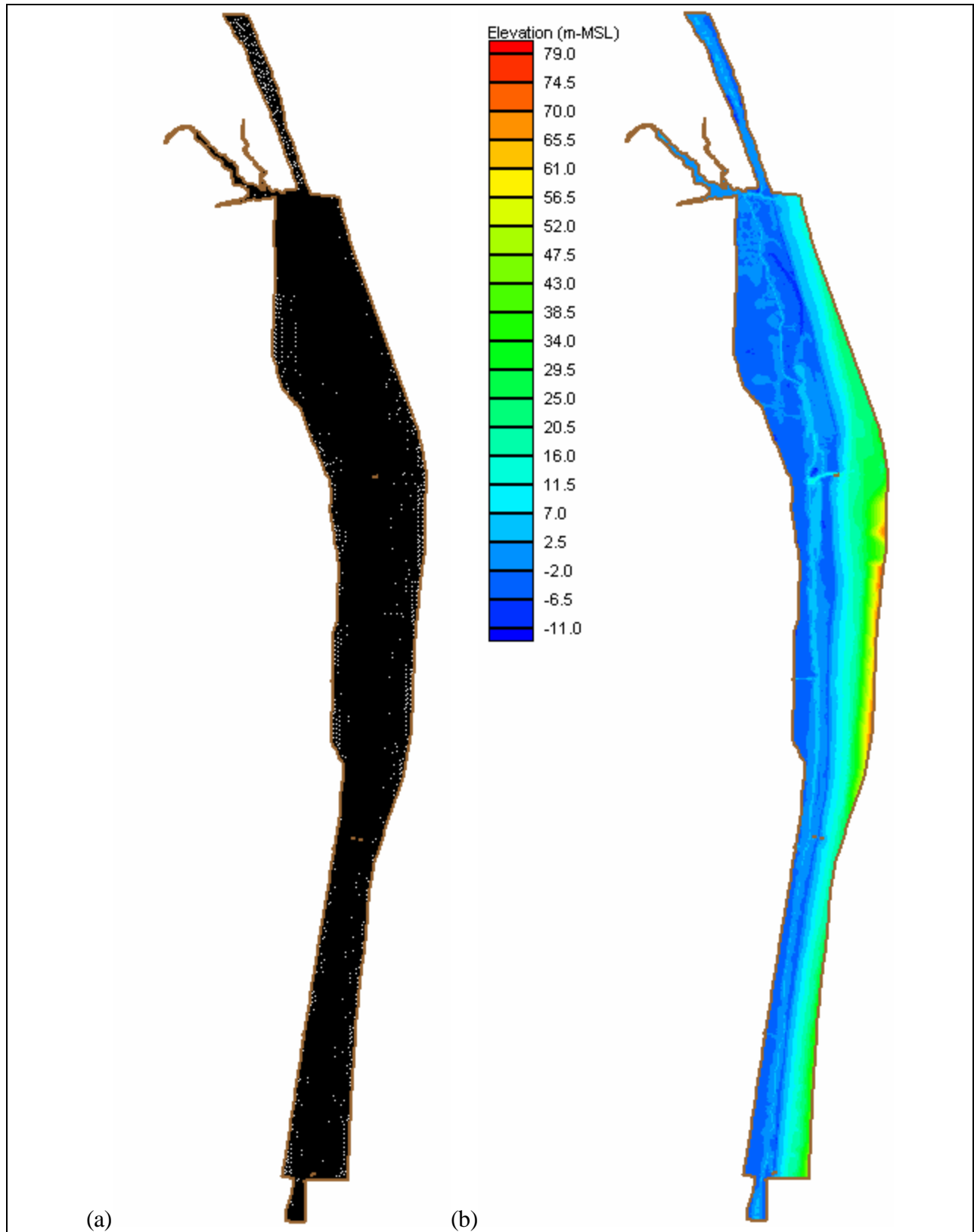


Figure 3.2 Lake Worth Inlet Model ADCIRC Mesh (a) Elements and (b) Elevations

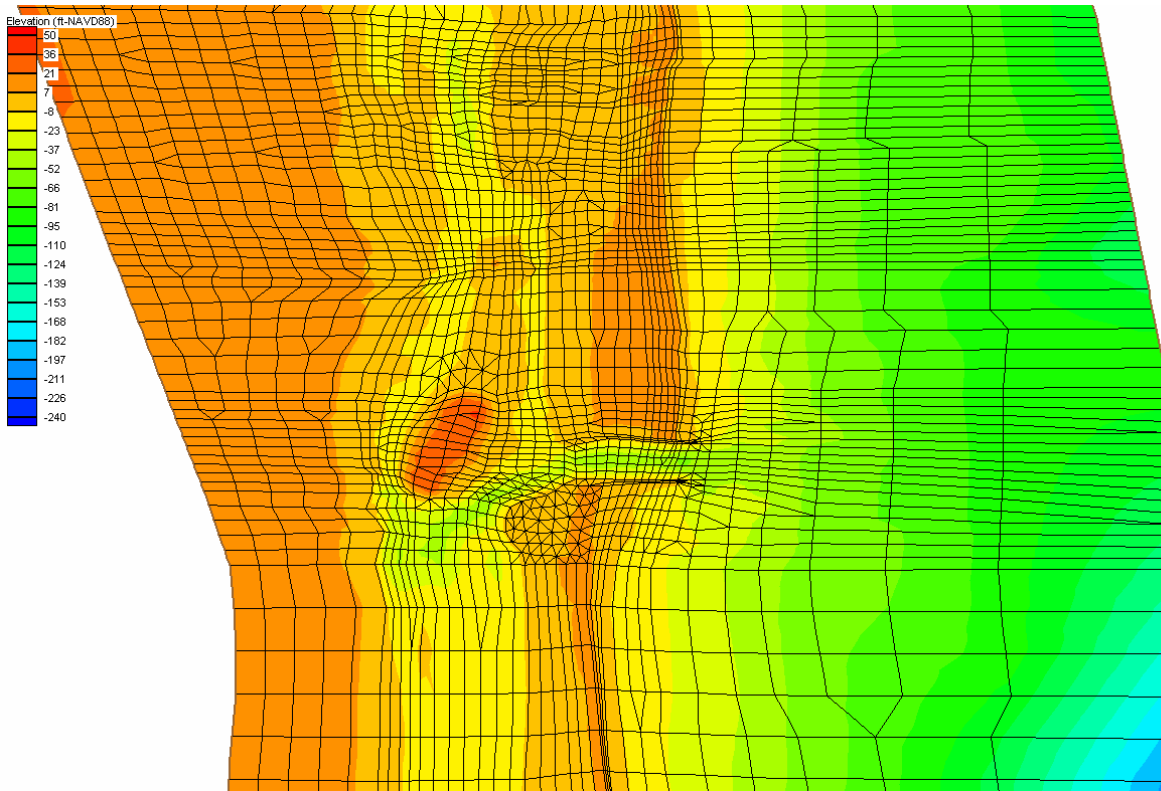


Figure 3.3 RMA2 Model Mesh at Lake Worth Inlet

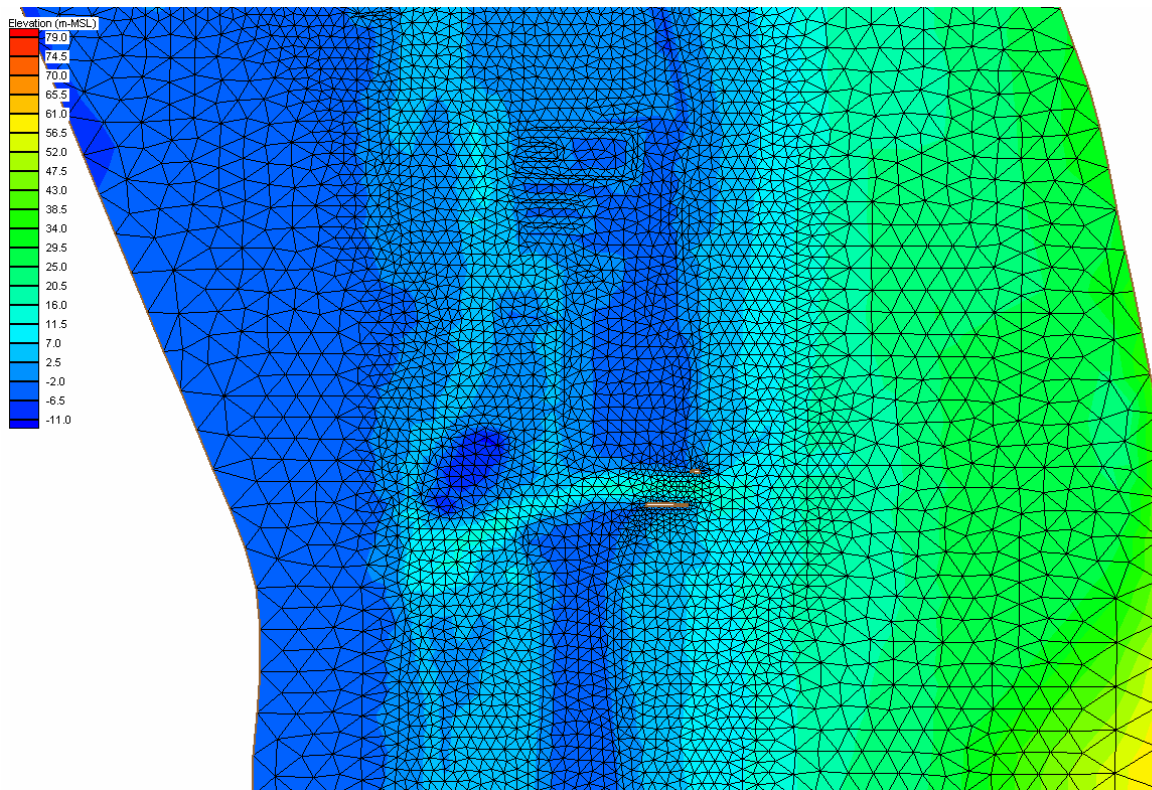


Figure 3.4 ADCIRC Model Mesh at Lake Worth Inlet

Multiple sources provided the data for constructing the meshes. These sources included aerial photography, topography obtained through stereoscopic photogrammetry, surveyed bathymetry and topography, and 5-ft contours from USGS quadrangle maps. The mesh construction procedure began with importing the aerial photography and Digital Terrain Model (DTM) contours into SMS. The aerials provide basemap information for delineating waterways and land areas. The DTM contours, imported as AutoCAD dxf files, provide information on the topographic layout. Given this information, the mesh developer can align elements along topographic contours to enable smooth wetting and drying of the land elements. From this information, the mesh developer constructed the mesh layout, which includes the location, size, and resolution of the triangular and quadrilateral elements that comprise the mesh.

The next step in mesh creation involved specifying the elevation of each node, located at the corners (RMA2 and ADCIRC) and midpoints (RMA2 only) of each element, in the meshes. This required importing all elevation data — the photogrammetric and surveyed data and digitized USGS quadrangle maps — into SMS. SMS represented this data as scatter points with associated scalar elevation values. Then, the program interpolated the elevations onto the mesh via a linear interpolation scheme.

Following specification of the nodal elevations, the mesh developer specified the material type for each mesh element for the RMA2 mesh. Material type specification includes assigning the friction and eddy viscosity for each element based on the land use or waterway that the element represents. The RMA2 Lake Worth Inlet model specifies eddy viscosity globally and automatically via the Peclet number automatic dynamic assignment. The Peclet number for the entire mesh ranged from 10 to 20. The friction values for the elements varied greatly between land and water body elements. For the ADCIRC model, friction specification was performed on a node-by-node basis. The lateral eddy viscosity coefficient (ESL) was specified globally and was set to values ranging from 2.5 to 5.0.

The final step in mesh creation involved specifying the location of the boundary conditions. Both RMA2 and ADCIRC allow specification of flow and water surface elevation boundary conditions along element edges (mesh boundaries). The Lake Worth Inlet model

contains a specified water surface elevation boundary condition along the eastern side of the model mesh (Atlantic Ocean). This boundary condition represents the water surface elevation as a function of time applied uniformly along the boundary. The time series data will vary depending on the simulated event — spring tide, 50-, 100-, or 500-year return period storm surge. Section 4.4 contains plots of the applied boundary condition for each of the simulations. The flow boundary conditions for the storm surge simulations included the 5-year return period flow rates at the C-15 Canal, C-16 Canal (Boynton Canal), C-51 Canal (West Palm Beach Canal), C-17 Canal / Earman River, C-18 Canal, and Loxahatchee River. Figure 3.5 through 3.10 illustrate the locations of these boundary conditions. For the calibration and spring tide simulations, the flow rates at these locations equaled a negligible (approximately 0 cfs) value. The sensitivity analyses show that setting these flow rates to a representative mean value had only negligible effects on flow rate and water surface elevation calibration, which justifies this choice.

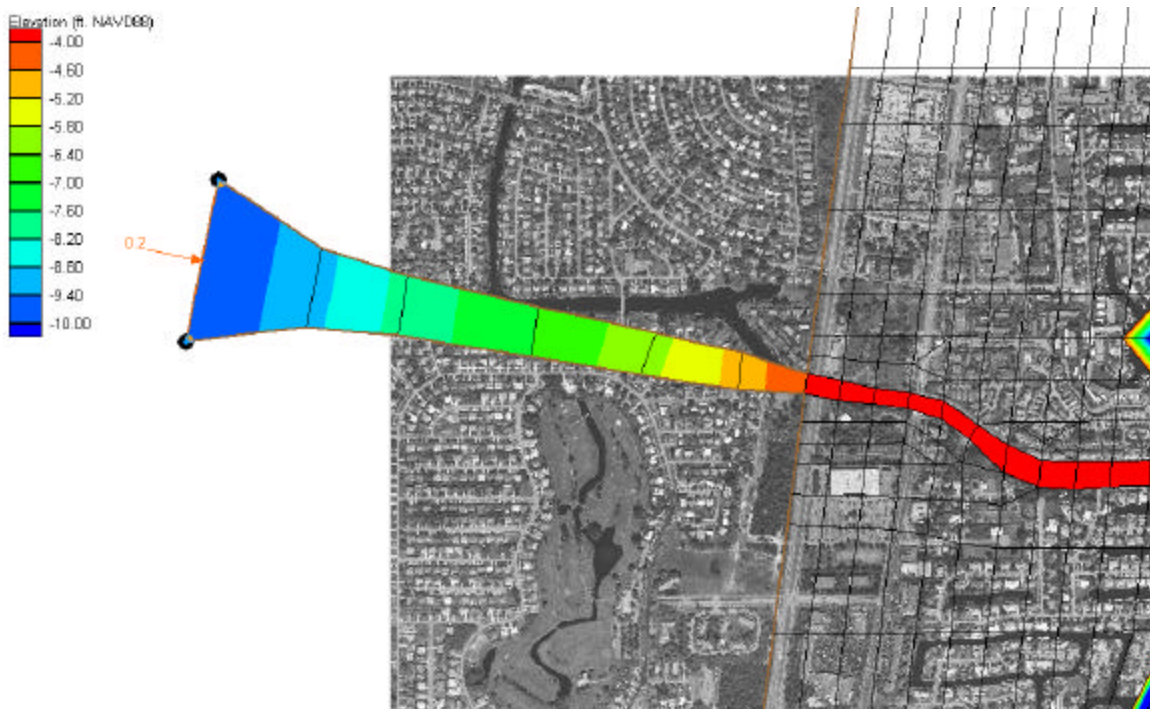


Figure 3.5 Flow Boundary Condition at the C-15 Canal

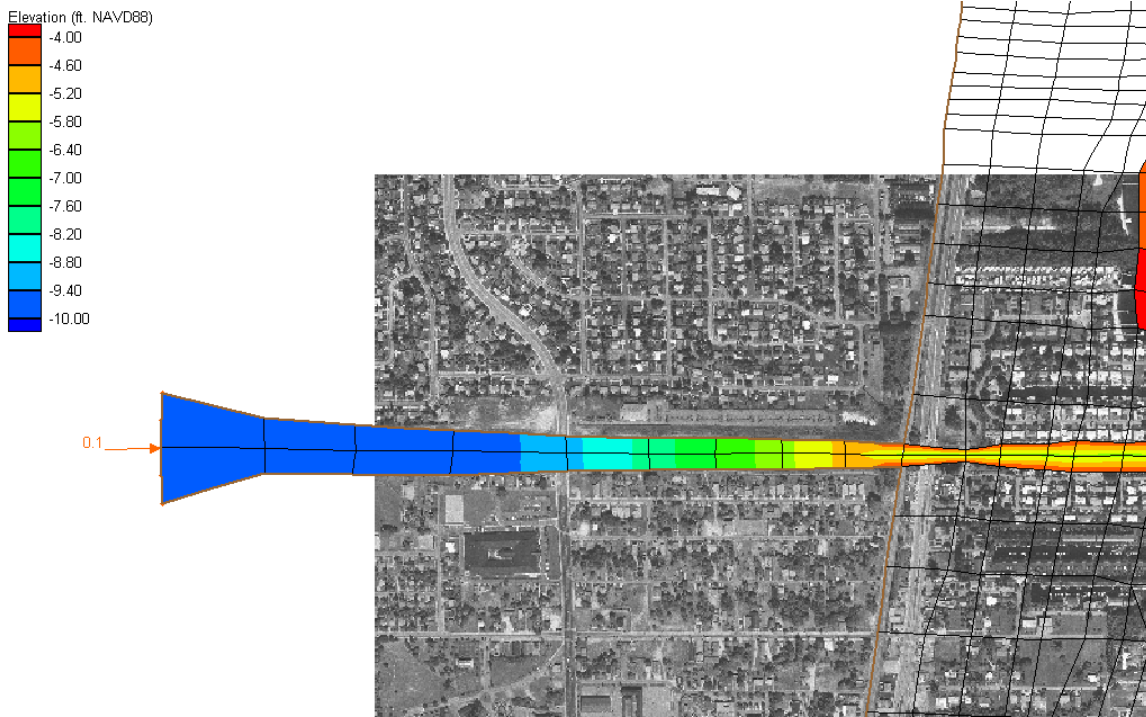


Figure 3.6 Flow Boundary Condition at the C-16 (Boynton) Canal

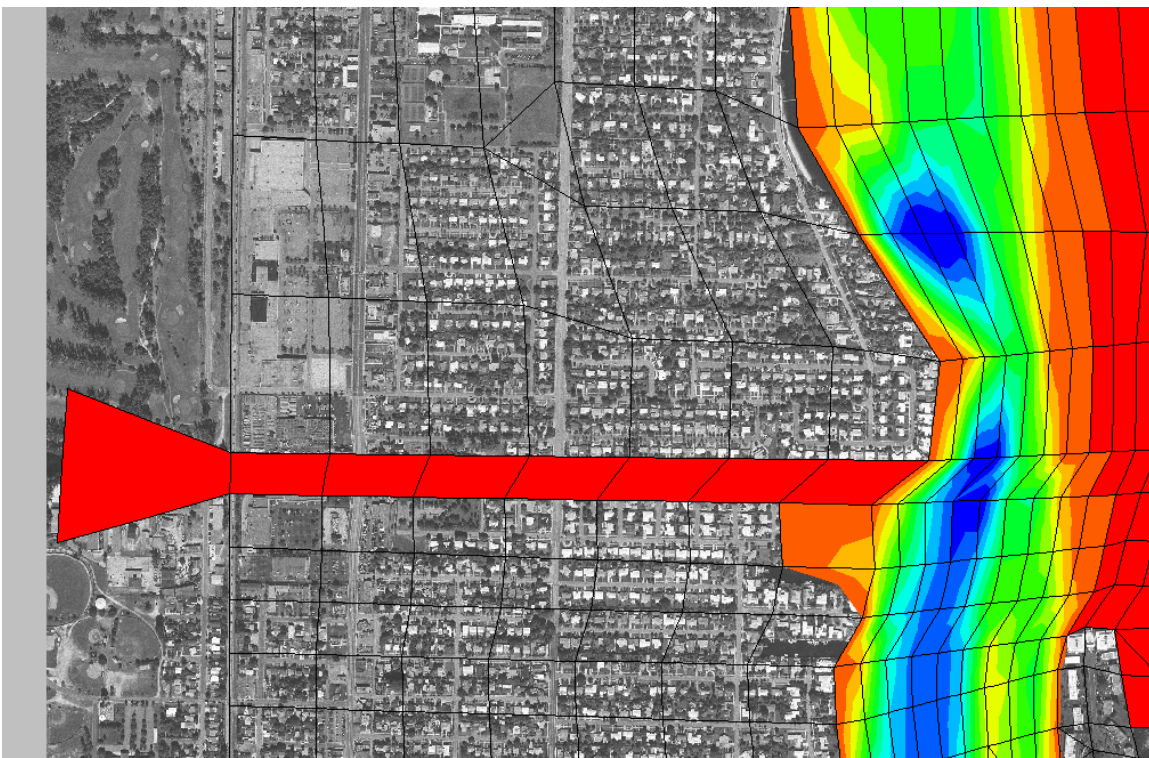


Figure 3.7 Flow Boundary Condition at the C-51 (West Palm Beach) Canal

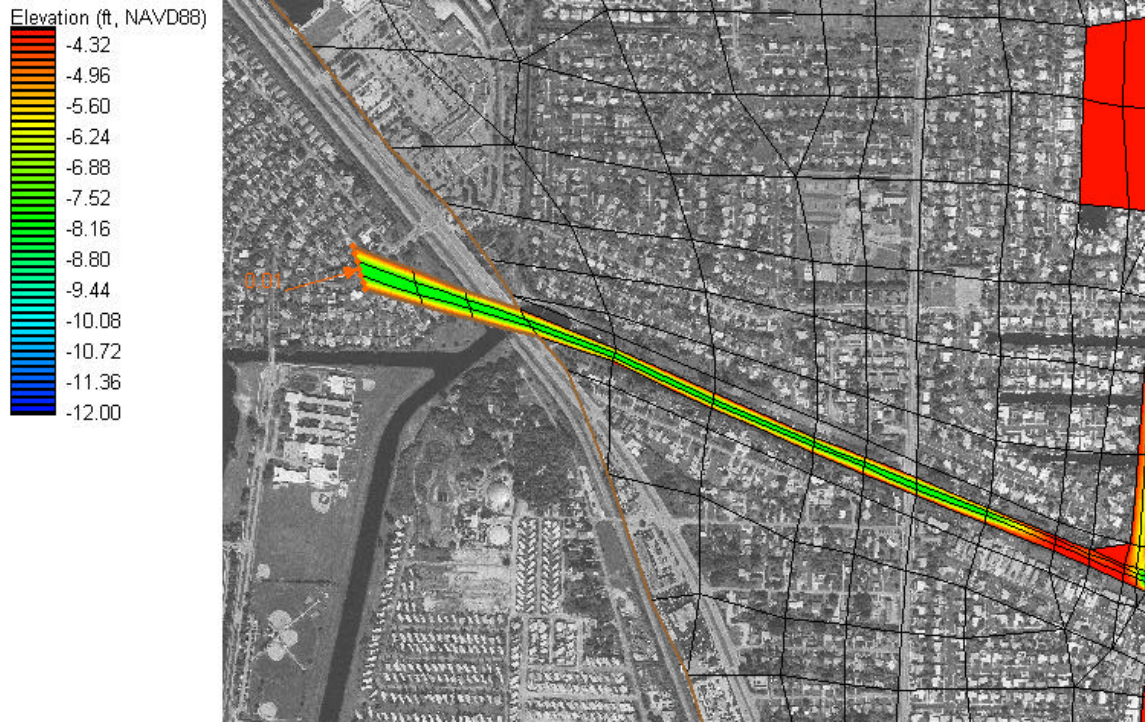


Figure 3.8 Flow Boundary Condition at the C-17 Canal / Earman River

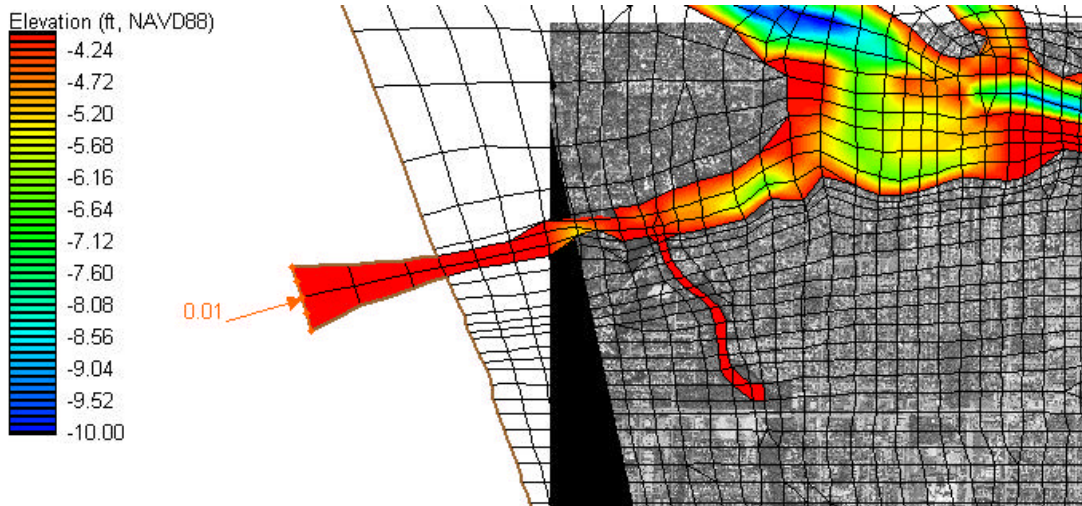


Figure 3.9 Flow Boundary Condition at the C-18 Canal

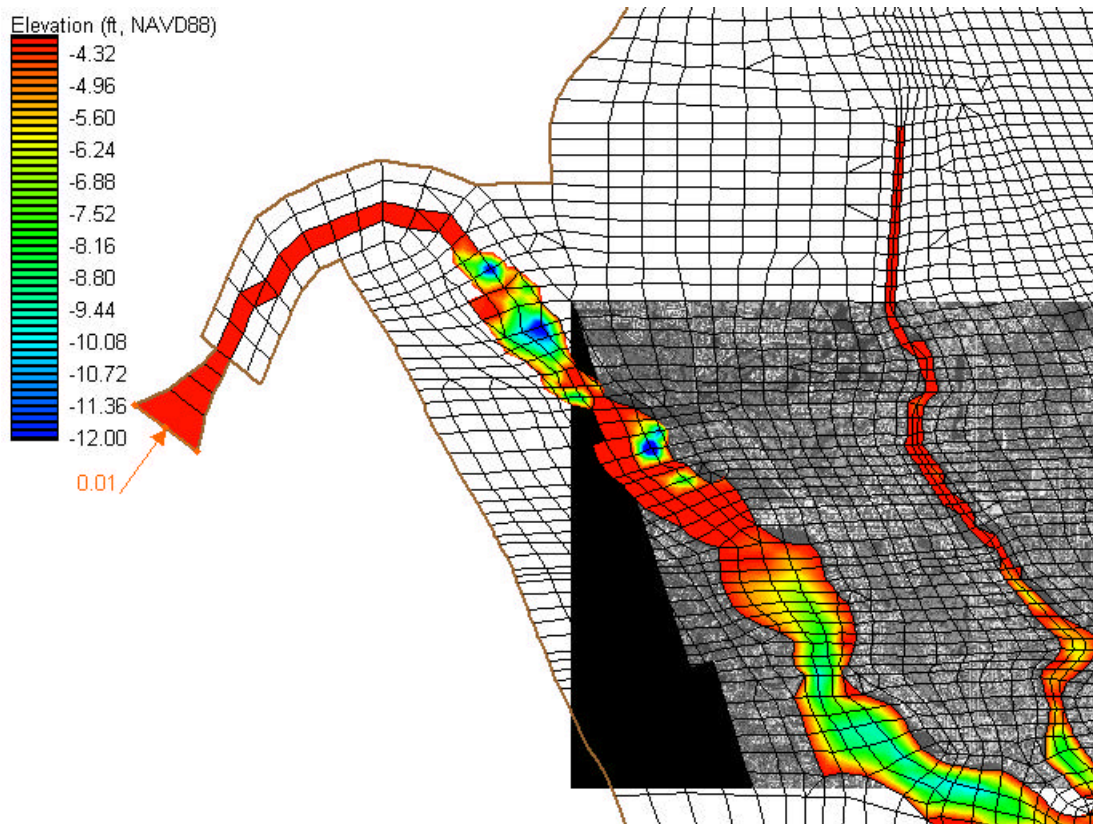


Figure 3.10 Flow Boundary Condition at the Loxahatchee River

3.2 Calibration

A calibrated model ensures an accurate depiction of the hydraulic characteristics in the area of interest. Calibration resulted from iterative adjustments to the model parameters and mesh extents until differences between measured and calculated flow properties became acceptable. Error calculations quantify these results. For this study, error estimation included mean error, root-mean square (rms) error, and percent error.

The following equation provides an estimate of the mean error, E , the average of the deviation of the calculated from the measured values (either water surface elevation or flow rate):

$$E = \frac{\sum_{i=1}^N (c_c - c_m)_i}{N} \quad (3.1)$$

where c_c is the calculated value, c_m is the measured value, and N is the total number of data points. A positive value for the mean error would indicate that the model overestimates the event, while a negative value would indicate the model underestimates the event.

The root-mean square error, E_{rms} , given by the following equation, indicates the absolute error of the comparison. The variables remain the same as indicated above.

$$E_{rms} = \sqrt{\frac{\sum_{i=1}^N (c_c - c_m)_i^2}{N}} \quad (3.2)$$

The final error estimator, E_{pct} , is the percent error. This variable gives an indication of the degree to which the calculated values misrepresent the measured values. Percent error, defined in terms of rms error, is given as

$$E_{pct} = 100 \frac{E_{rms}}{R} \quad (3.3)$$

where R is a representative range of the variable c . For the Lake Worth model, the R -value for the percent error water level calculations equals the total measured range of the tidal signal. This range, rather than the average of the measured tidal ranges (i.e., the average difference between consecutive high and low values over the period of the measurement) is more representative of the tidal signals near Lake Worth Inlet given that they are significantly affected by meteorological forcing. The R -value for the flow rate percent error calculations equals the average of the measured flow ranges (i.e., the average difference between consecutive ebb and flood flow rates over the period of the measurement).

The University of Florida Coastal and Oceanographic Engineering Laboratory, under contract to Kimley-Horn and Associates, Inc., provided the measured data for both the water level and flow rate calibration. The synoptic water surface elevation data, discussed in Chapter 3.0, spans a 4-week period from February 28, 2001 to March 30, 2001 and a 3-week period from

April 6, 2001 to April 26, 2001. For the calibration and spring tide simulation, the measurements obtained during a one month period from March 15, 2001 to April 15, 2001 provided the data for both calibration and specification of the boundary condition. For the Lake Worth Inlet model, two tide gages provide data for water surface elevation calibration: Frenchman's Marina and Bryant Park. The flow rate data, also discussed in Chapter 2.0, includes flow discharges measured at four cross sections on August 5, 2001.

Iterative adjustments of the element/nodal friction — Manning's n value (RMA2) and nodal friction factor (ADCIRC) — produced an average percent error for the water level calibration of the inshore gages of 8.5% for the ADCIRC simulation and 11.6% for the RMA2 simulation. Table 3.1 provides the final assigned Manning's n value by element type for the RMA2 simulation. For the ADCIRC simulation, the waterway nodes and land nodes were assigned friction factor values of 0.0025 and 0.015. Figure 3.11 and 3.12 compare the predicted model water level to the measured water level at the different gage locations. From the figures, the models adequately predicted the tidal fluctuations at these gages. Table 3.2 presents error calculations for the water level calibration. The table shows that the models accurately predicted the gage data and, as such, the models were considered calibrated for water surface elevation. A discussion of the relative performance of each model during calibration is presented in Chapter 4.0.

Table 3.1 Friction Assignment within the RMA2 Lake Worth Inlet Model Mesh

Element Type	Manning's n Value
Waterways (ICWW, Ocean, Inlets)	0.025
Golf Course	0.05
Jetties	0.06
Light Undeveloped	0.3
Dense Residential	0.4
Heavy Industry	0.4
Beach	0.025
Dredge Spoils and Shoaled Areas	0.03
Light Industry	0.15
Woods	0.2

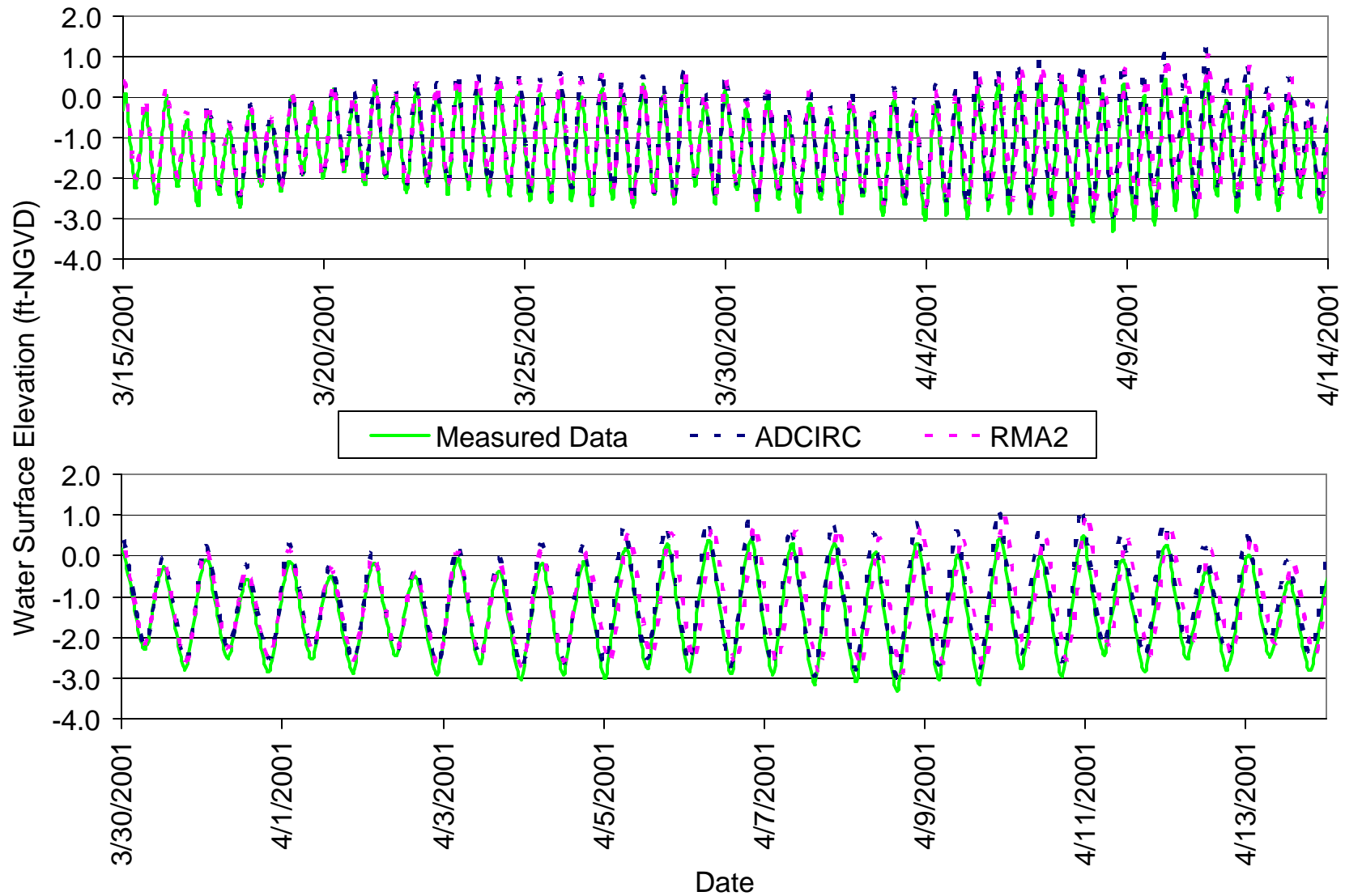


Figure 3.11 Measured and Predicted Water Surface Elevations at Frenchman's Marina

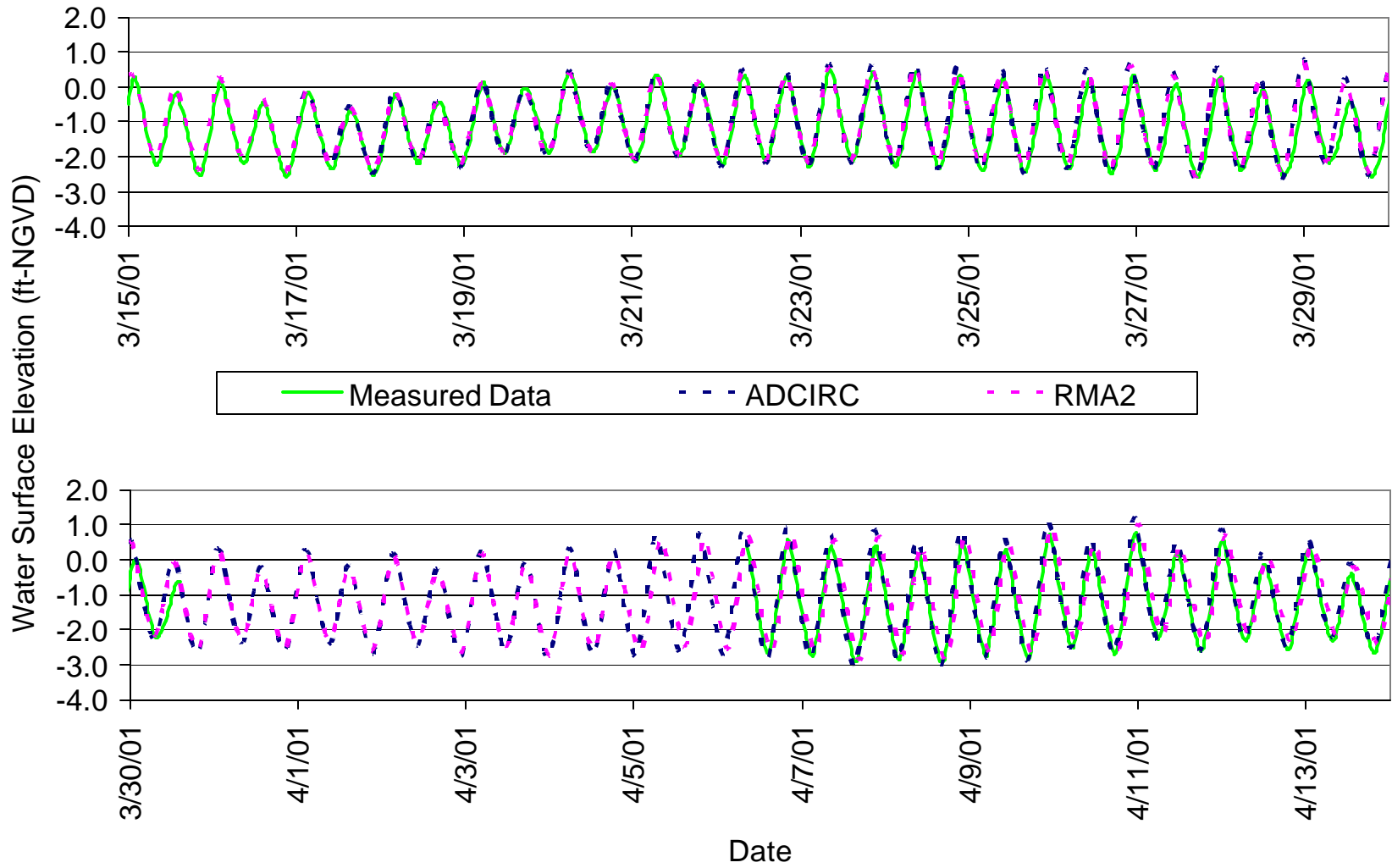


Figure 3.12 Measured and Predicted Water Surface Elevations at Bryant Park

Table 3.2 Error Summary for Water Level Calibration

Model	Error Type	Frenchman's Marina	Bryant Park
ADCIRC	Mean Error (cfs)	0.24	0.13
	RMS Error (cfs)	0.29	0.34
	Percent Error (%)	7.7%	9.3%
RMA2	Mean Error (cfs)	0.21	0.15
	RMS Error (cfs)	0.47	0.39
	Percent Error (%)	12.5%	10.8%

Model calibration also included matching measured flow rates. The flow rate measurements comprised four transects for almost 12 hours on April 5, 2001. Figure 3.13 through 3.16 compare the predicted model flow rates to the measured flow rates at the different cross section locations. The figures show the models accurately predicted the flow rates through the cross sections. Table 3.3 lists the errors associated with the flow rate calibration. From the table the average percent error equaled 5.5% for the ADCIRC simulation and 7.2% for the RMA2 simulation. As such, the models were considered calibrated for flow rate.

Table 3.3 Error Summary for Flow Rate Calibration

Model	Error Type	Lake Worth Inlet	ICWW-S	Peanut Island East	Peanut Island West
ADCIRC	Mean Error (cfs)	-647	-437	-811	-331
	RMS Error (cfs)	3881	3809	1768	1278
	Percent Error (%)	3.4%	5.5%	6.1%	6.6%
RMA2	Mean Error (cfs)	-137	5180	-1359	1433
	RMS Error (cfs)	4154	6332	1731	1936
	Percent Error (%)	3.6%	9.1%	6.0%	10.1%

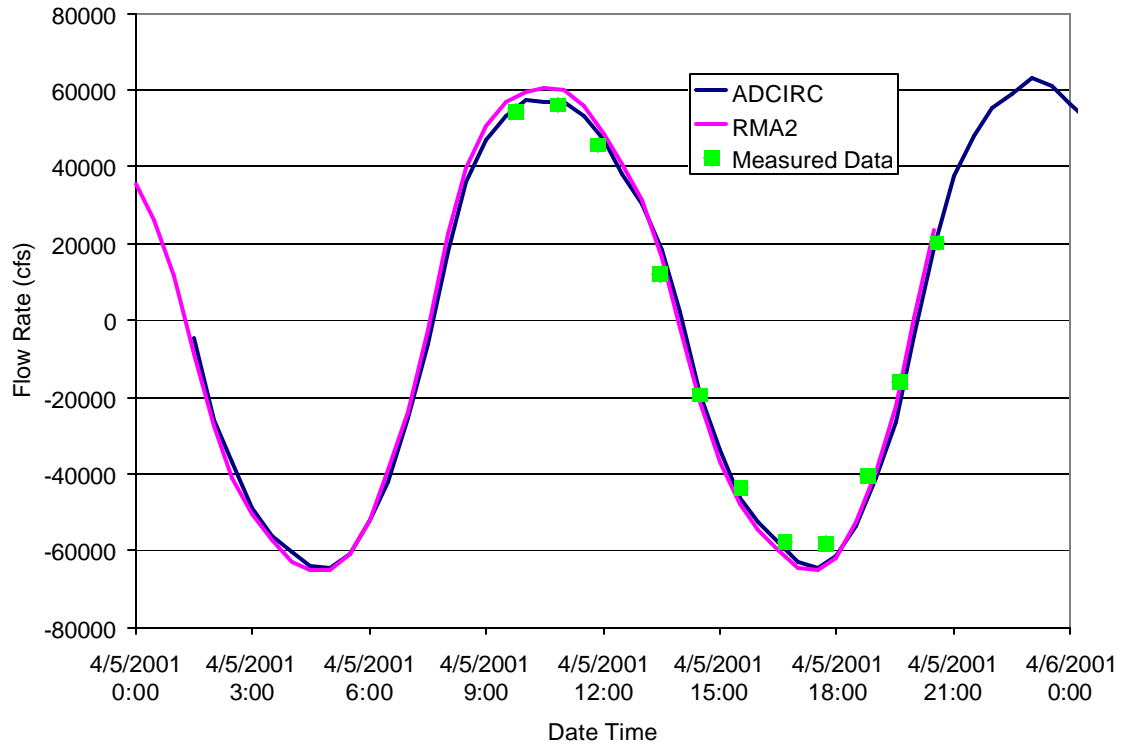


Figure 3.13 Flow Rate Calibration at Lake Worth Inlet

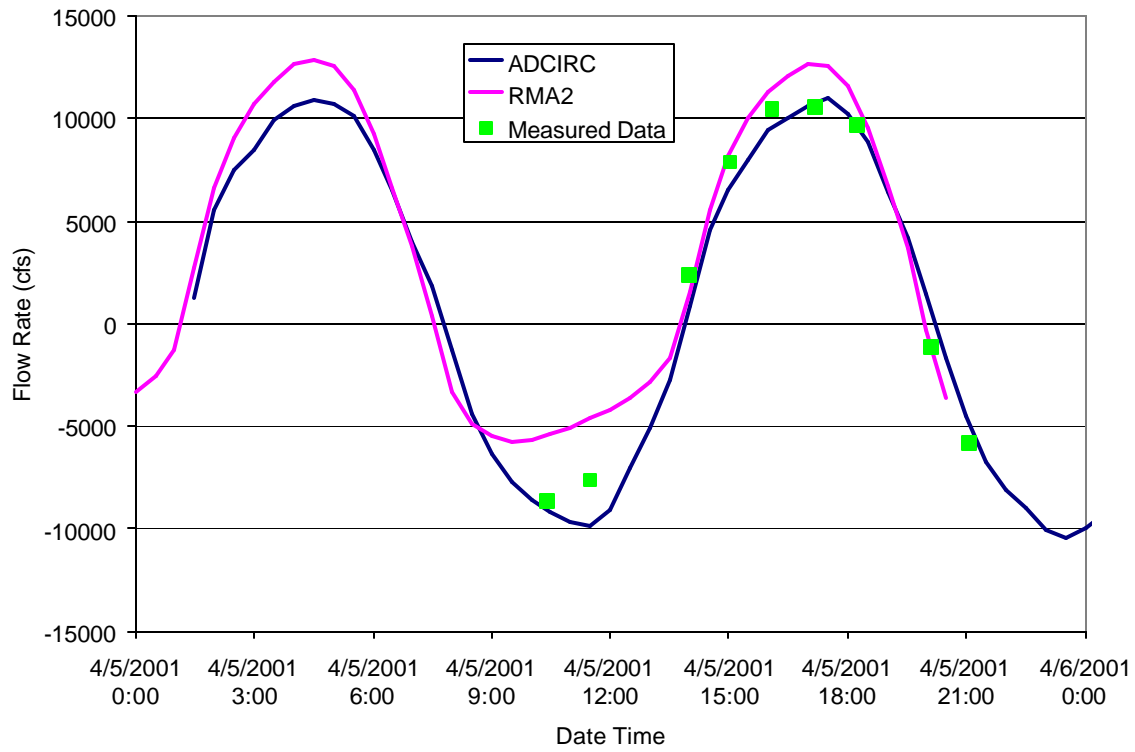


Figure 3.14 Flow Rate Calibration at Peanut Island West

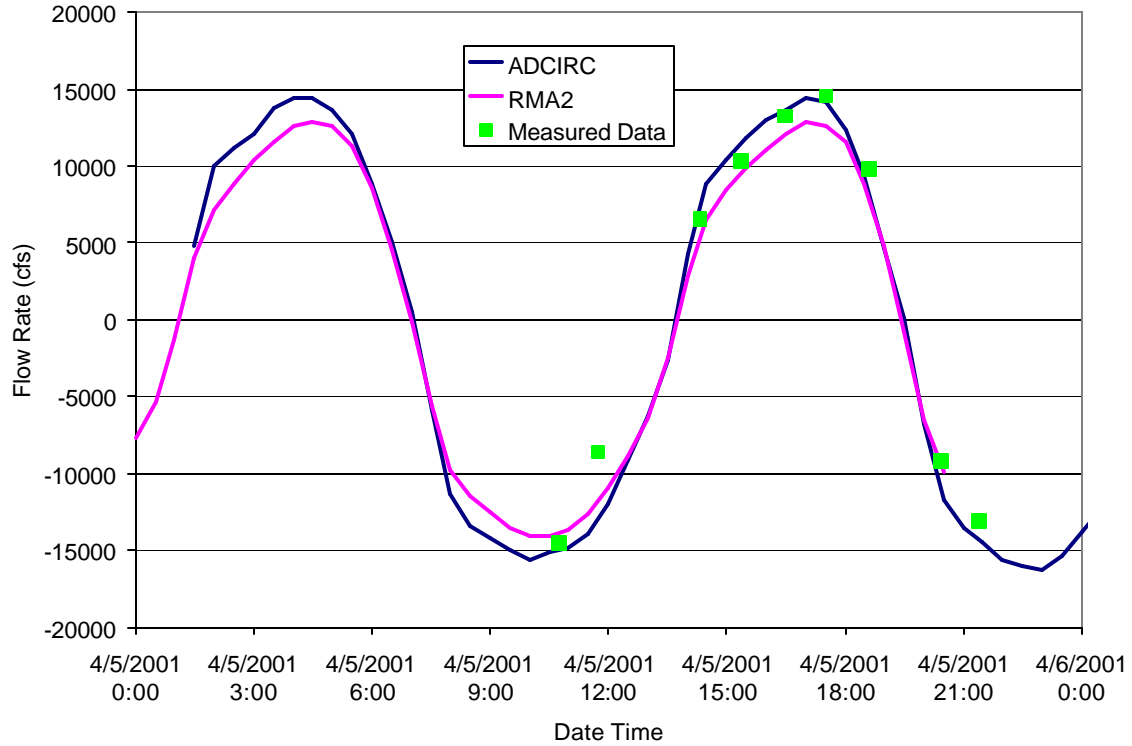


Figure 3.15 Flow Rate Calibration at Peanut Island East

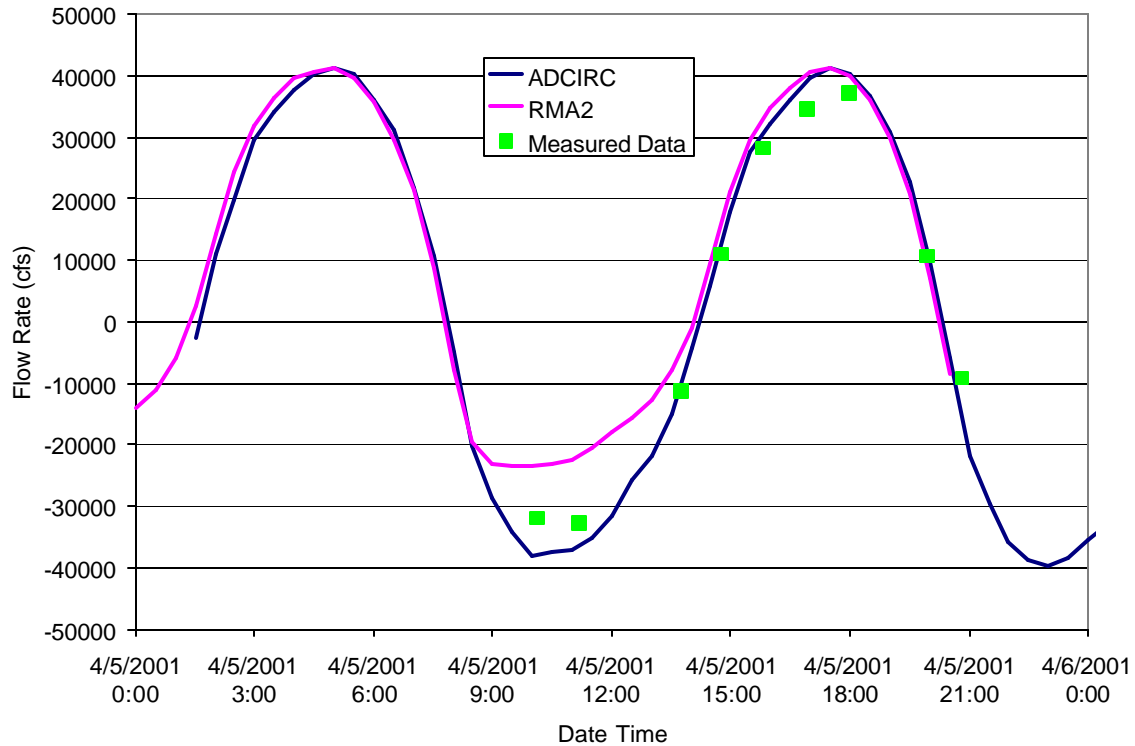


Figure 3.16 Flow Rate Calibration at ICWW-South

3.3 Model Simulations

The objective of this study is ultimately to identify the model that accurately describes the flows and water surface elevations during design storm conditions. The following subsections describe each of the simulations (the 50-, 100-, and 500-year return period storm surge events) performed in support of this study with both the RMA2 and ADCIRC hydrodynamic models. For the storm surge simulations, the offshore boundary conditions include an elevation time series that follow the hydrographs presented in Figure 2.6 and flow boundary conditions corresponding to the 5-year return period maximum flow as specified in Section 2.5 and applied at the locations indicated in Figures 3.5 through 3.10. For comparison's sake, the following two subsections present the results from the simulations at two of the bridges located within the models. Specifically, the subsections present the results at the Big Blue Heron Bridge (Bridge No. 930269, SR-A1A over the ICWW) and the Royal Palm Bridge (Bridges No. 930022 and 930411, SR-704 over the ICWW). Figure 3.17 shows the locations of the two bridges.

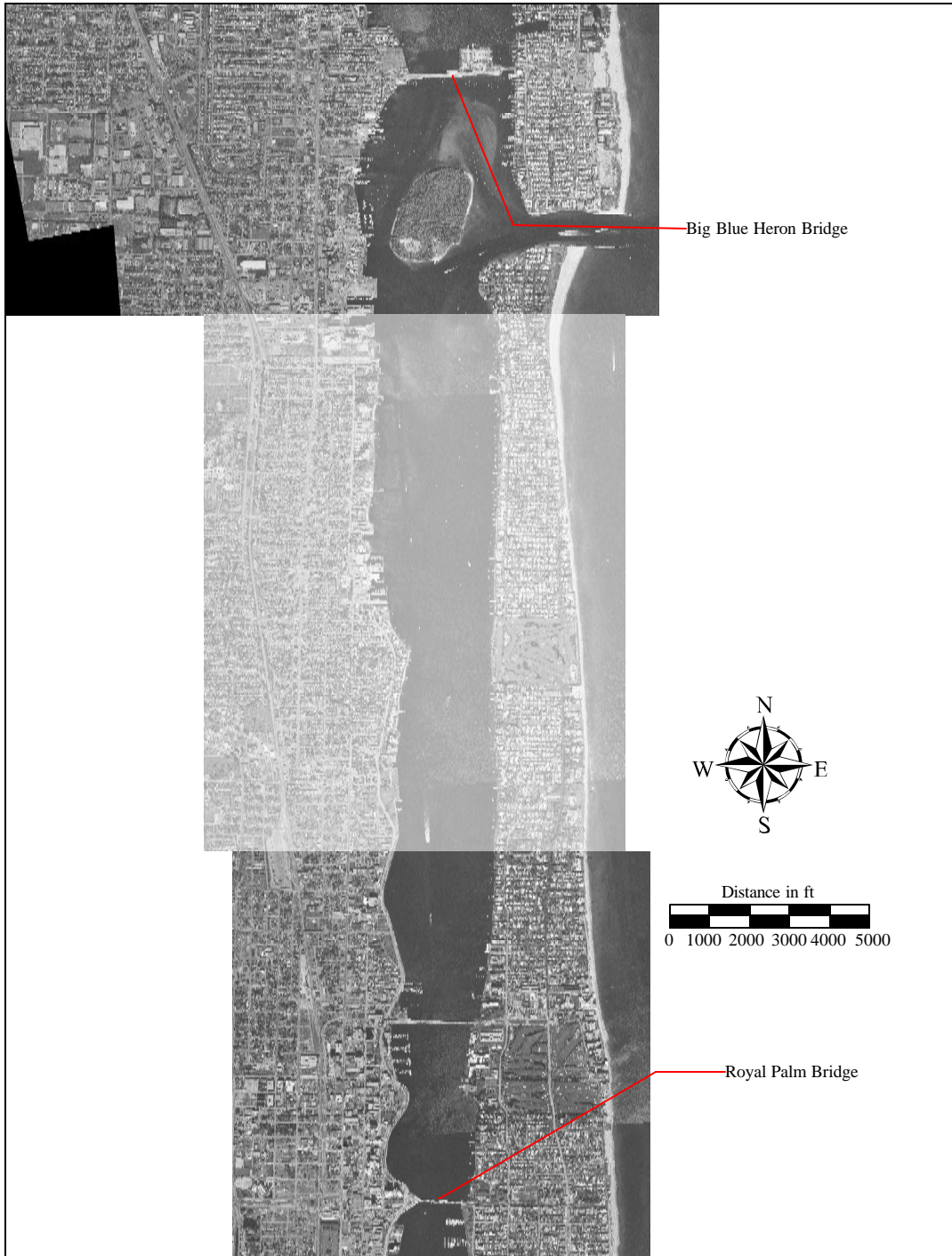


Figure 3.17 Locations of the Bridges Employed for the Presentation of the Simulation Results

3.3.1 RMA2 Simulations

The RMA2 model simulated storm surges associated with the 50-, 100-, and 500-year return period events through Lake Worth Inlet, the neighboring inlets, and the Intracoastal Waterway (ICWW). Figures 3.18 through 3.23 present results from the simulations at two locations within the model — at the Big Blue Heron Bridge and the Royal Palm Bridge. The figures present contours of velocity magnitude overlain with velocity vectors that indicate flow direction. The figures illustrate the flow patterns during the time of maximum velocity at the bridges. From the figures, the times of maximum velocity occur during the recession of the storm surge. In Figures 3.18 through 3.20, the location of the maximum velocity at the bridge occurs near Phil Foster Park (the island within the ICWW on the east side of the bridge). In Figures 3.21 through 3.23, the locations of the maximum velocities at the bridge occur near the center of the channel. Also, the figures show the intensification of velocities associated with the constriction of the shorelines as the flow approaches the bridge.

Time series plots of velocity magnitude and water surface elevations provide further understanding of the flow behavior at the bridges. Figures 3.24 and 3.25 present plots of the velocity magnitude and water surface elevations at the Big Blue Heron Bridge at the location of maximum velocity beneath the bridge for all three storm surge simulations. Figures 3.26 and 3.27 present plots of the velocity magnitude and water surface elevations at the Royal Palm Bridge at the location of maximum velocity beneath the bridge for all three storm surge simulations. Notably, all the figures also show the results from the ADCIRC simulations at the same locations. From the figures, the maximum velocities range from 3.4 ft/s during the 50-year simulation to 5.0 ft/s during the 500-year simulation at the Big Blue Heron Bridge and from 3.4 ft/s during the 50-year simulation to 4.8 ft/s during the 500-year simulation at the Royal Palm Bridge. The maximum water surface elevations range from 8.1 ft-NAVD during the 50-year simulation to 12.5 ft-NAVD88 during the 500-year simulation at the Big Blue Heron Bridge and from 8.1 ft-NAVD88 during the 50-year simulation to 12.4 ft-NAVD88 during the 500-year simulation at the Royal Palm Bridge. Table 3.4 contains a summary of the results from the storm surge simulations. Notably, the table also contains the results from the ADCIRC simulations.

Table 3.4 Summary of Simulation Results

Bridge	Model	Maximum Velocity (fps)			Maximum Water Surface Elevation (ft-NAVD88)		
		50-year	100-year	500-year	50-year	100-year	500-year
Royal Palm Bridge	ADCIRC	3.7	3.9	4.8	8.4	9.2	12.5
	RMA2	3.4	4.2	4.8	8.2	9.9	12.5
	Difference (RMA2-ADCIRC)	-0.3	0.3	<0.1	-0.2	0.7	0.0
Big Blue Heron	ADCIRC	3.6	3.8	4.4	8.3	9.1	12.3
	RMA2	3.4	4.4	5.0	8.1	9.8	12.5
	Difference (RMA2-ADCIRC)	-0.2	0.6	0.6	-0.2	0.7	0.2

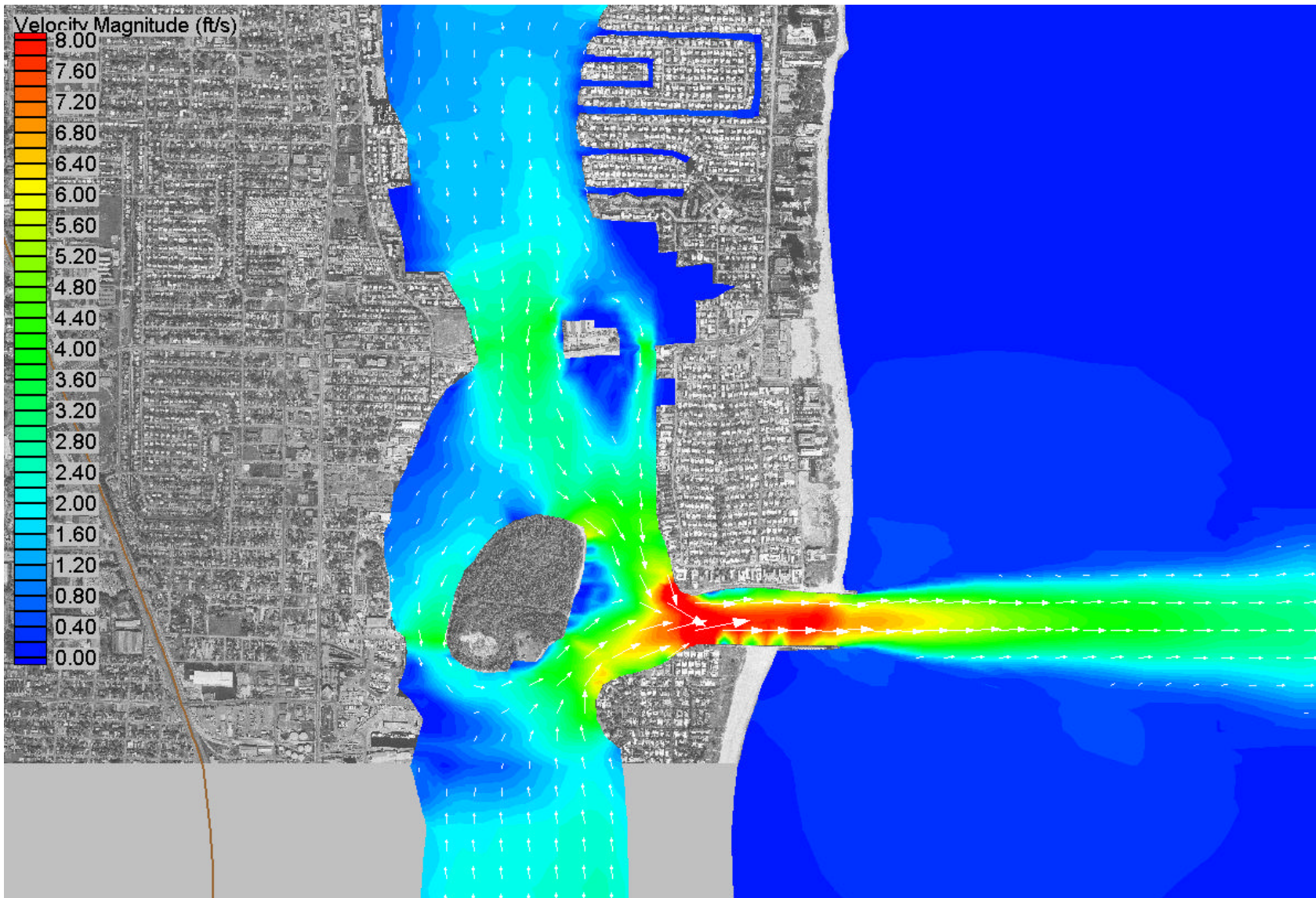


Figure 3.18 Contours of Velocity Magnitude and Velocity Vectors at the Time of Maximum Velocity near the Big Blue Heron Bridge for the 50-year Return Period Storm Surge Simulation (RMA2)

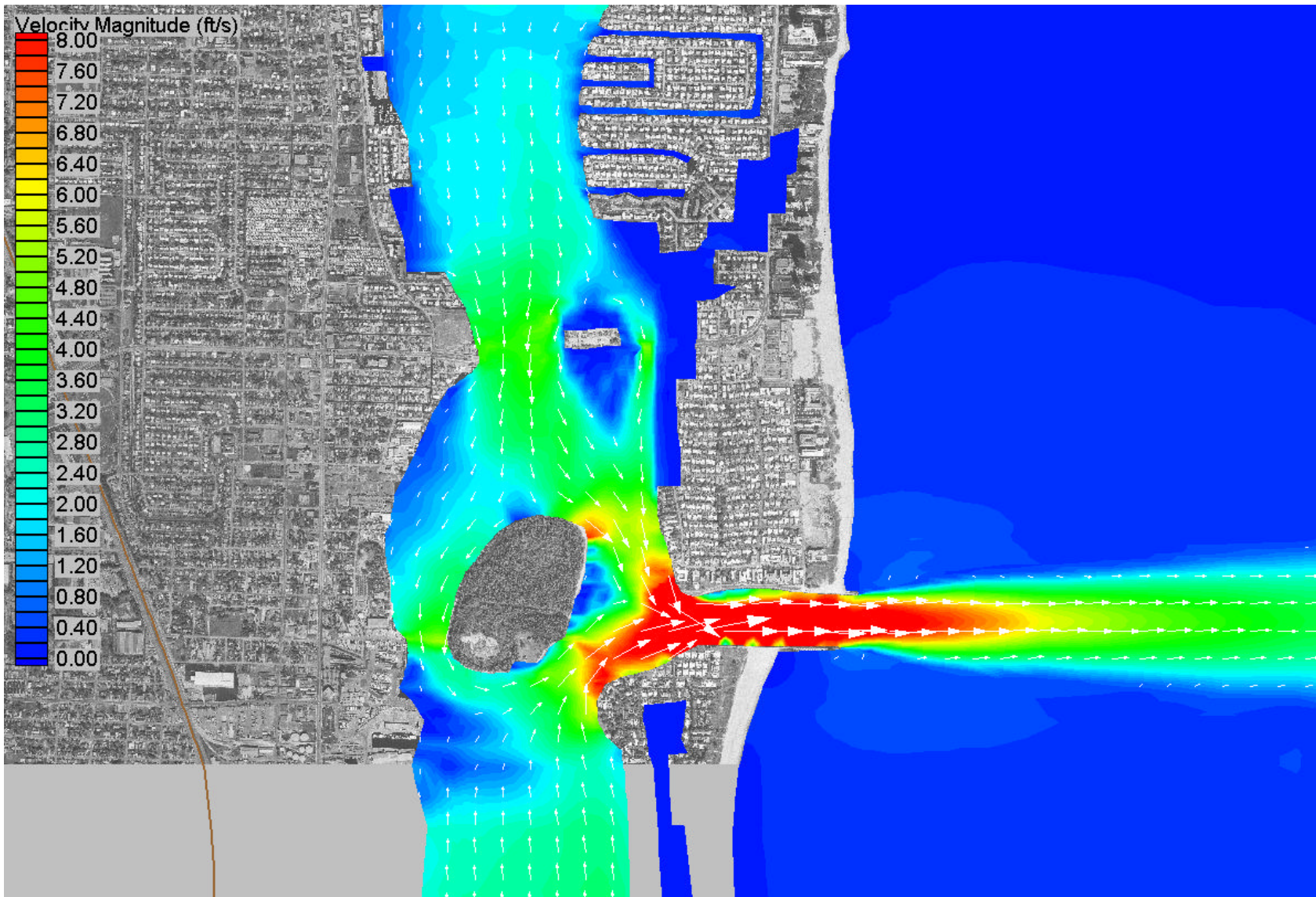


Figure 3.19 Contours of Velocity Magnitude and Velocity Vectors at the Time of Maximum Velocity near the Big Blue Heron Bridge for the 100-year Return Period Storm Surge Simulation (RMA2)

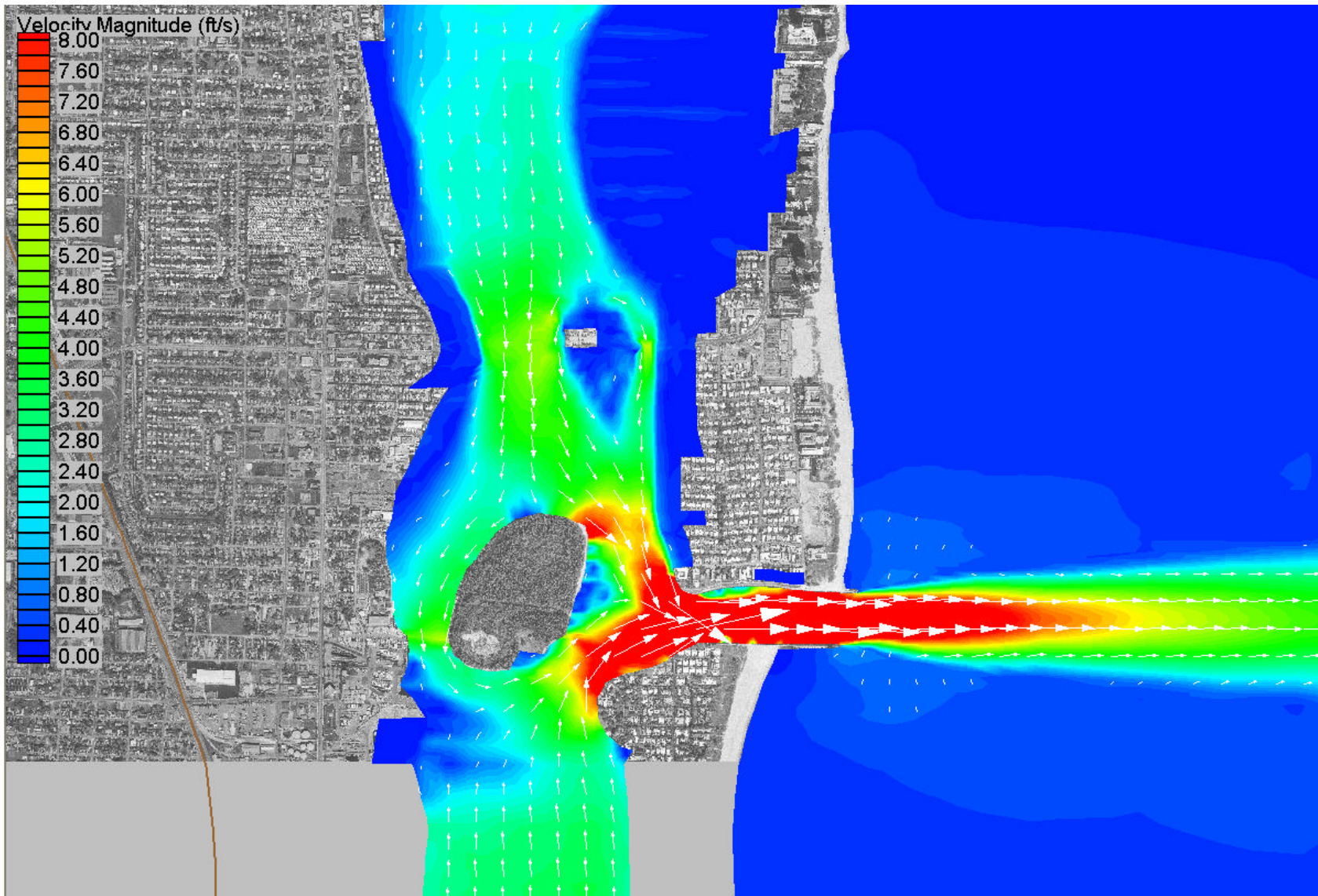


Figure 3.20 Contours of Velocity Magnitude and Velocity Vectors at the Time of Maximum Velocity near the Big Blue Heron Bridge for the 500-year Return Period Storm Surge Simulation (RMA2)

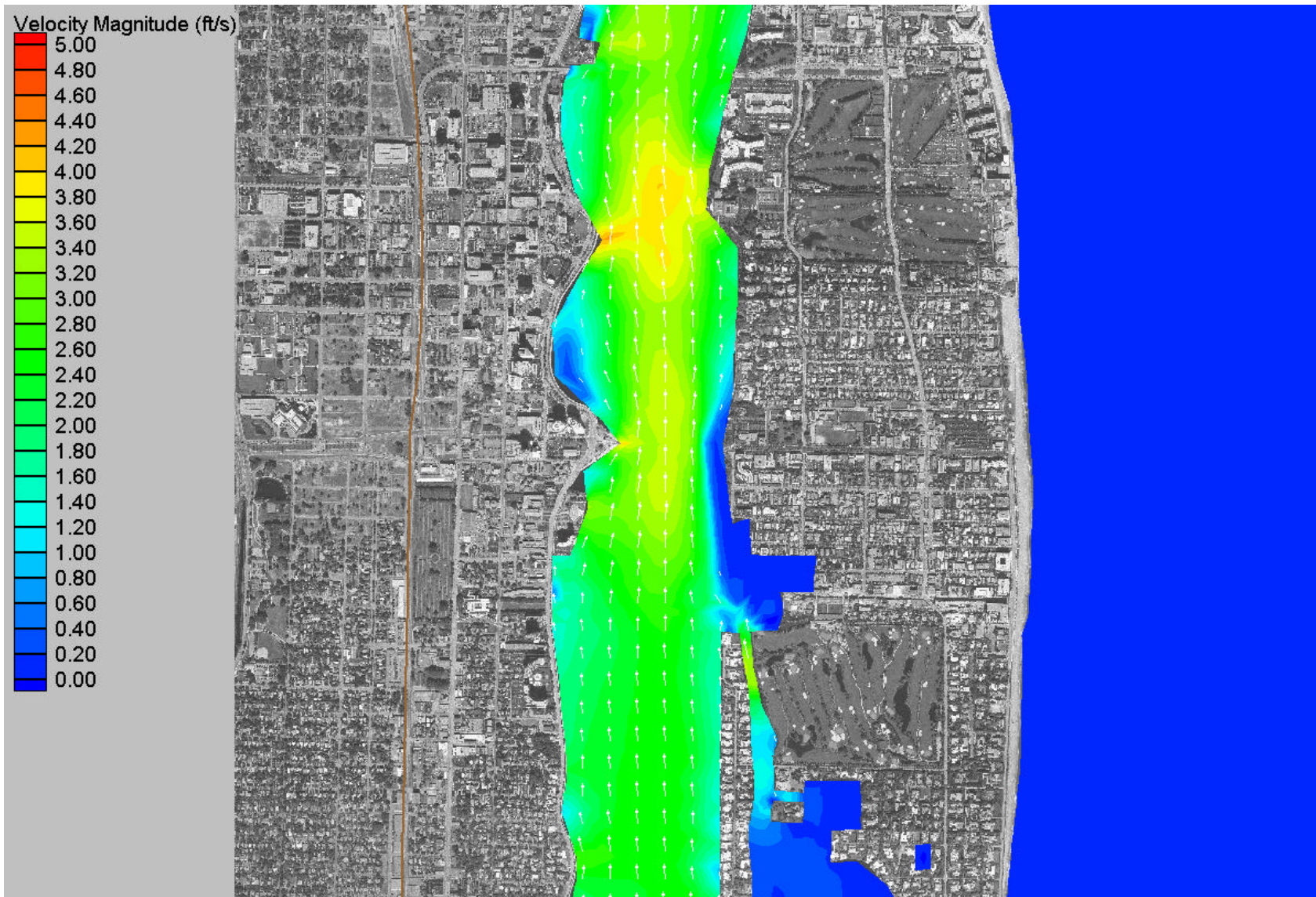


Figure 3.21 Contours of Velocity Magnitude and Velocity Vectors at the Time of Maximum Velocity near the Royal Palm Bridge for the 50-year Return Period Storm Surge Simulation (RMA2)

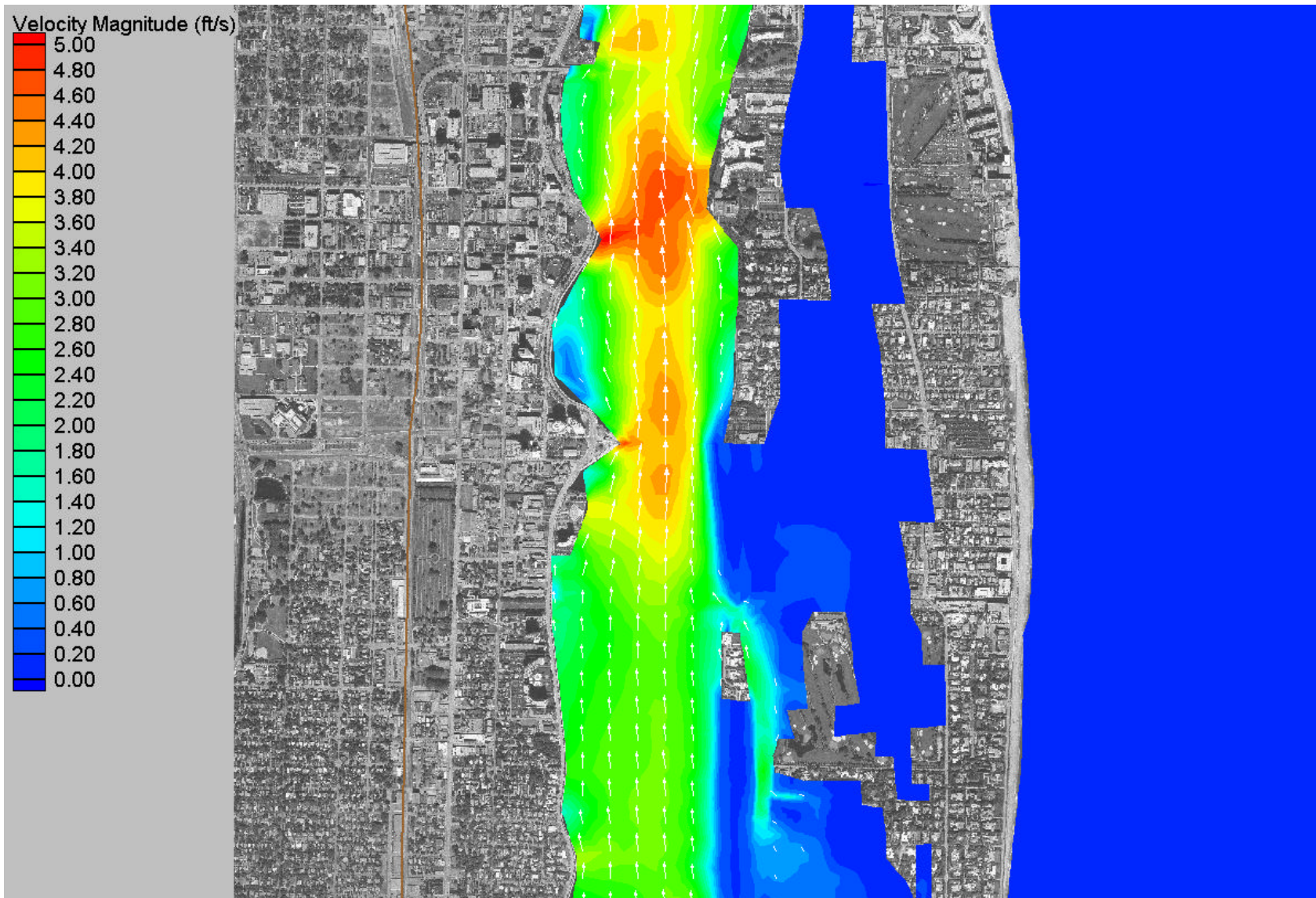


Figure 3.22 Contours of Velocity Magnitude and Velocity Vectors at the Time of Maximum Velocity near the Royal Palm Bridge for the 100-year Return Period Storm Surge Simulation (RMA2)

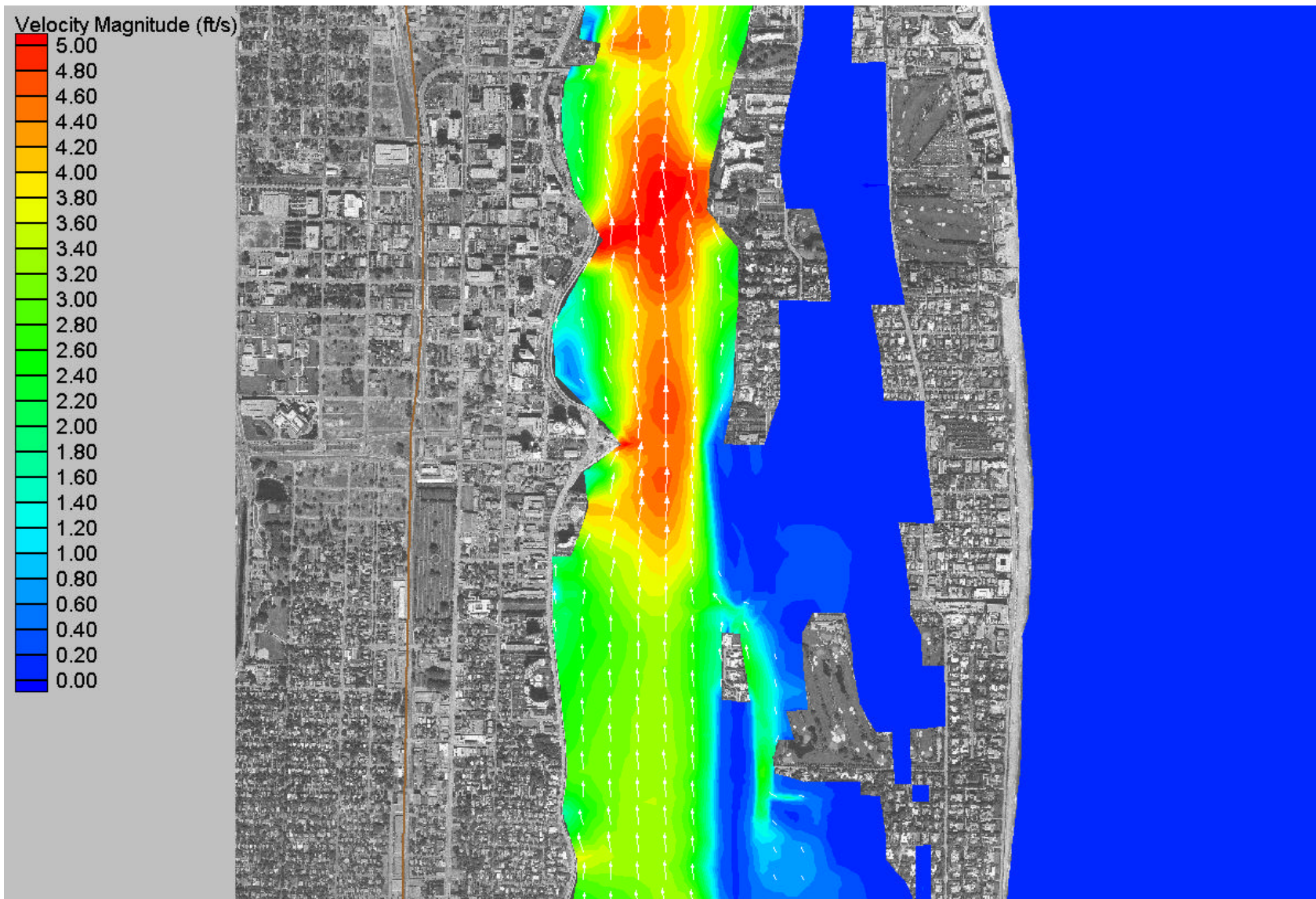


Figure 3.23 Contours of Velocity Magnitude and Velocity Vectors at the Time of Maximum Velocity near the Royal Palm Bridge for the 500-year Return Period Storm Surge Simulation (RMA2)

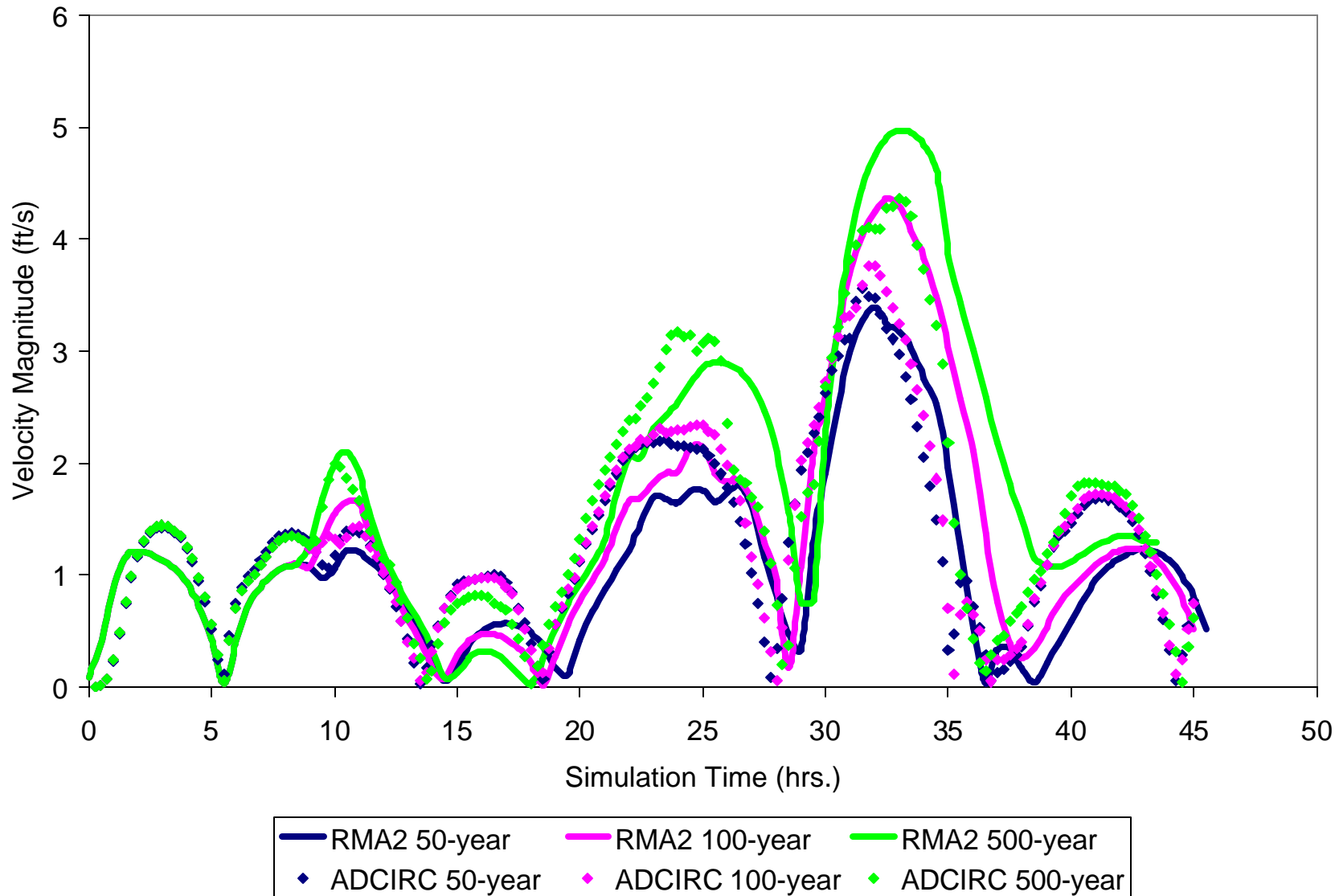


Figure 3.24 Velocity Magnitude Time Series at the Big Blue Heron Bridge for All Simulations

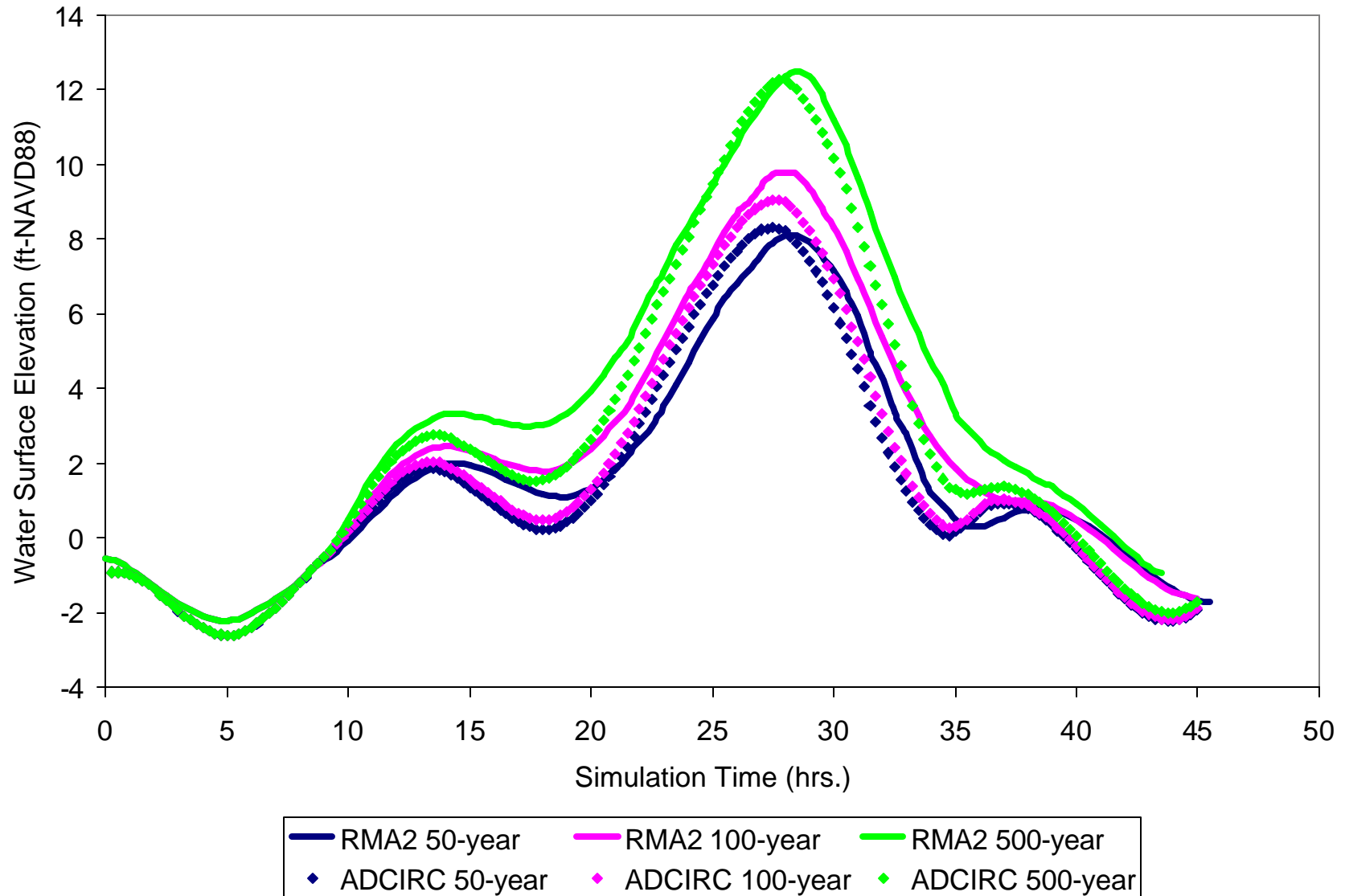


Figure 3.25 Water Surface Elevation Time Series at the Big Blue Heron Bridge for All Simulations

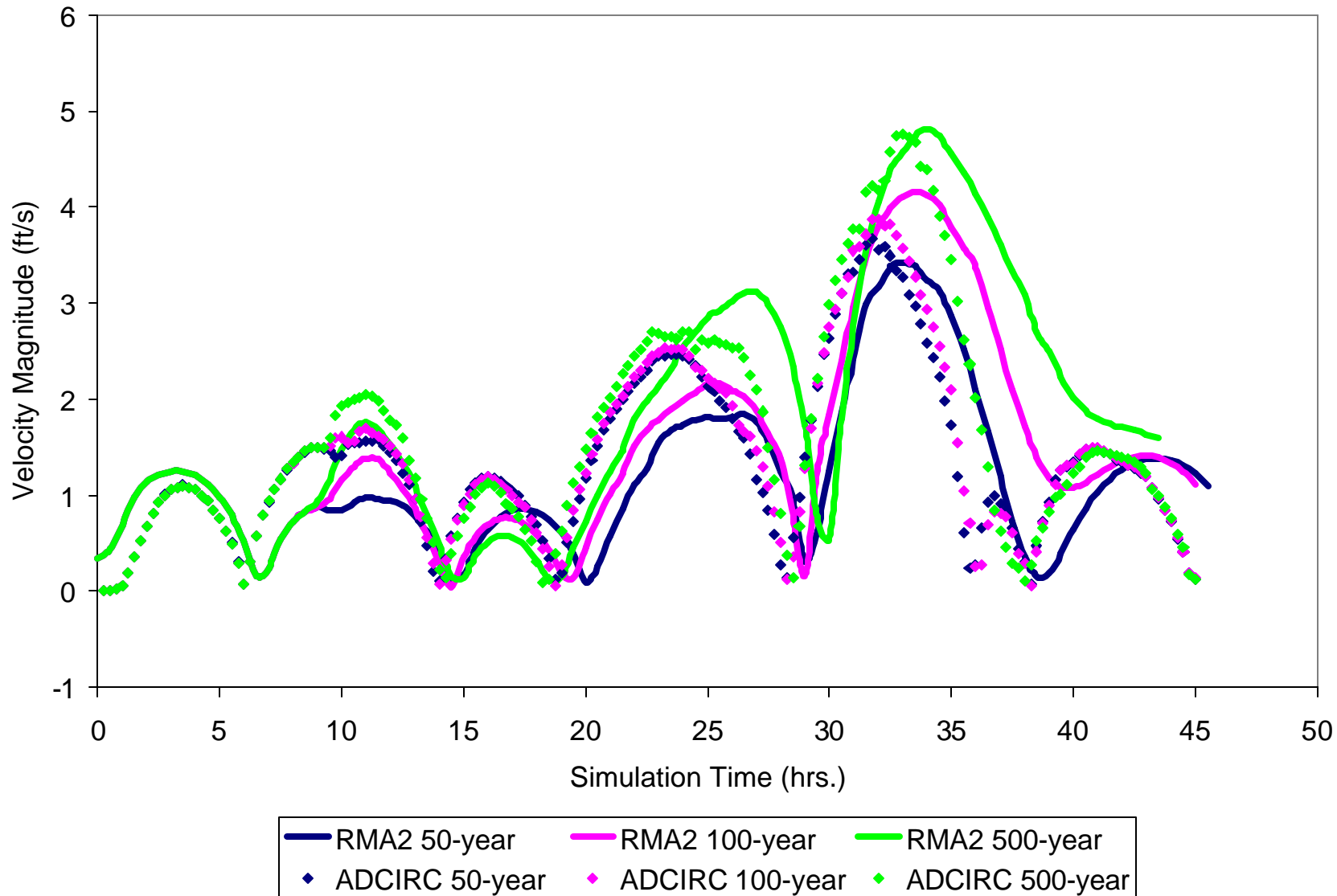


Figure 3.26 Velocity Magnitude Time Series at the Royal Palm Bridge for All Simulations

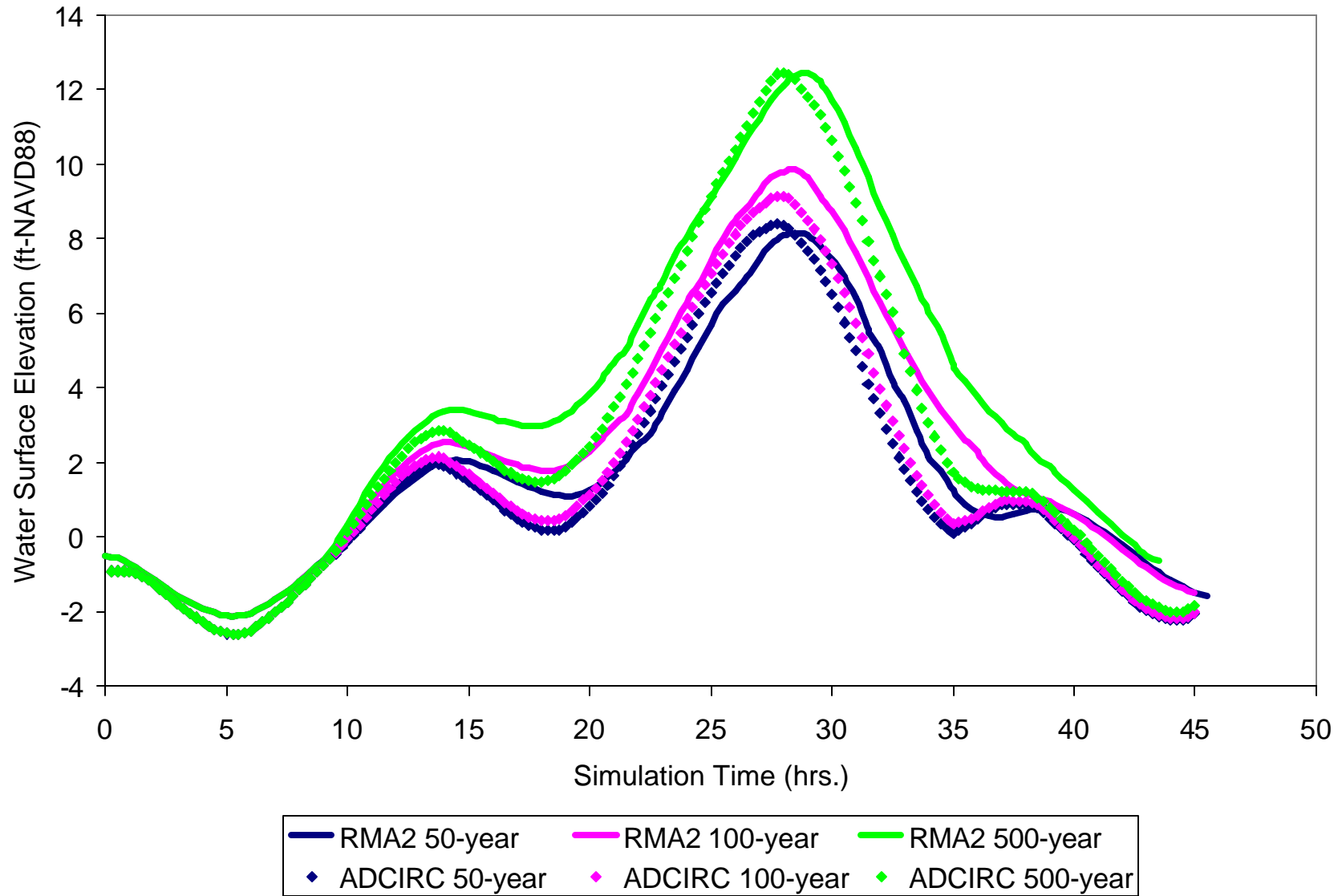


Figure 3.27 Water Surface Elevation Time Series at the Royal Palm Bridge for All Simulations

3.3.2 ADCIRC Simulations

The ADCIRC model simulated storm surges associated with the 50-, 100-, and 500-year return period events through Lake Worth Inlet, the neighboring inlets, and the Intracoastal Waterway (ICWW). Figures 3.28 through 3.33 present results from the simulations at two locations within the model — at the Big Blue Heron Bridge and the Royal Palm Bridge. The figures present contours of velocity magnitude overlain with velocity vectors that indicate flow direction. The figures illustrate the flow patterns during the time of maximum velocity at the bridges. As with the RMA2 simulations, the times of maximum velocity occur during the recession of the storm surge. In Figures 3.28 through 3.30, the locations of the maximum velocity at the bridge occur near Phil Foster Park (the island within the ICWW on the east side of the bridge). In contrast to the RMA2 simulations, the figures indicate less flooding of the overbanks during the time of maximum velocity. Additionally, the figures indicate a curvature to the ebb jet issuing from the inlet during the recession of the storm surge. The cause of this curvature is numerical and is discussed in the next chapter. In Figures 3.31 through 3.33, the locations of the maximum velocities at the bridge occur near the center of the channel. Also similar to the RMA2 simulations, the figures show the intensification of velocities associated with the constriction of the shorelines as the flow approaches the bridge. In contrast to the Big Blue Heron Bridge, there is flooding of the overbanks during the time of maximum velocity at the Royal Palm Bridge. However, the figures indicate a different pattern to the flooding than during the RMA2 simulations.

Time series plots of velocity magnitude and water surface elevations provide further understanding of the flow behavior at the bridges. Figures 3.24 and 3.25 present plots of the velocity magnitude and water surface elevations at the Big Blue Heron Bridge at the location of maximum velocity beneath the bridge for all three storm surge simulations. Figures 3.26 and 3.27 present plots of the velocity magnitude and water surface elevations at the Royal Palm Bridge at the location of maximum velocity beneath the bridge for all three storm surge simulations. Notably, all the figures also show the results from the RMA2 simulations at the same locations. From the figures, the maximum velocities range from 3.6 ft/s during the 50-year simulation to 4.4 ft/s during the 500-year simulation at the Big Blue Heron Bridge and from 3.7

ft/s during the 50-year simulation to 4.8 ft/s during the 500-year simulation at the Royal Palm Bridge. The maximum water surface elevations ranges from 8.3 ft-NAVD during the 50-year simulation to 12.3 ft-NAVD88 during the 500-year simulation at the Big Blue Heron Bridge and from 8.4 ft-NAVD88 during the 50-year simulation to 12.5 ft-NAVD88 during the 500-year simulation at the Royal Palm Bridge. Table 3.4 presents the results from both models' simulations. From the table, the results indicate little difference between the two models at the Royal Palm Bridge in either maximum velocity or water surface elevation with one exception — the maximum velocity during the 100-year simulation. At the Big Blue Heron Bridge, differences between the RMA2 and ADCIRC simulations are slightly greater than at the Royal Palm Bridge. Interestingly, the greatest difference also occurs during the 100-year return period storm surge in velocity magnitude. In summary, the largest difference in water surface elevation was 0.6 ft (~15%) and the largest difference in velocity was 0.7 ft/s (~7%). Reasons for these differences are discussed in the next chapter.

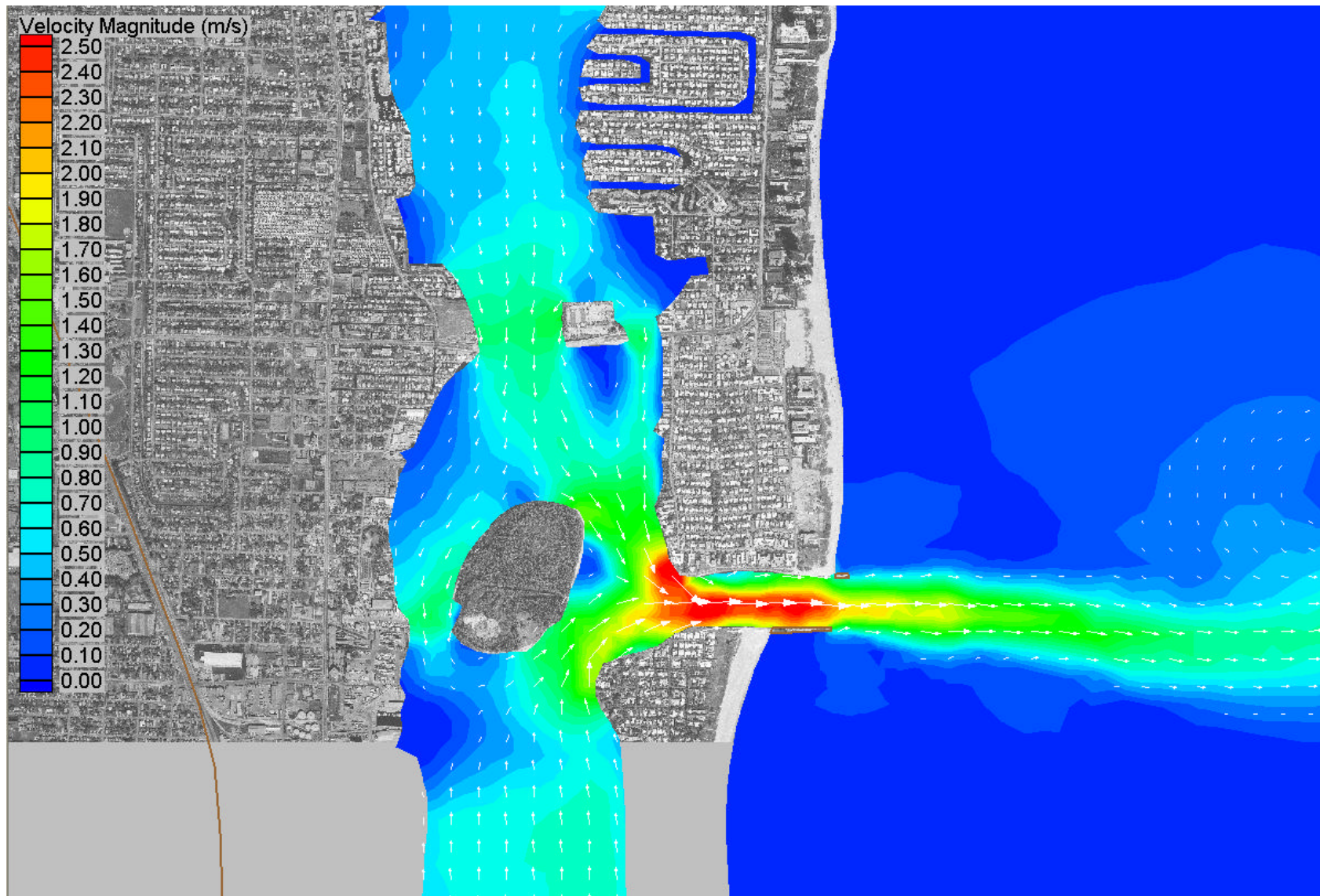


Figure 3.28 Contours of Velocity Magnitude and Velocity Vectors at the Time of Maximum Velocity near the Big Blue Heron Bridge for the 50-year Return Period Storm Surge Simulation (ADCIRC)

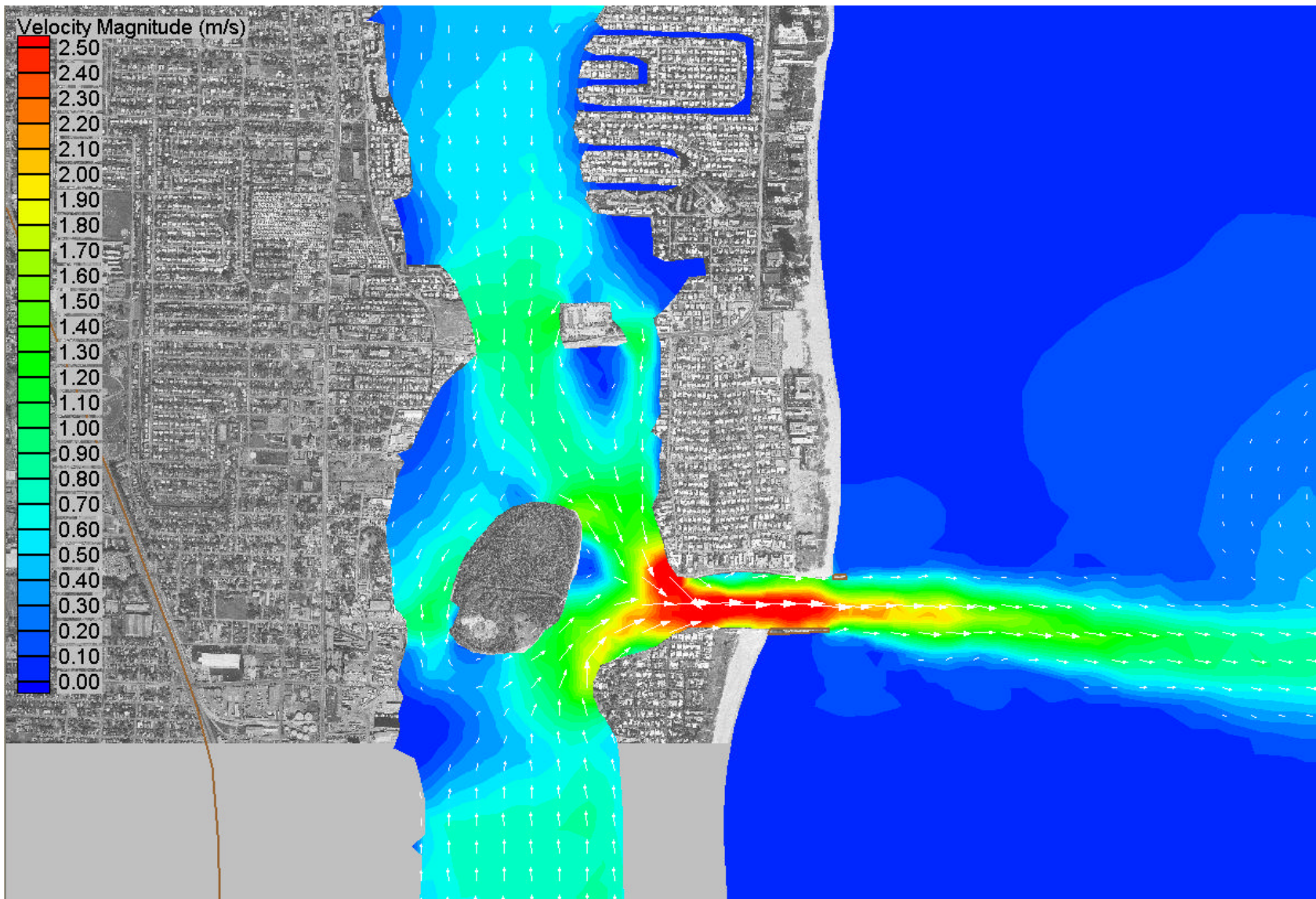


Figure 3.29 Contours of Velocity Magnitude and Velocity Vectors at the Time of Maximum Velocity near the Big Blue Heron Bridge for the 100-year Return Period Storm Surge Simulation (ADCIRC)

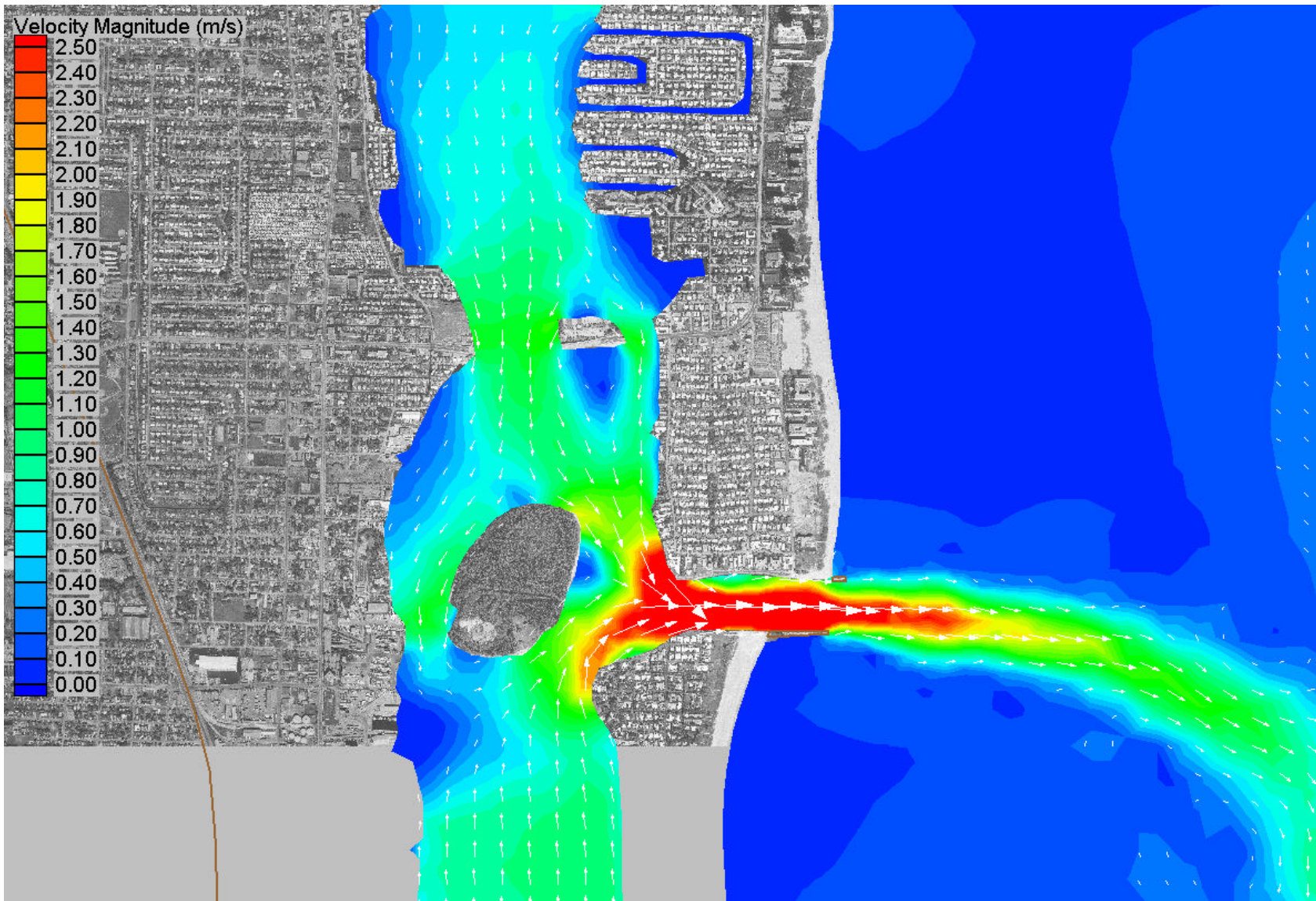


Figure 3.30 Contours of Velocity Magnitude and Velocity Vectors at the Time of Maximum Velocity near the Big Blue Heron Bridge for the 500-year Return Period Storm Surge Simulation (ADCIRC)

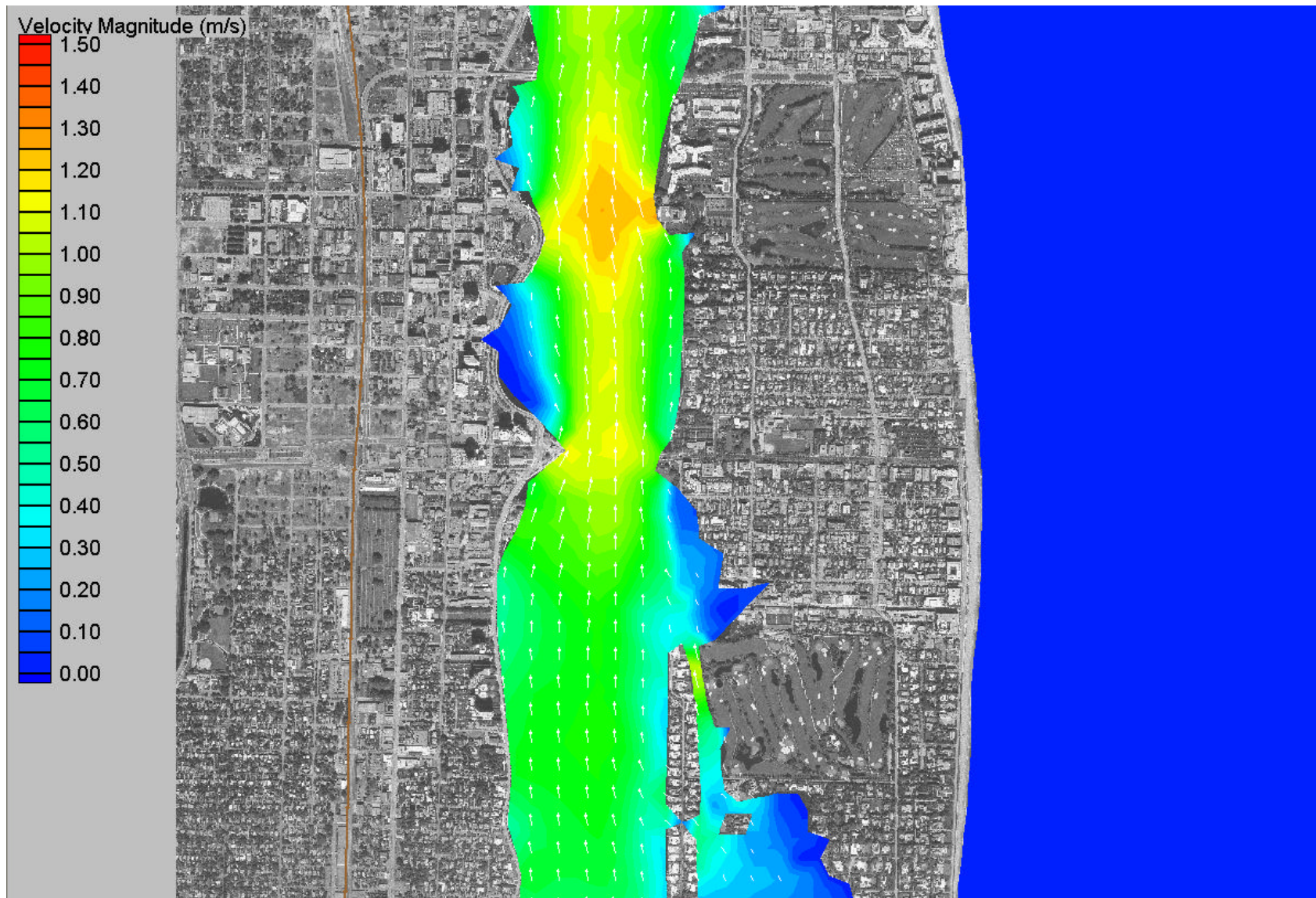


Figure 3.31 Contours of Velocity Magnitude and Velocity Vectors at the Time of Maximum Velocity near the Royal Palm Bridge for the 50-year Return Period Storm Surge Simulation (ADCIRC)

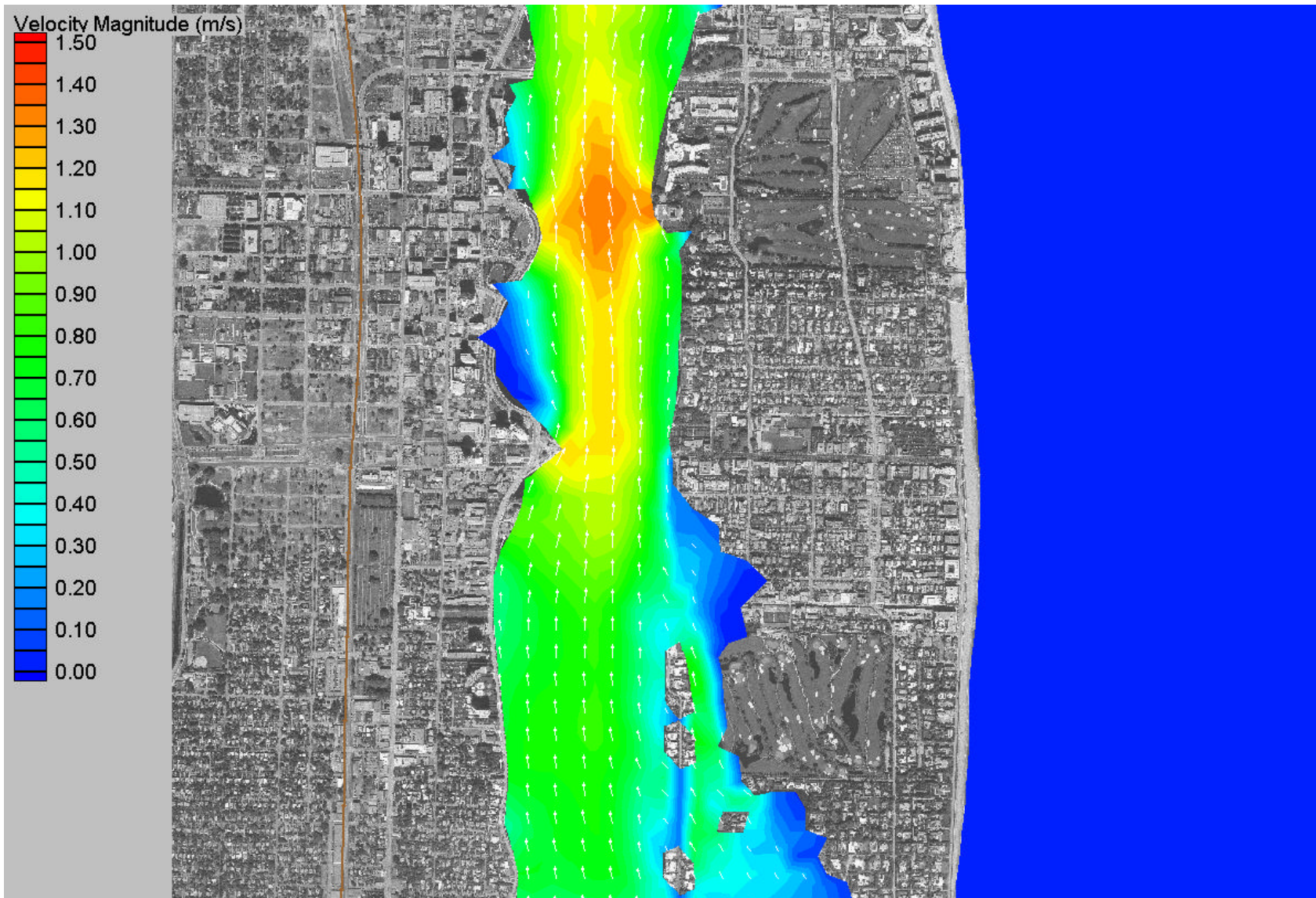


Figure 3.32 Contours of Velocity Magnitude and Velocity Vectors at the Time of Maximum Velocity near the Royal Palm Bridge for the 100-year Return Period Storm Surge Simulation (ADCIRC)

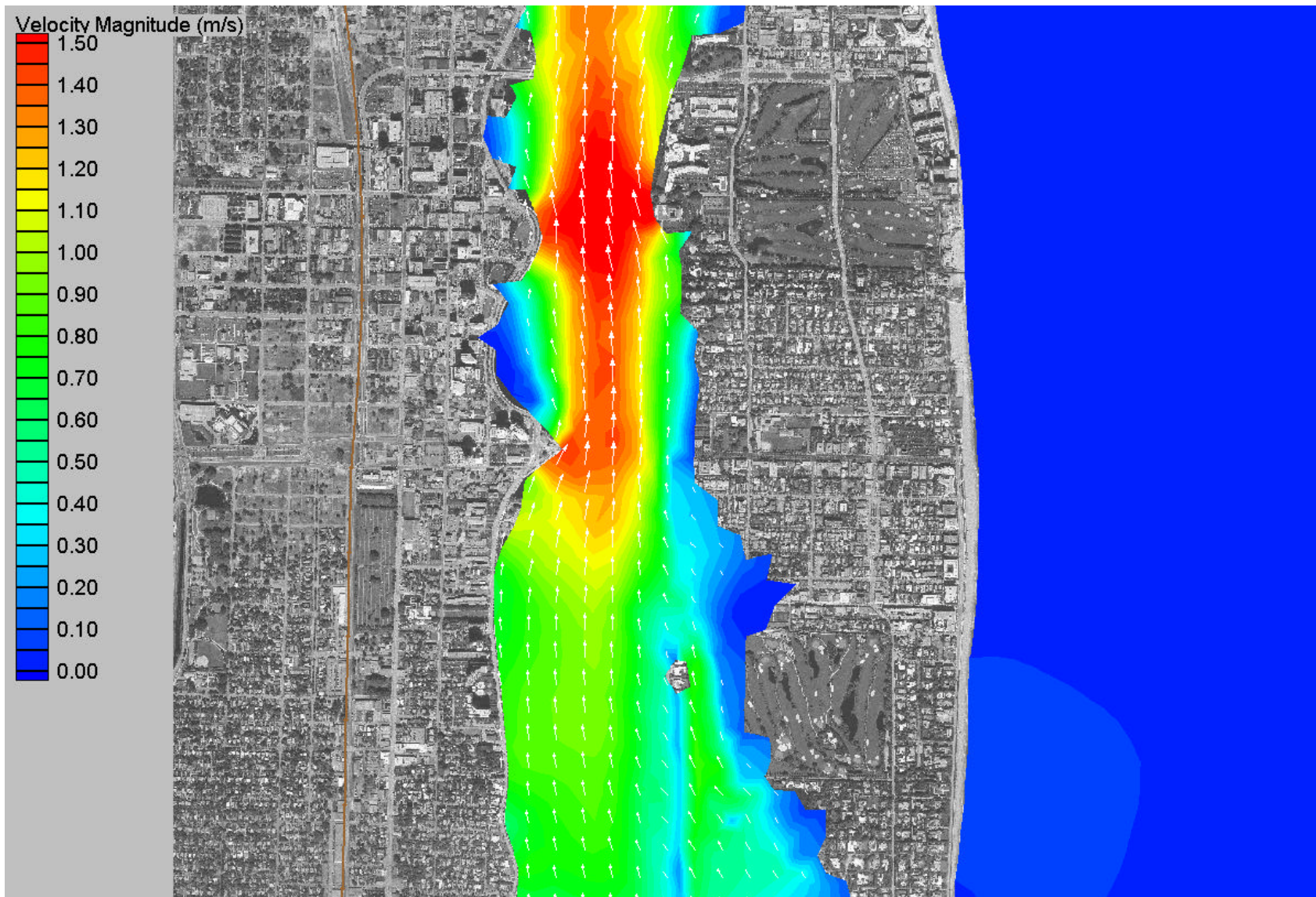


Figure 3.33 Contours of Velocity Magnitude and Velocity Vectors at the Time of Maximum Velocity near the Royal Palm Bridge for the 500-year Return Period Storm Surge Simulation (ADCIRC)

4.0 MODEL COMPARISON

The comparison of the two models presented herein comprises both a qualitative and quantitative analyses. Qualitatively, the models were compared by model features, ease of application, and relative time to construct, debug, and run the simulations. Quantitatively, the models were compared by their capability to predict water surface elevations and flow discharges relative to the measured calibration data. Additionally, the models are compared relative to each other in their predictions of the design storm surge flow properties.

4.1 Qualitative Comparison

A qualitative comparison of the models provides information on features of the modeling process other than model accuracy. For example, oftentimes work performed for the FDOT is under strict time constraints. If a model provides a more accurate answer but the modeling process cannot be completed within the allotted scheduling, then application of that model is inappropriate. Additionally, some applications may require models features that may point to one model over another. As such, a qualitative comparison plays an important role in the decision making process of selecting an appropriate model.

Before discussing the work performed for this contract, it is beneficial to review the specific features of each model that may affect the selection process. Both ADCIRC and RMA2 are finite element models. Both models provide specification of boundary conditions via specified elevation (time series), specified flow (time series), slip or no slip conditions for velocity, and surface stress (wind and/or wave radiation stress). Both models provide for spatially varying friction specification and a form of eddy viscosity for turbulence closure. Both models also contain provisions for wetting and drying and influence of Coriolis force.

Mesh creation within the RMA2 model takes place within either an English or SI coordinate system. The model provides several types of control structures:

- Type 1 — Point source or sink of flow, e.g. a pump or storm drain;
- Type 2 — Flow is a reversible function of head loss, e.g. an open culvert;

- Type 3 — Flow is an irreversible Type 2, e.g. a flap culvert;
- Type 4 — Flow is a function of water surface elevation, e.g. a weir;
- Type 5 — Type 2, with head loss as a function of flow; and
- Type 6 — Flow is an irreversible Type 5.

These control structures may be integrated into the mesh as either one- or two-dimensional features. The model is fully integrated within SMS and most of the features are accessible through this program.

Given its intended application over large domains, mesh creation within ADCIRC takes place within a geographic coordinate system. The vertical specification of the bathymetry is in meters from mean sea level as a depth (i.e., depths are positive and topography is negative). In addition to the boundary conditions listed previously, ADCIRC also provides complex meteorological forcing in several formats including US Navy Fleet Numeric format and PBL Hurricane Model format. Additionally, ADCIRC provides for elevation boundary conditions of the ocean boundary through specification of tidal constituents on a nodal basis. This specification is integrated into the program through access to a tidal constituent database. The program also provides for internal and external overflow and through-flow barriers. Additionally, the model provides a feature for accounting for the extra drag caused by subgrid scale obstructions such as bridge piers. Although SMS provides the interface for ADCIRC, several features of the program are not yet available through the GUI. As such, model setup and simulation runs required a certain amount of manual manipulation of the input files.

During the construction of the meshes, debugging of the models, calibration, and simulations, records were kept of the number of manhours spent for each task. Not surprisingly, most of the work involved construction of the meshes and debugging of the models. Problems common to both models included wetting and drying of the meshes and the formation of puddles within the model upon the recession of the storm surges. This “ponding” usually resulted in the model crashing or in numerical instability that propagated throughout the model domain. The approach to fixing the ponding involved manually smoothing the topography while attempting to ensure that the overall storage within the domain remained relatively constant. Both models

required approximately the same amount of time to construct and run. As such, both modeling efforts were deemed roughly equivalent in the amount of time it takes to perform an application. Additionally, since both models encountered the same types of problems during debugging, both models were deemed approximately equivalent in ease of application as well.

4.2 Quantitative Comparison

A quantitative comparison provided a direct measurement of the relative performance of the two models. This involved comparing the results from the calibration simulations to the measurements. Given the vagrancies associated with the measurement techniques (tide gages and ADCP measurements) and the inherent difference between the actual forcing and applied boundary conditions (a single offshore elevation boundary condition with no meteorological forcing), both models exhibited good calibration. For the water surface elevation calibration, ADCIRC performed slightly better than RMA2 at both gages (7.7% and 9.3% as compared with 12.5% and 10.8%). For the flow rate calibration, ADCIRC predicted the flows slightly more accurately than RMA2 at three of the four cross sections (3.4%, 5.5%, 6.1%, and 6.6% as compared with 3.6%, 9.1%, 6.0%, and 10.1%). Notably, calibration proceeded until acceptable convergence occurred. Both models achieved convergence within similar amounts of time. If more time was spent on calibration for either model, it is possible that these results might improve. However, given the very small difference in performance, both models were deemed roughly equivalent in capability to reproduce the measured results.

The storm surge simulations pointed out several differences in the model performance. Table 3.4 indicates that at two of the bridges within the models there exist slight differences, on the order of 10% to 15%, in both the predicted maximum water surface elevations and maximum velocity. This was particularly evident in the 100- and 500-year return period storm surge simulations at the Big Blue Heron Bridge. Interestingly, the 50-year simulations exhibited slightly smaller deviations. This may be attributed to one of two factors. First, the two models differ markedly in the resolution of the topography. Figures 4.1 and 4.2 illustrate the model meshes in the area of the Big Blue Heron Bridge. From the figures, the ADCIRC mesh contains more resolution in the topography, especially in the bank areas, than does the RMA2 mesh. This

simply reflects the choices made by the modeler concerning the need for additional resolution in these areas. Certainly the RMA2 model could be modified to include additional resolution in these areas. That said, the difference in resolution may have led to differences in the way the model wets and dries elements and, as such, may have affected the overall storage on either side of the bridges. This, in turn, would influence both the water surface elevation and the velocities associated with the storm surge propagation. A second, and more likely, reason for the differences involves the smoothing of the mesh by the model developer during the debugging process. As problems occurred during the simulations, the model developer would stop the simulation, locate the problem element(s), and attempt to fix the problem through slight adjustments to the topography — in effect, manual smoothing of the topography to avoid ponding. Given the differences in the wetting and drying algorithms and the difference in solution schemes, problems with the models would occur in different areas. As such, the models experienced different smoothing. Although model developers attempted to maintain the same overall storage and characteristics of the topography, numerous adjustments may have had an additive effect. This additive effect may have been sufficient to noticeably change the results. Evidence of this lies in the fact that while the 100-year and the 500-year simulations exhibit noticeable differences, the 50-year does not. This suggests that the differences in the mesh between the +8 and +12 ft-NAVD contour had a direct influence on the flow behavior at the bridges. Regardless of this fact, proper perspective must be maintained. The differences between the results only reached on the order of 10% to 15% of the overall elevations and velocity magnitudes at the bridges examined. These differences compare well with the calibration of the models which ranged from 3 to 13% in flow and elevation.

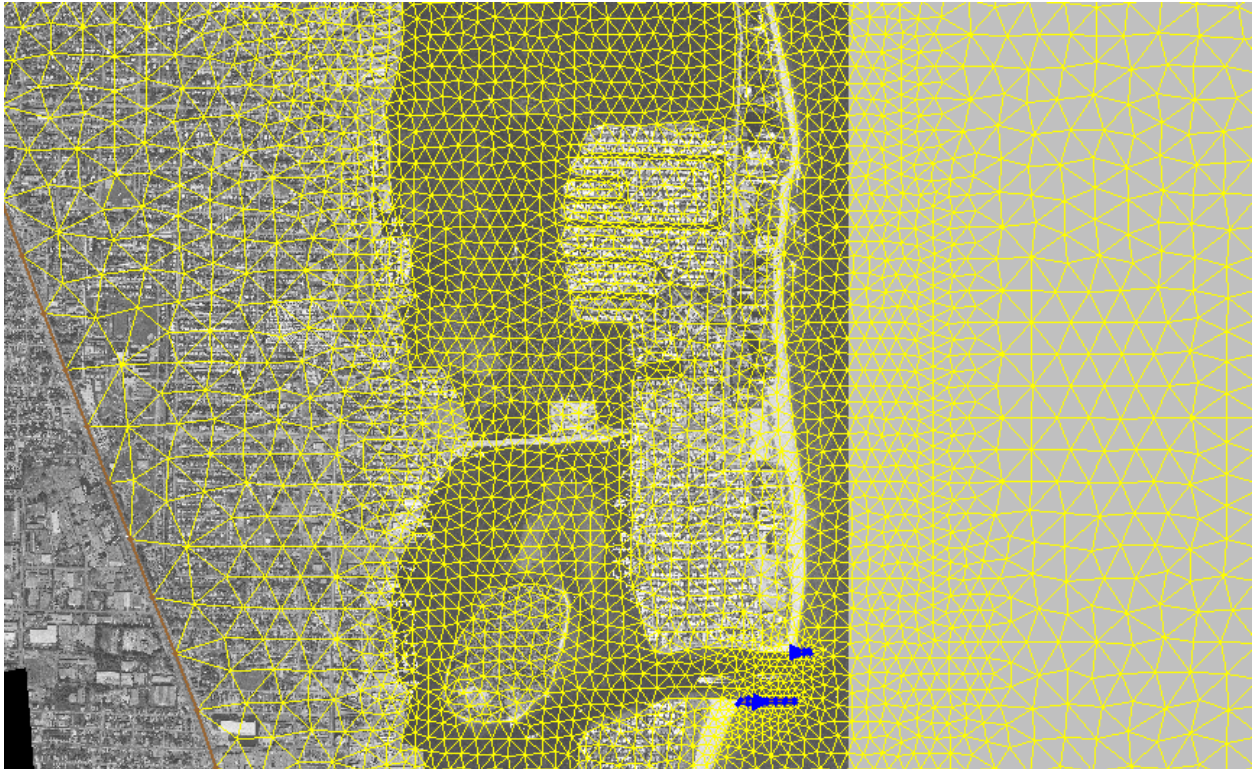


Figure 4.1 ADCIRC Model Mesh in the Vicinity of the Big Blue Heron Bridge

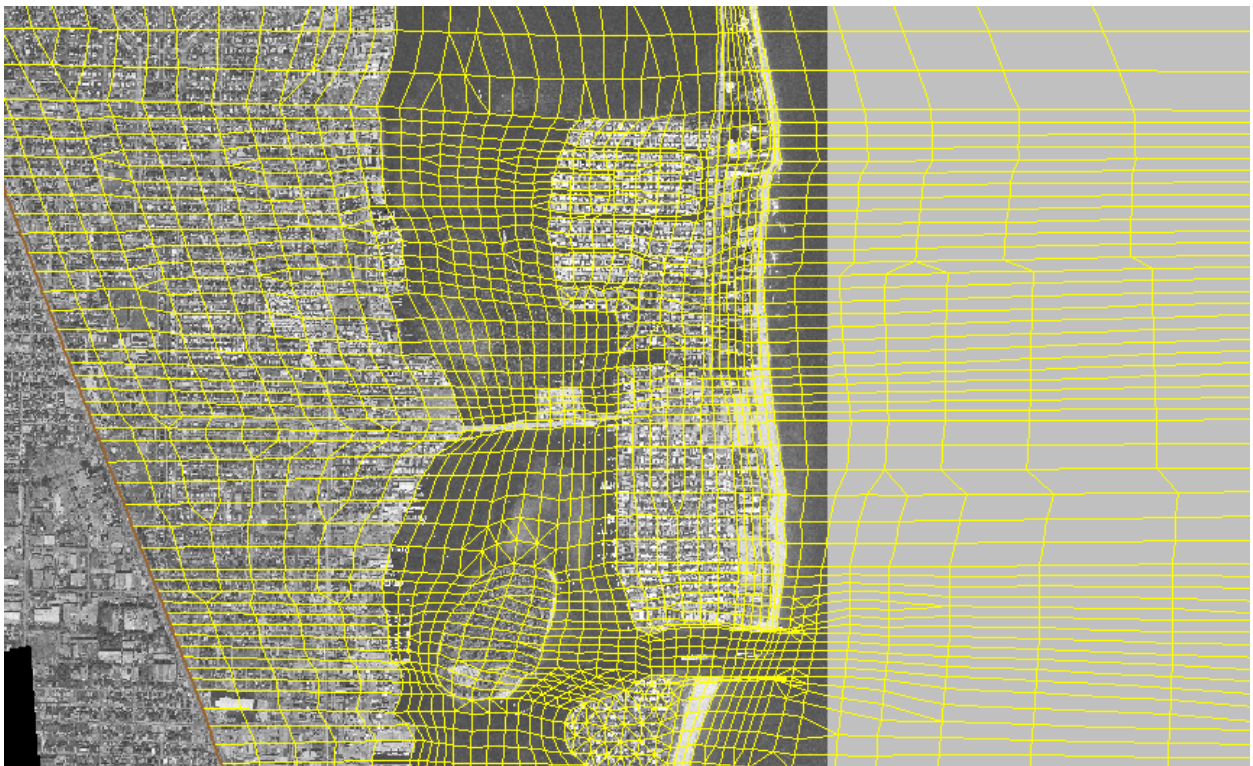


Figure 4.2 RMA2 Model Mesh in the Vicinity of the Big Blue Heron Bridge

Before continuing, another notable difference in the model results deserves mention. As noted previously, the ADCIRC results portrayed a curvature in the jet that issues from Lake Worth Inlet on ebb tide. This behavior is particularly apparent during the 500-year storm surge simulation (Figure 3.30). In fact, viewing a time series of velocity magnitude contours indicates that the ebb jet oscillates, curving both the north and south, during the storm surge recession. This is directly attributable to the location of the boundary condition residing only 2 miles offshore. The conditions placed on this boundary require very low flow through the boundary in order to maintain constant elevation across it. As such, the ebb jet must wag north and south in order to maintain this condition. This illustrates an ill-conceived model domain for the ADCIRC application. Interestingly, the RMA2 results do not exhibit the same behavior. Although this was known going into this work, the decision was made to maintain the same domain boundaries as the RMA2 model mesh in order to conduct a one-to-one comparison of model construction and ease of application. A larger domain for the ADCIRC model may have increased the amount of work associated with mesh development. Additionally, application of the measured tidal boundary conditions for calibration in a different location may also skew the results. This behavior underscores the importance of locating ones boundary conditions sufficiently far from the inlet to avoid these types of problems.

5.0 SUMMARY AND RECOMMENDATIONS

The objective of this work was to evaluate the capabilities of the ADCIRC and RMA2 models to simulate hurricane storm surge propagation through inland waterways for the purpose of determining design flow properties in support of FDOT's bridge hydraulics interests. This report presented the work associated with constructing a model of Lake Worth Inlet, its neighboring inlets, and connecting waterways, debugging and calibrating the model, and employing the model to simulate the storm surge propagation associated with the 50-, 100-, and 500-year return period hurricane storm surges. This work built upon work previously performed for FDOT District 4 in support of its scour evaluation program. The models' performance was judged both qualitatively and quantitatively.

Both models took approximately the same amount of time to construct, calibrate, and run. Both models achieved good calibration when compared with measured flow and water surface elevations. Although the ADCIRC model performed slightly better in the overall all calibration than did the RMA2 model, the differences were minor at best and might be reduced with additional work. The models did exhibit slight differences in flow behavior during the storm surge simulations at the bridges examined. These differences (10% to 15%) may be attributed to different choices made by the model developer concerning model resolution and topography smoothing during the model development and debugging processes. Additionally, differences occurred in the flow behavior offshore of the inlet. This resulted from selection of the location of the offshore boundary too close to shore for the ADCIRC application. This underscores the importance of placing the boundary conditions far from the area of interest. In summary, the models appear approximately equivalent in both their accuracy and their ease of application.

Given the minor differences in the two models, both models appear acceptable for this type of application. As such, OEA recommends the application of either model for the purpose of simulating hurricane storm surge propagation for FDOT applications where open coast storm surge boundary conditions are known. Selection of a model should therefore fall to which model contains the features most appropriate to the model domain and available boundary conditions. For example, simulation of specific hurricanes through meteorological forcing would suggest

application of the ADCIRC model. Conversely, if a bridge site contains numerous control structures such as culverts or flap gates, then RMA2 would be the preferred model.

REFERENCES

- Dean, R. G., Chiu, T. Y., and Wang, S. Y. (1992). *Combined Total Storm Tide Frequency Analysis for Palm Beach County, Florida*. Division of Beaches and Shores Department of Natural Resources. Beaches and Shores Resource Center, Institute of Science and Public Affairs. Tallahassee, Florida.
- Donnell, Barbara P., Letter, Joseph V., McAnally, W. H., et al. (2001), "User's Guide for RMA2 Version 4.5." US Army, Engineer Research and Development Center, Waterways Experiment Station, Coastal and Hydraulics Laboratory. Vicksburg, MS.
- Interagency Advisory Committee on Water Data (1982) *Guidelines for determining flood-flow frequency: Bulletin 17B of the Hydrology Subcommittee*. Office of Water Data Coordination, U.S. Geological Survey. Reston, Va.
- Luettich, R.A. and Westerink, J.J. (2000). ADCIRC, A (Parallel) ADvanced CIRCulation Model for Oceanic, Coastal and Estuarine Waters.
http://www.marine.unc.edu/C_CATS/adcirc/document/users_manual_pdf_version/ADCIRC_manual.pdf.
- Thomas, Jr., W. O., Lumb, A. M., Flynn, K. M., and Kirby, W. H. (1998). *Users Manual for Program PEAKFQ, Annual Flood Frequency Analysis Using Bulletin 17B Guidelines (Draft)*. U.S. Geological Survey Water-Resources Investigations Report. Reston, Va.
- U. S. Army Corps of Engineers (1986). *Storm Surge Analysis and Design Water Level Determinations*. Department of the Army, EM 1110-2-1412. Washington, D. C.

ACKNOWLEDGMENTS

The authors would like to thank Mr. Rick Renna, the State Drainage Engineer for the Florida Department of Transportation, for inspiring and sponsoring this research. Additionally, the authors would like to thank Dr. Scott Hagen from the University of Central Florida for providing his insight regarding the application and development of the ADCIRC model.